Copyright Warning & Restrictions

The copyright law of the United States (Title 17, United States Code) governs the making of photocopies or other reproductions of copyrighted material.

Under certain conditions specified in the law, libraries and archives are authorized to furnish a photocopy or other reproduction. One of these specified conditions is that the photocopy or reproduction is not to be "used for any purpose other than private study, scholarship, or research." If a, user makes a request for, or later uses, a photocopy or reproduction for purposes in excess of "fair use" that user may be liable for copyright infringement,

This institution reserves the right to refuse to accept a copying order if, in its judgment, fulfillment of the order would involve violation of copyright law.

Please Note: The author retains the copyright while the New Jersey Institute of Technology reserves the right to distribute this thesis or dissertation

Printing note: If you do not wish to print this page, then select "Pages from: first page # to: last page #" on the print dialog screen

ABSTRACT

NEURAL CORRELATES OF POST-TRAUMATIC BRAIN INJURY (TBI) ATTENTION DEFICITS IN CHILDREN

by
Meng Cao

Traumatic brain injury (TBI) in children is a major public health concern worldwide. Attention deficits are among the most common neurocognitive and behavioral consequences in children post-TBI which have significant negative impacts on their educational and social outcomes and compromise the quality of their lives. However, there is a paucity of evidence to guide the optimal treatment strategies of attention deficit related symptoms in children post-TBI due to the lack of understanding regarding its neurobiological substrate. Thus, it is critical to understand the neural mechanisms associated with TBI-induced attention deficits in children so that more refined and tailored strategies can be developed for diagnoses and long-term treatments and interventions.

This dissertation is the first study to investigate neurobiological substrates associated with post-TBI attention deficits in children using both anatomical and functional neuroimaging data. The goals of this project are to discover the quantitatively measurable markers utilizing diffusion tensor imaging (DTI), structural magnetic resonance imaging (MRI), and functional MRI (fMRI) techniques, and to further identify the most robust neuroimaging features in predicting severe post-TBI attention deficits in children, by utilizing machine learning and deep learning techniques. A total of 53 children with TBI and 55 controls from age 9 to 17 are recruited. The results show that the systems-level topological properties in left frontal regions, parietal regions, and medial occipitotemporal regions in structural and functional brain network are significantly associated with

inattentive and/or hyperactive/impulsive symptoms in children post-TBI. Semi-supervised deep learning modeling further confirms the significant contributions of these brain features in the prediction of elevated attention deficits in children post-TBI. The findings of this project provide valuable foundations for future research on developing neural markers for TBI-induced attention deficits in children, which may significantly assist the development of more effective and individualized diagnostic and treatment strategies.

NEURAL CORRELATES OF POST-TRAUMATIC BRAIN INJURY (TBI) ATTENTION DEFICITS IN CHILDREN

by
Meng Cao

A Dissertation
Submitted to the Faculty of
New Jersey Institute of Technology
and Rutgers University Biomedical and Health Sciences – Newark
in Partial Fulfillment of the Requirements for the Degree of
Doctor of Philosophy in Biomedical Engineering

Department of Biomedical Engineering

May 2023

.

APPROVAL PAGE

NEURAL CORRELATES OF POST-TRAUMATIC BRAIN INJURY (TBI) ATTENTION DEFICITS IN CHILDREN

Meng Cao

Dr. Xiaobo Li, Dissertation Advisor — Date
Associate Professor of Biomedical Engineering, NJIT

Dr. Tara L. Alvarez, Dissertation Co-Advisor — Date
Distinguished Professor of Biomedical Engineering, NJIT

Dr. Bharat Biswal, Committee Member — Date
Distinguished Professor of Biomedical Engineering, NJIT

Dr. Ozlem Gunal, Committee Member — Date
Assistant Professor of Psychiatry, Rutgers New Jersey Medical School, Newark, NJ

Dr. Sridhar Kannurpatti, Committee Member — Date
Assistant Professor of Radiology, Rutgers New Jersey Medical School, Newark, NJ

BIOGRAPHICAL SKETCH

Author: Meng Cao

Degree: Doctor of Philosophy

Date: May 2023

Undergraduate and Graduate Education:

- Doctor of Philosophy in Biomedical Engineering,
  New Jersey Institute of Technology, Newark, NJ, 2023

- Master of Science in Electrical Engineering,
  Stevens Institute of Technology, Hoboken, NJ, 2016

- Bachelor of Science in Electrical Engineering,
  Michigan State University, East Lansing, MI, 2013

Major: Biomedical Engineering

Presentations and Publications:

Cao, M., Wu, K., Halperin, J.M., and Li, X. (2023). Abnormal structural and functional network topological properties associated with left prefrontal, parietal and occipital cortices significantly predict childhood TBI-related attention deficits: a semi-supervised deep learning study. *Frontiers in Neuroscience, 17*, 311.

Cao, M., Luo, Y., Wu, Z., Wu, K., and Li, X. (2022). Abnormal neurite density and orientation dispersion in frontal lobe link to elevated hyperactive/impulsive behaviors in young adults with traumatic brain injury. *Brain Communications 4*, fcac011.

Cao, M., Wu, Z., and Li, X. (2022). GAT-FD: an integrated MATLAB toolbox for graph theoretical analysis of task-related functional dynamics. *PLoS One 17*, e0267456.

Cao, M., Halperin, J.M., and Li, X. (2022). Abnormal functional network dynamics implicate post-TBI attention deficits in children. *Organization of Human Brain Mapping (OHBM) Annual Meeting, Glasgow, Scotland, UK*.

Baboli, R., Cao, M., Halperin, J.M., and Li, X. (2022). Distinct thalamic and frontal neuroanatomical substrates in children with familial vs. non-familial attention-deficit/hyperactivity disorder (ADHD). *Brain Sciences 13*.

Cao, M., Halperin, J.M., and Li, X. (2021). Abnormal functional network topology and its dynamics during sustained attention processing significantly implicate post-TBI attention deficits in children. *Brain Sciences 11*.

Cao, M., Luo, Y., Wu, Z., Mazzola, C.A., Catania, L., Alvarez, T.L., Halperin, J.M., Biswal, B., and Li, X. (2021). Topological aberrance of structural brain network provides quantitative substrates of post-traumatic brain injury attention deficits in children. *Brain Connectivity 11*, 651-662.

Wu, Z., Cao, M., Di, X., Wu, K., Gao, Y., and Li, X. (2021). Regional topological aberrances of white matter- and gray matter-based functional networks for attention processing may foster traumatic brain injury-related attention deficits in adults. *Brain Sciences 12*.

[Blank]

ACKNOWLEDGMENT

I would like to express my deepest gratitude to my dissertation advisor, Dr. Xiaobo Li for her academic supervision, remarkable mentoring, and invaluable patience through all my years in graduate school. Her immense knowledge, motivation and experience have guided and shaped my ability as a researcher and will influence me for the rest of my life.

I extend my great appreciation to Dr. Tara L. Alvarez and Dr. Bharat B. Biswal from NJIT, and Dr. Ozlem Gunal and Dr. Sridhar Kannurpatti from Rutgers New Jersey Medical School for their time and invaluable feedback to improve the quality of this dissertation. They all have played a major role in polishing my research.

This endeavor would not have been possible without the generous support from New Jersey Institute of Technology (Provost's Doctoral Assistantship Award), the National Institute of Mental Health (R03MH109791, R15MH117368, and R01MH126448), and the New Jersey Commission on Brain Injury Research (CBIR17PIL012 and CBIR22PIL002).

I would also like to thank current and former members of the Computational Neuroanatomy and Neuroinformatics Laboratory: Dr. Elizabeth Martin, Rahman Baboli, Chirag Lalitbhai Motwani, Dr. Ziyan Wu, Dr. Yuyang Luo, and Jincheng Li for giving me the motivation and supports I needed to finish my work.

Last, but not least, I am genuinely grateful to my parents, Jinrui Cao and Rongli Pan, and my wife, Wanzhen Sheng, whose love and good wishes are with me wherever I go.

TABLE OF CONTENTS

TABLE OF CONTENTS
(Continued)

Chapter **Page**

TABLE OF CONTENTS
(Continued)

TABLE OF CONTENTS
(Continued)

Chapter **Page**

LIST OF TABLES

LIST OF FIGURES

CHAPTER 1

INTRODUCTION

1.1 Background and Significance

Traumatic brain injury (TBI) is a major public health concern in children, with estimated more than 1 million emergency department visits annually in the United State (Dewan et al., 2016; Taylor et al., 2017). Population under the potential impact of TBI is rather high when considering additional outpatients or individuals who did not receive any medical attention (Arbogast et al., 2016). Children after TBI are typically at risk of having behavioral and psychiatric problems, including attention problems, depression and mood disorders, anxiety, and posttraumatic stress disorder (Hooper et al., 2004; Konigs et al., 2015; Emery et al., 2016). Pediatric TBI results in substantial financial burden and health system costs in the United State (Miller et al., 2021). In addition, the neurocognitive impairments and behavioral abnormalities cause substantial burdens in affected individuals and caregivers (Aitken et al., 2009; Polinder et al., 2015; Dewan et al., 2016; Lumba-Brown et al., 2018).

1.1.1 Attention deficits in children post traumatic brain injury

Attention deficits are among the most common long-term sequalae in pediatric TBI patients (Gerring et al., 1998; Max et al., 2005; Narad et al., 2018). Deficits in attention are prominent in the subacute phase of recovery and often persist into chronic phase (Ginstfeldt and Emanuelson, 2010). Significant attention deficits were reported in about 35% of children within two years of their TBI (Max et al., 2005), and were observed to strongly contribute to elevated risk for severe psychopathology and impairments in overall

functioning in late adolescence, with the pathophysiological underpinning yet to be fully elucidated (Le Fur et al., 2019; Narad et al., 2019). Clinical studies reported that the post-TBI attention deficits were associated with poor performance in executive function, lapse of attention, or poor inhibitory controls (Konigs et al., 2015; Yang et al., 2016; Sinopoli et al., 2011). The persistent attention deficits after TBI have significant impacts on the affected individual's educational and social outcomes, which further compromise the life quality of themselves and their families' (Stancin et al., 2010; Wehmeier et al., 2010; Narad et al., 2019). There is a paucity of evidence to guide the optimal treatment strategies of attention deficits related symptoms in children post-TBI (Backeljauw and Kurowski, 2014; Resch et al., 2018). Evaluation and treatment procedures on attention deficits post-TBI have been based on endorsement of symptoms of attention deficit/hyperactivity disorder (ADHD) (Napolitano et al., 2005; Pangilinan et al., 2010; Barnett and Reid, 2020). However, mixed results were observed, with some reported benefits of pharmacologic and cognitive therapies, while others resulted in suboptimal efficacy (Senior et al., 2013; Backeljauw and Kurowski, 2014; Resch et al., 2018; Kurowski et al., 2019; LeBlond et al., 2019). The limited consensus regarding appropriate evaluation and treatment of attention deficits in children post-TBI is due to the lack of understanding of the neurobiological substrate associated with this syndrome in children. Therefore, elucidation of the underlying neural mechanisms of post-TBI attention deficits in children is vitally critical, so that timely and tailored strategies can be developed for diagnoses and long-term treatments and interventions.

1.1.2 Neuroimaging studies of traumatic brain injury

Existing neuroimaging studies on pediatric TBI utilizing multimodal neuroimaging modalities, including the structural magnetic resonance imaging (MRI), diffusion tensor imaging (DTI), and functional MRI (fMRI), have revealed widespread structural and functional alterations in both gray matter (GM) and white matter (WM) tissues. In specific, structural MRI studies have reported significant alterations of GM thickness and volume in frontal, parietal, and temporal regions (Merkley et al., 2008; Wilde et al., 2012b; Dennis et al., 2013; Yeates et al., 2014; Dennis et al., 2016; Dennis et al., 2017). Among them, although a few have shown the relationship between morphometry and functional outcomes, including working memory (Merkley et al., 2008), executive function (Wilde et al., 2012b), social cognition (Dennis et al., 2013; Yeates et al., 2014), and overall cognitive function (Dennis et al., 2016; Dennis et al., 2017), no studies have focused on the attention domain (King et al., 2019).

The majority of anatomical neuroimaging studies in pediatric TBI utilized DTI technique, and have shown reduced WM integrity in a wide range of association fibers, projection fibers, and commissural fibers in pediatric TBI patients at chronic phase relative to controls, including the superior longitudinal fasciculus, inferior longitudinal fasciculus, inferior occipitofrontal fasciculus, uncinate fasciculus, arcuate fasciculus, cingulum, corona radiata, corpus callosum, and fornix (Wilde et al., 2012a; Liegeois et al., 2013; Treble et al., 2013b; Dennis et al., 2018; Konigs et al., 2018; Wu et al., 2018a; Lindsey et al., 2019; Molteni et al., 2019). Meanwhile, associations between WM damages and working memory deficits and executive dysfunctions were frequently found in children with chronic TBI. For instance, a number of DTI studies reported that disrupted WM integrity in corpus callosum (Ewing-Cobbs et al., 2008; Treble et al., 2013a; Lindsey et al.,

2019), superior longitudinal fasciculus and inferior fronto-occipital fasciculus (Dennis et al., 2015), uncinate fasciculus (Lindsey et al., 2019), and cingulum bundle (Wilde et al., 2011) were associated with working memory impairments in children with TBI. There were also diverse findings reported in children post-TBI that linked with executive dysfunction, that better executive function performance was correlated with higher WM integrity in frontal regions (Wozniak et al., 2007b; Kurowski et al., 2009), superior longitudinal fasciculus and anterior corona radiata (Adamson et al., 2013), and ventral striatum (Faber et al., 2016). A more recent pediatric TBI study reported that reduced fractional anisotropy (FA) in the inferior longitudinal fasciculus, inferior fronto-occipital fasciculus, superior longitudinal fasciculus, and corpus callosum were associated with impaired attention and working memory (Konigs et al., 2018). Despite the increasing evidence in the relationship between anatomical properties and functional outcomes in the field, only a few DTI studies mentioned above have investigated the associations between brain structural properties and attention problems in children post-TBI (Wozniak et al., 2007b; Konigs et al., 2018).

Task-based fMRI is widely used to explore the brain activations that involved in a specific task performance for children with chronic-TBI. The majority of task-based fMRI studies used working memory paradigms and have found increased activations in prefrontal cortex, superior temporal gyrus, middle temporal gyrus, and precentral gyrus, while also reported decreased activation in medial frontal region, parahippocampal gyrus, and insula (Newsome et al., 2008; Kramer et al., 2009; Sinopoli et al., 2014; Westfall et al., 2015). A more recent study found no significant difference in Blood-oxygen-level dependent (BOLD) activation between children with TBI and children with orthopedic injury when

performing working memory tasks (Brooks et al., 2020). Olsen and colleagues reported relations between neurocognitive outcomes and functional activation alterations during spatial working memory task, where poor outcome group demonstrated hyperactivations while normal outcome group showed hypoactivation, when compared both TBI groups to controls (Olsen et al., 2020). Other task-based fMRI studies also reported functional alterations in frontal, parietal, temporal, and occipital regions in children with TBI during motor task (Caeyenberghs et al., 2009), language task (Karunanayaka et al., 2007), and social cognition task (Newsome et al., 2010). A few pediatric TBI studies have investigated brain activations during attention tasks (Kramer et al., 2008; Tlustos et al., 2011; Strazzer et al., 2015; Tlustos et al., 2015). During sustained attention task, studies have reported that children with TBI demonstrated reduced activation in frontal, parietal, and occipital regions when compared to healthy controls (Strazzer et al., 2015) and children with orthopedic injuries (Kramer et al., 2008). Tlustos and colleagues reported that children with TBI, relative to controls, showed decreased activation in anterior cingulate and motor cortex during inhibition task (Tlustos et al., 2015). Children with TBI have higher activation in middle frontal gyrus, precentral gyrus, and parietal lobule when performing interference control (Tlustos et al., 2011). In addition, a few TBI studies using resting-state fMRI have reported that the reduced connectivity in default mode network and motor network were associated with poor inhibitory control (Stephens et al., 2017; Stephens et al., 2018). Although the behavioral and neurocognitive outcomes have gained increased attention in neuroimaging studies in pediatric TBI, the field still lacks investigations that target the severe attention deficits in children post-TBI and the associated functional and structural alterations.

1.1.3 Graph theoretical analysis studies of traumatic brain injury

The existing voxel- and region-of-interest (ROI)-based studies have limitations in addressing how, in the systems-level, certain brain regions are vulnerable to TBI and contribute to related cognitive and behavioral consequences. The graph theoretical technique (GTT)-based approaches have been increasingly implemented in human brain imaging data to construct structural and/or functional brain networks in a systems-level, and to characterize the network integration, segregation, centrality, and small-worldness in both the global and regional (sub-network) scales (Bullmore and Sporns, 2009). In the context of TBI in children, diffuse axonal injury has been demonstrated to damage the structural networks, resulting in disrupted functional information transfer across distal brain regions and cognitive and behavioral impairments. For instance, structural network studies found that children with chronic TBI, relative to controls, showed altered global network metrics, including increased characteristic path length and decreased local efficiency (Caeyenberghs et al., 2012; Konigs et al., 2017; Yuan et al., 2017a). In addition, global and regional network properties were found to correlate with postural control (Caeyenberghs et al., 2012), IQ and working memory (Konigs et al., 2017), and overall cognitive performance (Yuan et al., 2017a). Although an increasing number of studies have successfully used graph theoretical analysis to evaluate relationships between graph metrics and neurocognitive and behavioral outcomes, the anatomical network property alterations associated with post-TBI attention deficits have not yet been investigated.

Decreased functional network integration, including decreased network global efficiency and increased characteristic path length, was often observed in adult with TBI when compared to controls (Nomura et al., 2010; Pandit et al., 2013; Han et al., 2016). A more recent longitudinal study reported that increased functional network integrations were

associated with better cognitive recovery in adults with TBI (Kuceyeski et al., 2019). TBI-induced disruptions in long range fibers have the potential to affect the information processing in the functional brain network, which can be reflected in the integration metrics, i.e. network global efficiency, or connectivity metrics, i.e., nodal degree. Regional network properties also have the sensitivity to identify the regions that have altered roles in specific function networks. However, no studies have used graph theoretical analysis to determine the topological alterations in functional network in children post-TBI.

1.1.4 Machine learning studies of traumatic brain injury

Conventional statistical analysis does not always guarantee to identify features with adequate accuracy in differentiating TBI patients and controls. Compared to conventional parametrical models, machine learning techniques have the capacity in learning the joint effects of measures in high dimensional space and have the sensitivity in detecting subtle information that have high discriminative/predictive power (Nielsen et al., 2020). When aided with feature selection methods and cross-validation methods, machine learning techniques can deliver efficient and robust classifications between different groups.

Machine learning techniques have been successfully employed in several adult TBI studies recently and have shown improvements in classification accuracies. In specific, Lui et al. used five classifiers to build prediction models with features selected from demographic information, structural MRI, DTI, and resting-state fMRI with minimal-redundancy-maximal-relevance feature selection model (Lui et al., 2014). The feature selection process was able to increase the accuracy of varies algorithms by 2-20% and achieved 86% prediction accuracy using multilayer perceptron algorithm. One combined fMRI-DTI study got 83.59% accuracy in differentiating active-duty soldiers with post-

traumatic syndrome and controls by using recursive cluster elimination as feature selection method, and support vector machine (SVM) as prediction model (Rangaprakash et al., 2017). Another study used only DTI extracted features and demonstrated that both random forest and SVM can achieve approximate 70% accuracy in differentiate adult TBI patients and controls in a large dataset with 325 participants (Mitra et al., 2016). Vergara et al. compared resting-state fMRI data with DTI data as features for SVM and demonstrated that SVM using resting-state fMRI data can achieve 84.1% accuracy, which was higher than using DTI data or combined data of both (Vergara et al., 2017). The high accuracies achieved in adult TBI studies indicate that machine learning technique could help to develop effective classification models in pediatric TBI studies.

A few existing studies in children with TBI have applied machine learning techniques. By constructing classification model using SVM and edge density image, one study was able to differentiate 14 children with TBI and 10 controls with an area under the receiver-operating-characteristic-curve (AUC) of 0.94 (Raji et al., 2020). Another study built an SVM-based classification model using structural MRI data and DTI data from 29 student athletes (aged from 15 to 20 years) and 27 controls and achieved an AUC of 0.84 (Tamez-Pena et al., 2021). A longitudinal study reported that when combining resting-state MRI data and structural MRI data in 99 children with TBI at 4 weeks after the injury, SVM algorithm was able to predict the recovery of post-concussion symptoms at 8 weeks with an AUC of 0.86 (Iyer et al., 2019). However, the majority of these machine learning studies in children with TBI applied supervised models that only focused on discriminating labels of the two diagnostic groups, and none of these studies have intended to detect the neurobiological features associated with the most common TBI-related cognitive deficits.

In addition, the features that contribute to a highly accurate classification model can improve the understanding of be neural mechanism of attention deficits in children post-TBI and provide potential targets for interventions and treatments.

1.2 Innovations

The current research investigates the neural mechanisms associated with attention deficits in children post-TBI in a more homogeneous subgroup of children with clinically confirmed post-TBI attention deficits. The functional consequences and brain alterations after TBI are heterogenous by nature. Existing neuroimaging studies that investigated the attention domain included TBI subjects without considering whether they have attention problem or not. Therefore, the current study with a more homogeneous will increase the statistical power in detecting the difference between children with severe post-TBI attention deficits and controls. In addition, the proposed research utilizes multimodal neuroimaging techniques. Studies in the existing literature mainly focused on the anatomical alterations or working memory related functional alterations in children with TBI. The combined structural and functional imaging technique in the same cohort will significantly advance our understanding of the neural mechanisms associated with severe post-TBI attention deficits in children. Moreover, this study implements combinations of features selection, cross-validation, machine learning, and deep learning techniques to construct classification models of attention deficits in children post-TBI. Relative to conventional statistical methods, machine learning is able to detect the complex patterns between different neuroimaging modalities.

1.3 Objective and Specific Aims

Therefore, the overarching goals of this study are 1) to understand the neural mechanisms associated with TBI-induced attention deficits (TBI-A) in children; 2) to develop a novel procedure to identifying the most robust neuroimaging predictors of TBI-A in children.

Specific Aim 1: Determine the topological alterations of structural connectivity network in children with TBI-A. The structural connectivity network is constructed based on the anatomical regions and the interconnecting fibers. The topological properties are calculated in global level and nodal level. The brain network hubs are characterized by the nodal strength and betweenness centrality. Associations between attention deficits symptoms and network properties are investigated in children with TBI-A. **Hypothesis:** Compared to controls, TBI-A group shows significantly reduced local connectivity (e.g., local efficiency and clustering coefficient) in frontal lobe and parietal regions and altered network traffic topology with different hub combinations. Greater local connectivity in frontal and parietal regions are associated with better behavioral outcomes in TBI-A group.

Specific Aim 2: Assess topological dynamics in functional connectivity network for sustained attention processing in children with TBI-A. fMRI data are collected from subjects while they are performing a continuous performance task. The functional network is constructed for each individual using graph theoretic technique. Global level and nodal level topological properties and their dynamics are calculated. Associations between attention deficits symptoms and network properties are investigated. **Hypothesis:** Relative to controls, TBI-A group shows significantly decreased nodal global efficiency and degree, and reduced stability in frontal and parietal regions. Decreased nodal efficiency in frontal and parietal regions are associate with increased attention deficits symptoms in TBI-A group.

Specific Aim 3: Develop a novel procedure that utilize the machine learning and deep learning techniques to identify the most robust neuroimaging predictors of TBI-A in children. Combinations of feature selection methods are used to construct the classification models. Classification accuracies are compared to conventional machine learning techniques. **Hypothesis:** The most important features identified by the proposed procedure are the functional and structural network topological properties of regions within frontal and parietal lobe.

CHAPTER 2

GENERAL METHODOLOGY

2.1 Participants

The study received institutional review board approval at the New Jersey Institute of Technology, Rutgers University, and Saint Peter's University Hospital.

The TBI-A group included children with a clinically diagnosed mild or moderate non-penetrating TBI at least 6 months prior to the study date; and T score ≥ 65 in the inattention subscale (or T scores ≥ 65 in both inattention and hyperactivity subscales) in the Conners 3rd Edition-Parent Short form (Conners 3-PS) assessed during the study visit (Conners, 2008). Children with TBI who had overt focal brain damages or hemorrhages were excluded. To rule out confounding factors associated with pre-TBI attention deficits, children who had a history of diagnosed ADHD (any sub-presentations) prior the diagnosis of TBI, or severe pre-TBI inattentive and/or hyperactive behaviors that were reported by a parent, were excluded from the TBI-A group. The control group included children with no history of diagnosed TBI, no history of diagnosed ADHD, and T scores ≤ 60 in all of the subscales in the Conners 3-PS assessed during the study visit. The two groups were matched on sex (male/female) distribution and socioeconomic status (SES) that was estimated using the average education year of both parents.

To further improve the homogeneity of the study sample, the general inclusion criteria for both groups were:

1. Right-handed, to remove handedness-related potential effects on brain structures.
2. Full scale IQ ≥ 80, to minimize neurobiological heterogeneities in the study sample.
3. Ages of 11 – 15 years, to reduce neurodevelopment-introduced variations in brain

structures.

The general exclusion criteria for both groups were:

1. Current or previous diagnosis of Autism Spectrum Disorders, Pervasive Development Disorder, psychotic, Major Mood Disorders (except dysthymia not under treatment), Post-Traumatic Stress Disorder, Obsessive-Compulsive Disorder, Conduct Disorder, Anxiety (except simple phobias), or substance use disorders, based on Diagnostic and Statistical Manual of Mental Disorders 5 (DSM-5) and supplemented by the Kiddie Schedule for Affective Disorders and Schizophrenia for School-Age Children-Present and Lifetime Version (K-SADS-PL) (Kaufman et al., 2000);

2. Any types of diagnosed chronic medical illnesses, neurological disorders, or learning disabilities, from the medical history;

3. Treatment with long-acting stimulants or non-stimulant psychotropic medications within the past month;

4. Any contraindications for MRI scanning, such as claustrophobia, tooth braces or other metal implants;

5. Pre-puberty subjects were also excluded, to reduce pubertal stage-related confounders (Blakemore and Choudhury, 2006);

In the study, handedness was evaluated using the Edinburgh Handedness Inventory (Oldfield, 1971). Full scale IQ was estimated by the Wechsler Abbreviated Scale of Intelligence II (WASI-II) (Wechsler, 2011). Puberty status was evaluated using the parent version of Carskadon and Acebo's self-administered rating scale (Carskadon and Acebo, 1993).

Severity of TBI was characterized using the Glasgow Coma Scale (GCS) (Teasdale and Jennett, 1974), with the scores ranging from 9 to 15 in the TBI-A subjects. Severities of the inattentive and hyperactive/impulsive symptoms were dimensionally measured using the raw scores and T scores of the subscales in Conners 3-PS. The CogState brief battery for children (Eckner et al., 2011), which included five computerized tests, was administered to each subject. The normalized overall scores of the tests were used to

evaluate neurocognitive capacities in executive function, psychomotor speed, visual attention, visual learning/memory and working memory.

A total of 53 children with TBI and 55 controls from age 9 to 17 were recruited. Due to availability of the structural and function MRI data, the total number of participants in each aim varied between 66 and 105.

2.2 Multimodal Magnetic Resonance Imaging Data Acquisition Protocol

For each subject, high-resolution T1-weighted structural MRI, DTI, and task-based fMRI data were acquired using a 3-Tesla Siemens TRIO (Siemens Medical Systems, Germany) scanner from the Rutgers University Brain Imaging Center. The T1-weighted anatomical images were obtained with a sagittal multi-echo magnetization-prepared rapid acquisition gradient echo (MPRAGE) sequence (voxel size = 1 mm^3 isotropic, repetition time (TR) = 1900 ms, echo time (TE) = 2.52 ms, flip angle = 9°, field of view (FOV) = 250 mm × 250 mm, and 176 sagittal slices). The scan time was 3 minutes. The DTI data was acquired using echo planar imaging (EPI) sequence (voxel size = 2.0 mm × 2.0 mm × 2.5 mm, TR = 7700 ms, TE = 103 ms, FOV = 250 mm × 250 mm, 30 diffusion-sensitizing gradient directions with b-value = 700 s/mm^2, and one image with b-value = 0 s/mm^2). The scan time was 4.5 minutes. The fMRI data acquisition utilized whole brain gradient EPI sequence (voxel size = 1.5 mm × 1.5 mm × 2.0 mm, TR = 1000 ms, TE = 28.8 ms, and FOV = 208 mm × 208 mm). The scan time was 5.5 minutes. T2-Weighted Field Map without diffusion weighting was collected for fMRI geometric distortion corrections. Each participant was placed in a supine position in the scanner. Foam pads were placed under the knees and between the head and the coil, in order to maximize comfort, minimize muscle strain during fMRI task responses, and minimize head motion. The study procedure

was carefully explained to each subject before entering the scanner.

2.3 General Techniques of Multimodal Magnetic Resonance Imaging

MRI is one of the most utilized neuroimaging techniques in studying the anatomical and functional brain properties. In psychiatric research, MRI have become a critical tool for understanding the brain alterations that associated with etiology, pathophysiology, and treatment response (Kalin, 2021). MRI is a noninvasive medical imaging technique that based on the nuclear magnetic resonance phenomenon. Under strong magnetic field, hydrogen atoms can be excited by radio waves of certain frequency. Combined with magnetic field gradients, the radio wave can excite selected regions. And by measuring the emitted radio wave from the excited hydrogen atoms, the rate of excited atoms that returns to equilibrium state can used as the contract between different tissues, due to the density differences. Compared to other medical imaging techniques, MRI has higher contrast between different brain tissues, e.g., gray matter and white matter.

2.3.1 Structural magnetic resonance imaging

Structural MRI was commonly used in characterizing anatomical properties of the brain. The different density of hydrogen atoms in different brain tissues resulted in different magnetic properties of the transition from excited state to equilibrium state. The relaxation processes are usually described by T1, magnetization in the same direction as the static magnetic field, and T2, magnetization transverse to the static magnetic field. The T1-weighted image has high contrast between gray matter and white matter, which is generally used to obtain morphological information. T2-weighted, on the other hand, has high contrast between normal tissue and abnormal tissues, such as inflammation, infection, or

tumor.

2.3.2 Diffusion-weighted magnetic resonance imaging

Diffusion-weighted Imaging (DWI) is a type of MRI technique that generate image using the diffusion of water molecule as contrast. Diffusion is a physical phenomenon that refers to the random, microscopic movement of water and other small molecules due to thermal agitation. In the brain tissues, the movement of the water molecule was limited by obstacles such as fibers and membranes. Therefore, measuring the diffusion pattern can serve as the method of characterizing the microscopic details of tissue architecture. DWI has been used in the detection of cerebral ischemia, axonal shearing injury, brain tumors, or abscesses (Mukherjee et al., 2008). The most common quantitative measure from a DWI is apparent diffusion coefficient (ADC), which is a measure of the magnitude of diffusion within tissue.

The convention DWI only provide a general diffusion coefficient for each voxel. However, it is not sufficient to characterize the diffusion property in highly structured biological tissues, e.g., brain tissues. The concept of anisotropic refers to different diffusion coefficient along different direction, compared to isotropic, which refers diffusion in a homogenous environment. Brain tissues, especially white matters, where water molecule moves along nerve fibers, is highly anisotropic. Diffusion tensor imaging (DTI) is a diffusion MRI technique that estimate the diffusion coefficient along different directions. In DTI, multiple diffusion images with different directions are collected to calculate a diffusion tensor, a 3 by 3 matrix with each number corresponding to the diffusion coefficient of a direction combination (e.g., x-y, x-z), for each voxel. The key quantitative measures include fraction anisotropy (FA, a index of the diffusion asymmetry), mean

diffusivity (MD, average diffusion coefficient of all three directions), and radial diffusivity (RD, average diffusion coefficient in the two minor axes). In addition to voxel measure, DTI data can also be used to estimate white matter fibers. The application is called tractography.

Recently, a more advanced diffusion MRI modality, the neurite orientation dispersion and density imaging (NODDI), has been developed (Zhang et al., 2012). This innovative technique acquires imaging data at multiple levels of diffusion weight, with each sampling many different spatial orientations at high angular resolution. The main parameters derived from NODDI are neurite density index (NDI), and neurite orientation dispersion index (ODI). The intracellular component of NODDI is designed to be representative of both axons and dendrites, thus providing an improved description of gray matter microstructure. In addition, NODDI enables differentiation of changes to tissue density and tissue ODI (both expressed by FA changes when using DTI), ultimately offering superior sensitivity to micro-level tissue changes.

2.3.3 Functional magnetic resonance imaging

Functional MRI is an MRI technique for measuring brain activity in association with task-induced mental processes or during resting-state (Kim and Ogawa, 2012). The contrast is the blood oxygenation level-dependent (BOLD). Because the cerebral blood flow is coupled with neuronal activation, the relative levels of oxygenated hemoglobin and deoxygenated hemoglobin in the blood can be used as an indicator of regional activation. Each type of hemoglobin has different magnetic properties that can be differentiated using MRI. Relative to other functional neural imaging techniques, fMRI have higher spatial resolution, and the ability to measure the activity of deep brain structures.

2.4 Graph Theoretical Techniques

Known as a foundation of neuroscience, human brain regions do not work in an isolated manner. When processing sensory and higher-order cognitive information, cortical and subcortical brain regions have been found to dynamically reassemble into small-world networks, to maintain optimal communication efficiency (Bassett et al., 2011; Spreng et al., 2013). The existing voxel- and region-of-interest (ROI)-based studies have limitations in addressing cognitive or behavioral problems in the systems-level. The graph theoretical technique (GTT)-based approaches have been increasingly implemented in human brain imaging data to construct structural and/or functional brain networks in a systems-level, and to characterize the network integration, segregation, centrality, and small-worldness in both the global and regional (sub-network) scales, as show in **Figure 2.1**.

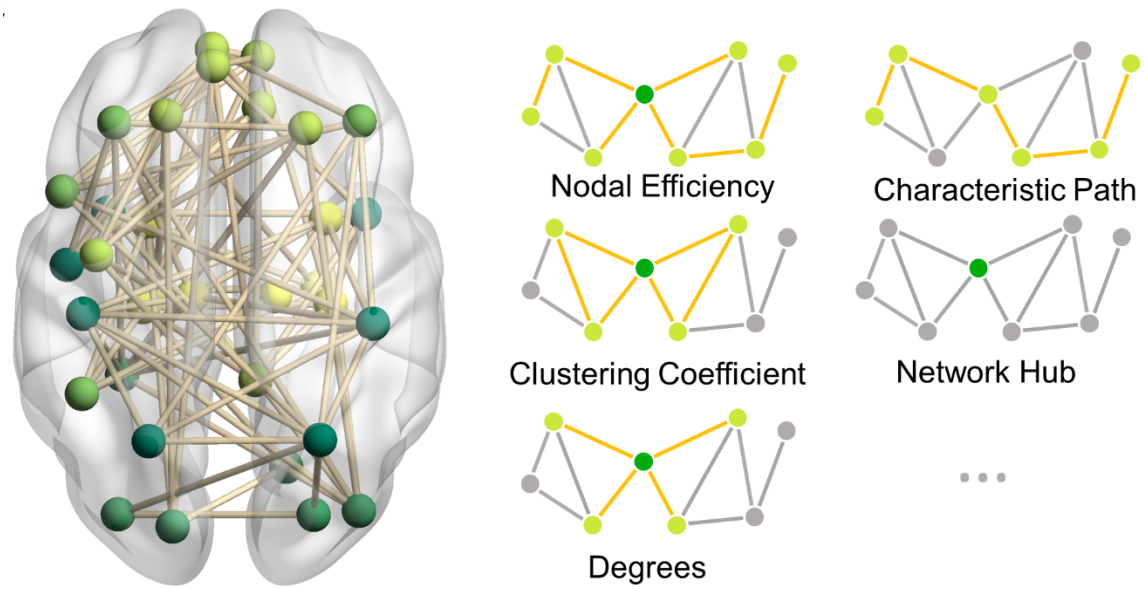

Figure 2.1 Examples of different network topological measures.

The network global efficiency is a metric of the network integration that reflects the ability of information transferring across distributed brain areas (Latora and Marchiori,

2001). It was defined as

$$E_{glob}(G) = \frac{1}{n(n-1)} \sum_{i,j \in N, j \neq i} \frac{1}{d_{ij}} \tag{2.1}$$

where d_{ij} was the inverse of the shortest distance between node i and j that was represented using the edge's normalized weight. When two nodes were not directly connected, the shortest distance was the sum of the shortest connecting edges.

The network local efficiency estimates the network segregation and represents the fault tolerance level of the network (Latora and Marchiori, 2001), which was defined as

$$E_{network-loc}(G) = \frac{1}{n} \sum_{i \in N} E_{glob}(G_i) \tag{2.2}$$

where G_i was the subnetwork consisted of all neighbor nodes of node i, and the global efficiency of subnetwork G_i is calculated using **Equation (2.1).**

The network overall strength was defined as the average of the normalized weights of the edges in the network, which was used to represent the overall connectivity of the network.

The nodal global efficiency of node i is a measure of its nodal communication capacity with all other nodes in the network, which was defined as

$$E_{nodal}(i) = \frac{1}{n-1} \sum_{j \in N, j \neq i} \frac{1}{d_{ij}} \tag{2.3}$$

nodal local efficiency of node i represents the robustness and integration of the subnetwork it belongs, which was defined as the global efficiency of the subnetwork consist of all the neighbors of i.

The nodal clustering coefficient describing the likelihood of whether the neighboring nodes of node i are interconnected with each other (Onnela et al., 2005). It was defined as

$$C(i) = \frac{1}{k_i(k_i-1)} \sum_{j,h \in N_i} (w_{ij} w_{ih} w_{jh})^{1/3} \tag{2.4}$$

where j, k were neighbors of node i, and k_i was the number of neighbors of node i.

In a communicative network, there are certain nodes that have strong connections with other nodes, and/or frequently appear in the shortest between-node paths. These critical nodes are called “network hubs”, which serve to connect multiple segregated subnetworks and facilitate the intermodular integrations (Rubinov and Sporns, 2010). In our study, nodal strength and betweenness-centrality (BC) were estimated to characterize the hub property of each node in a network. The strength of a node was defined as the sum of the weights of its edges; whereas the BC attempted to measure the ability for one node to bridge indirectly connected nodes (Freeman, 1978). BC was defined as

$$BC(i) = \frac{1}{(n-1)(n-2)} \sum_{j,k \in N, j \neq k} \frac{p(i \mid j,k)}{P(j,k)} \quad (2.5)$$

where j, k were node pairs in the network. $p(i \mid j,k)$ was whether the shortest path between node j and node k passes through node i. $P(j,k)$ was the total number of unique shortest path between node j and node k.

2.5 Machine Learning Techniques

The increasing interest of machine learning models in applying such models to investigate psychiatric disorders. Generally, machine learning models are mathematical models that learn complex patterns in an existing dataset. These learned patterns can then be used for prediction in a novel dataset (e.g. patient vs control participant, symptom scores), as well as to highlight the most important variables in creating this prediction. Models like support vector machine (SVM), random forests, and deep learning methods have proved effective in capturing the complex interactions between discrete alterations in schizophrenia, Alzheimer's disease, and autism spectrum disorder (ASD) (Arbabshirani et al., 2017; Quaak et al., 2021). Most psychiatric studies have developed models that can differentiate patient groups and controls using classification algorithms like SVM, random forest and linear discriminative analysis (LDA). Others predict symptom severity or behavioral performance using regression algorithms, for example, random forest regression, support vector regressor, and elastic net regression. The general steps involve splitting data into training set and validation set, feature selection, and model training, as shown in **Figure 2.2**. Then, the effectiveness of the classification models can then be evaluated using accuracy, specificity, sensitivity, or area-under-the-curve (AUC) and the performance of

the regression models can be evaluated by the mean square error or the correlation(Scheinost et al., 2019). Most machine learning studies have been able to differentiate patients with psychiatric disorders and controls with AUC from 60% to 90% (Quaak et al., 2021). For diagnostic purposes, models with AUC of less than 60% were considered as having bad performance while models with AUC of more than 80% were considered as having very good performance (Simundic, 2009).

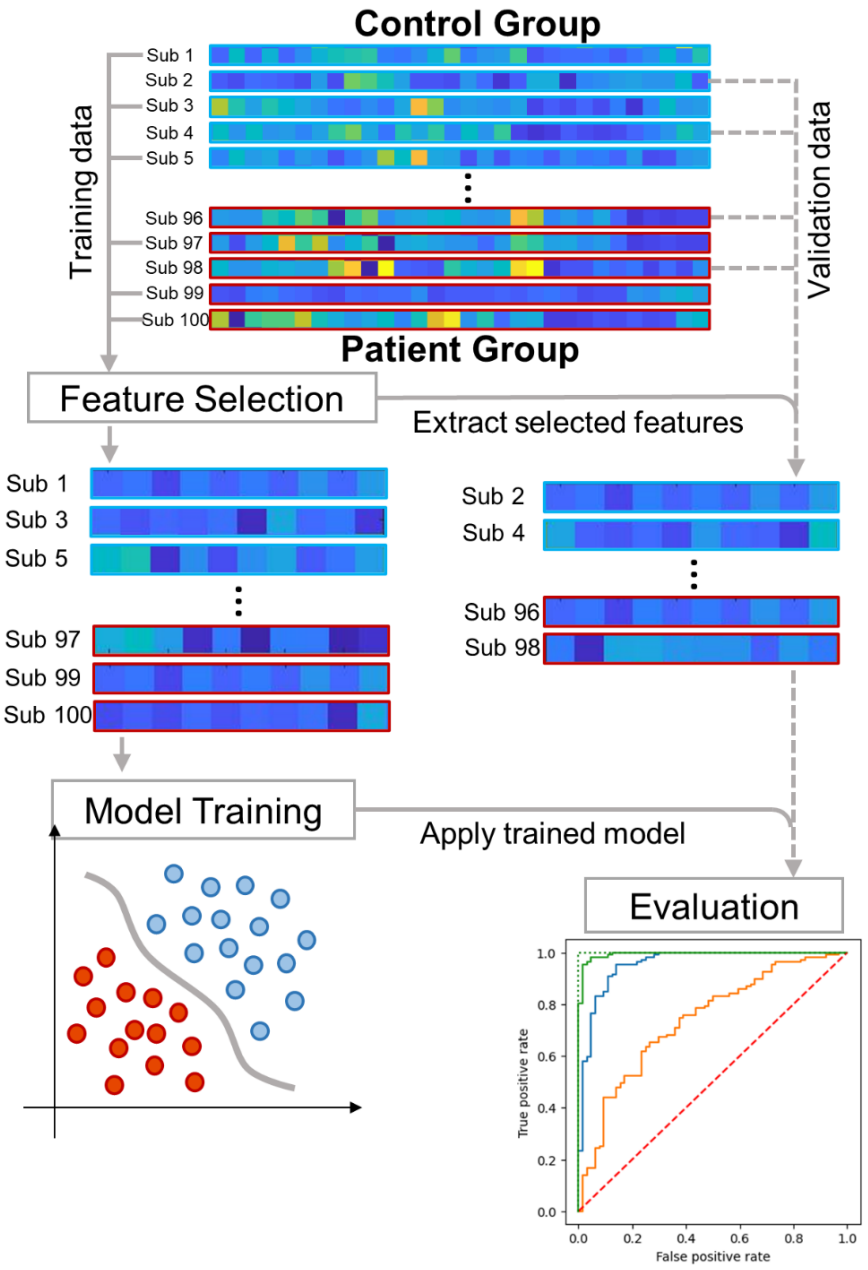

Figure 2.2 General steps for machine learning studies. Before processing, data are separated into training data and validation data. For psychiatric studies, the number of generated features is usually greater than the number of subjects. Therefore, feature selection methods are commonly implicated only in the training data to avoid over-fitting and information leakage from the validation data. Training data with the selected features are then used to train the machine learning model. After training, same features from the validation data are used to evaluation the model using accuracy or other metrics.

Even though machine learning can construct highly accurate classification models, the performance may not be consistent with new data. Therefore, cross-validation is required to avoid overfitting of a classification model. This phenomenon is especially common with data that have a larger number of features than the sample sizes. The cross-validation is used to minimize the effect of overfitting by validating the prediction model using different data distribution (Janssen et al., 2018). Cross-validation repeatedly validates the model by splitting the dataset into training set and testing set. As cross-validation can evaluate the generalizability of the trained model, it is often included as part of the training process to optimize the parameters for machine learning algorithms. A hierarchical cross-validation, nested cross-validation, is necessary to avoid overfitting of the overall training process.

The predictive value of each feature in a prediction model may vary, depending on the choices of classification algorithms, feature selection models, and validation methods. The lack of standardized procedure in determining the most informative features could lead to inconsistent and incomparable results across different study designs. Using robust features to train the classification model will increase generalizability, which indicates the performance of this model on new testing data. Combining multiple machine learning algorithms in one classification model can increase both accuracy and generalizability, which has been successfully employed in detecting patients with ADHD, Alzheimer's disease, and schizophrenia (Liu et al., 2012; Suk et al., 2017; Kalmady et al., 2019; Luo et al., 2020).

CHAPTER 3

TOPOLOGIAL ALTERATIONS OF STRUCTURAL BRAIN NETWORK IN CHILDREN WITH POST-TRAUMATIC BRAIN INJURY ATTENTION DEFICITS

3.1 Introduction

Pediatric traumatic brain injury (TBI) is a major public health concern, which occurs in more than 100,000 children each year and incurs an estimated annual medical cost of more than $1 billion (Watson et al., 2019). Neurocognitive impairments and behavioral abnormalities have been consistently observed in children with TBI (Konigs et al., 20Polinder et al., 2015; Dewan et al., 2016; Lumba-Brown et al., 2018). Among the most common cognitive consequences, significant attention deficits were reported in about 35% of children within two years of their TBI (Max et al., 2005), and were observed to strongly contribute to elevated risk for severe psychopathology and impairments in overall functioning in late adolescence, with the pathophysiological underpinning yet to be fully elucidated (Le Fur et al., 2019; Narad et al., 2019). The post-TBI attention problems in children have been evaluated and treated based on endorsements of behavioral symptoms from subjective observations and have resulted in largely divergent results regarding effectiveness (Backeljauw and Kurowski, 2014; Kurowski et al., 2019; LeBlond et al., 2019). Understanding the neurobiological substrates of post-TBI attention deficits in children is thus vitally critical, so that timely and tailored strategies can be developed for diagnoses and long-term treatments and interventions.

3.1.1 Anatomical alterations in children with traumatic brain injury

In literature of pediatric TBI, injury-induced regional structural brain alterations and associated cognitive and behavioral impairments have been increasingly reported. Structural MRI studies have investigated the relationship between cortical thickness and functional outcomes in children with chronic TBI, and found that the abnormal cortical gray matter (GM) thickness in frontal, parietal, and temporal regions were significantly associated with working memory impairments (Merkley et al., 2008) and executive dysfunctions (Wilde et al., 2012b). Existing diffusion tensor imaging (DTI) studies in children with TBI have also reported widespread white matter (WM) structural abnormalities and their linkage with post-TBI cognitive and behavioral impairments in the chronic stage.

For instance, a number of DTI studies have demonstrated that disrupted WM integrity in corpus collosum (Ewing-Cobbs et al., 2008; Wilde et al., 2011; Treble et al., 2013a; Lindsey et al., 2019), uncinate fasciculus (Lindsey et al., 2019), superior longitudinal fasciculus and inferior fronto-occipital fasciculus (Dennis et al., 2015) were significantly associated with working memory impairments in children with TBI. Lower fractional anisotropy (FA) in frontal regions (Wozniak et al., 2007a; Kurowski et al., 2009), superior longitudinal fasciculus and anterior corona radiata (Adamson et al., 2013), and ventral striatum (Faber et al., 2016) have been found to significantly link to post-TBI executive dysfunctions in children. Reduced FA in inferior longitudinal fasciculus, inferior fronto-occipital fasciculus, superior longitudinal fasciculus and corpus callosum were also found to be associated with impaired attention function (Konigs et al., 2018). The large inconsistency of these findings was partially resulted from factors of the study samples, such as heterogeneity regarding TBI-induced cognitive and behavioral impairments and

their severity levels, variations in terms of the biological and modifiable factors, differences in injury severity and mechanism, sample sizes, differences in imaging and data analysis techniques, etc. In addition, for understanding relations of the anatomical and cognitive/behavioral alterations in TBI, the region-of-interest (ROI)-based investigations of the injured human brain can be biased without considering the fact that human brain is formed as a structurally and functionally connected network for information-transferring.

3.1.2 Structural brain network analysis studies of traumatic brain injury

Indeed, human brain regions do not work in an isolated manner. When processing sensory and higher-order cognitive information, cortical and subcortical brain regions have been found to dynamically reassemble into small-world networks, to maintain optimal communication efficiency (Bassett et al., 2011; Spreng et al., 2013). Structural connectome, facilitated by WM structural connectivity, has been highlighted to play important role in supporting functional brain processes (Baum et al., 2017; Chu et al., 2018). A handful of studies involving adults with TBI have employed graph theoretical techniques to explore the structural network alterations and have reported inconsistent results. Some studies reported significant structural network segregation in adults with TBI, including increased shortest path length and decreased global efficiency when compared to controls (Caeyenberghs et al., 2014; Kim et al., 2014; Hellyer et al., 2015), while others reported no significant alterations in global network metrics (Caeyenberghs et al., 2013; Kuceyeski et al., 2019).

One study found that the reduction of structural network connectivity at chronic stage might be related to the severity of injury, where adult with severe TBI demonstrated significant lower network topological measures than adult with mild TBI and controls

(Raizman et al., 2020). A longitudinal study found that increased structural segregation was associated with better cognitive recovery within the patient group (Kuceyeski et al., 2019). The relationship between reduced structural network connectivity and cognitive impairment have also been observed in the group of professional fighters (Mishra et al., 2019). Relative to controls, adult TBI patients also demonstrated reduced structural connectivity in subnetworks that identified using network-based statistic (Mitra et al., 2016; Dall'Acqua et al., 2017).

In the context of pediatric TBI, structural brain network studies have found that children with TBI had altered global network properties. At acute and subacute stage, children with TBI were shown to have reduced global efficiency and increased clustering coefficient, characteristic path length, and modularity (Yuan et al., 2015; Yuan et al., 2017b; Watson et al., 2019). For children with chronic TBI, the structural networks were found to have increased characteristic path length and decreased local efficiency, suggesting a more segregated, instead of a normally more coordinated, architecture for information processing, when compared to matched controls (Caeyenberghs et al., 2012; Konigs et al., 2017; Yuan et al., 2017a). In addition, the reduced connectivity in the network was found to associate with deficits in postural control (Caeyenberghs et al., 2012), and decreased IQ and impaired working memory (Konigs et al., 2017) in TBI children. A longitudinal intervention study reported that improved overall cognitive performance after intervention was associated reduced network segregation in TBI children (Yuan et al., 2017a). A more recent study categorized the edges of the structural brain network into rich club (connections between different hubs), feeder (connections between hubs and other nodes), and local (connections between different non-hub nodes)

connections, and reported that children with TBI had significantly lower overall strength in rich club connections and higher overall strength in local connections; while none were associated with their significantly impaired executive function (Verhelst et al., 2018). Although increasing number of studies have started to focus their effort on understanding the relations of TBI-induced structural brain network alterations and cognitive/behavioral impairments (Imms et al., 2019), the neuroanatomical substrates of severe post-TBI attention deficits in children have not yet been fully investigated.

The current study proposed to utilize the probabilistic tractography in DTI and graph theoretical techniques to assess the structural connectome properties in a carefully evaluated cohort of children with severe post-TBI attention deficits and group-matched controls. In previous functional MRI studies, significant functional hyper-activations in frontal and parietal regions have been consistently observed in children with TBI, during sustained attention and inhibitory control processes (Kramer et al., 2008; Tlustos et al., 2011; Strazzer et al., 2015). Based on these findings, we hypothesized that altered regional structural network properties in frontal and parietal areas may exist in children with severe post-TBI attention deficits.

3.2 Materials and Methods

3.2.1 Participants

A total of 66 children, including 31 with severe post-TBI attention deficits (TBI-A) and 35 group-matched controls, were initially involved in this study. A subject in the TBI-A group must have had a clinically diagnosed mild or moderate non-penetrating TBI at least 6 months prior to the study date; and T score ≥ 65 in the inattention subscale (or T scores ≥ 65 in both inattention and hyperactivity subscales) in the Conners 3rd Edition-Parent Short

form (Conners 3-PS) (Conners, 2008) assessed during the study visit. Children with TBI who had overt focal brain damages or hemorrhages were excluded. To rule out confounding factors associated with pre-TBI attention deficits, children who had a history of diagnosed attention-deficit/hyperactivity disorder (ADHD) (any sub-presentations) prior the diagnosis of TBI, or severe pre-TBI inattentive and/or hyperactive behaviors that were reported by a parent, were excluded from the TBI-A group. The control group included children with no history of diagnosed TBI, no history of diagnosed ADHD, and T scores ≤ 60 in all of the subscales in the Conners 3-PS assessed during the study visit.

To further improve the homogeneity of the study sample, the general inclusion criteria for both groups included 1) only right-handed, to remove handedness-related potential effects on brain structures; 2) full scale IQ ≥ 80, to minimize neurobiological heterogeneities in the study sample; 3) ages of 11 – 15 years, to reduce neurodevelopment-introduced variations in brain structures. In the study, handedness was evaluated using the Edinburgh Handedness Inventory (Oldfield, 1971). Full scale IQ was estimated by the Wechsler Abbreviated Scale of Intelligence II (WASI-II) (Wechsler, 2011). The two groups were matched on sex (male/female) distribution and socioeconomic status (SES) that was estimated using the average education year of both parents.

The general exclusion criteria for both groups were 1) current or previous diagnosis of Autism Spectrum Disorders, Pervasive Development Disorder, psychotic, Major Mood Disorders (except dysthymia not under treatment), Post-Traumatic Stress Disorder, Obsessive-Compulsive Disorder, Conduct Disorder, Anxiety (except simple phobias), or substance use disorders, based on Diagnostic and Statistical Manual of Mental Disorders 5 (DSM-5) and supplemented by the Kiddie Schedule for Affective Disorders and

Schizophrenia for School-Age Children-Present and Lifetime Version (K-SADS-PL) (Kaufman et al., 2000); 2) any types of diagnosed chronic medical illnesses, neurological disorders, or learning disabilities, from the medical history; 3) treatment with long-acting stimulants or non-stimulant psychotropic medications within the past month; 4) any contraindications for MRI scanning, such as claustrophobia, tooth braces or other metal implants; 5) pre-puberty subjects were also excluded, to reduce confounders associated with different pubertal stages (Blakemore and Choudhury, 2006). Puberty status was evaluated using the parent version of Carskadon and Acebo's self-administered rating scale (Carskadon and Acebo, 1993).

After initial processing of the neuroimaging data from each subject, 3 subjects were excluded from further analyses, due to heavy head motion. Therefore, a total of 31 patients with TBI-A and 32 controls were included in group-level analyses.

The TBI-A subjects were recruited from the New Jersey Pediatric Neuroscience Institute (NJPNI), North Jersey Neurodevelopmental Center (NJNC), Children's Specialized Hospital (CSH), Brain Injury Alliance of New Jersey (BIANJ), and local communities in New Jersey. Controls were solicited from the local communities by advertisement in public places. The study received institutional review board approval at the New Jersey Institute of Technology (NJIT), Rutgers University, and Saint Peter's University Hospital. Prior the study, all the participants and their parents or guardians provided written informed assents and consents, respectively.

Severity of TBI was characterized using the Glasgow Coma Scale (GCS) (Teasdale and Jennett, 1974), with the scores ranging from 9 to 15 in the TBI-A subjects. Severities of the inattentive and hyperactive/impulsive symptoms were dimensionally measured

using the raw scores and T scores of the subscales in Conners 3-PS. The CogState brief battery for children (Eckner et al., 2011), which included 5 computerized tests, was administered to each subject. The normalized overall scores of the tests were used to evaluate neurocognitive capacities in executive function, psychomotor speed, visual attention, visual learning/memory and working memory.

All of the demographic, clinical, and neurocognitive performance measures were summarized in **Table 3.1**.

Table 3.1 Demographic, Clinical, and Neurocognitive Characteristics

	Controls Mean (SD)	**TBI-A Mean (SD)**	**t or χ^2 value**	***p* value**
N	35 (M:18, F:17)	31 (M:16, F:15)	0.0002	*0.988*
Age	13.83 (1.29)	14.13 (1.69)	-0.817	*0.417*
Ethnicity/Race			0.2418	*0.886*
Caucasian	25	23		
Hispanic	6	4		
Others	4	4		
Socio-Economic Status	32.00 (3.70)	31.16 (4.16)	0.872	*0.387*
Full Scale IQ	115.08 (11.27)	111.13 (12.59)	1.348	*0.183*
Inattention	45.97 (5.86)	70.52 (7.32)	-18.031	*< 0.001*
Hyperactivity/Impulsivity	48.31 (5.55)	62.00 (14.08)	-6.546	*< 0.001*
Groton Maze Learning Test	106.34 (4.76)	105.58 (4.71)	0.653	*0.516*
Detection	100.54 (6.02)	101.39 (4.96)	-0.617	*0.540*
Identification	102.17 (5.25)	100.39 (6.68)	1.213	*0.230*
One Card Learning	101.34 (7.36)	100.16 (7.53)	0.644	*0.522*
One Back (Speed)	92.63 (9.18)	93.58 (10.61)	-0.391	*0.697*
One Back (Accuracy)	101.77 (6.94)	104.55 (8.20)	-1.490	*0.141*

Cognitive performance was evaluated using CogState Brief Neurocognitive Testing Battery. TBI-A: TBI induced attention deficit; SD: Standard deviation; N: Number of subjects; M: Males; F: Females.

3.2.2 Preprocessing of structural magnetic resonance imaging data and diffusion tensor imaging data

DTI data pre-processing was performed using the Diffusion Toolbox from FMRIB Software Library v6.0 (FSL) (Jenkinson et al., 2012). Each DTI data (**Figure 3.1A** as an example) was first manually checked for any missing slides or heavy geometric distortions.

The head-motions and eddy-current distortion were then corrected with affine transformation and predictions estimated by a Gaussian Process (Andersson and Sotiropoulos, 2016). Heavy head movement is a critical issue that can significantly affect the quality of imaging data and cause inaccurate results of tractography. In the current study, the cutoffs of heavy head movements were defined as data with ≥ 2 mm translational displacement or ≥ 3° rotational displacement, with which data from 3 subjects were excluded from further analyses. Subjects involved in further analyses did not show significant between-group differences in the head movement measures (in mean translation ($t=0.623$, $p=0.536$), maximum translation ($t=0.638$, $p=0.526$), mean rotation ($t=0.941$, $p=0.350$), and maximum rotation ($t=0.847$, $p=0.400$).

Non-brain voxels were removed by performing brain extraction over the non-diffusion-weighted image (b0 image). The parameters for probabilistic tractography were estimated using the FSL/BedpostX toolbox (Behrens et al., 2007). This process estimated a 2-fiber model in each voxel based on the probability distribution generated by Markov Chain Monte Carlo sampling (**Figure 3.1B**).

In each subject, a total of 78 cortical and subcortical ROIs were generated from the T1-weighted data (**Figure 3.1C**) using the standardized brain atlas parcellation procedures from FreeSurfer v6.0.0 (Fischl, 2012). There ROIs (**Figure 3.1D**) included 68 cortical regions bilaterally, and 10 subcortical regions (bilateral putamen, caudate, hippocampus, thalamus, and pallidum). All of the ROIs in structural space were linearly registered into each individual's native diffusion space by referencing to the b0 image and binarized into ROI masks to serve as seed masks for tractography (**Figure 3.1E**).

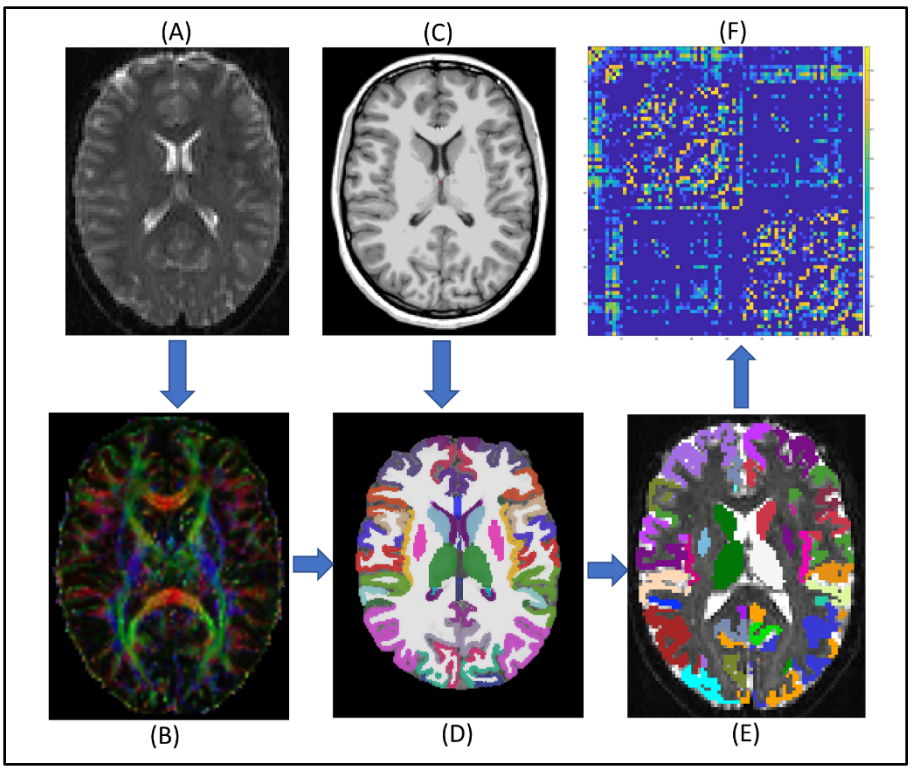

Figure 3.1 Individual level imaging data analysis and network construction. (A) DTI data; (B) Estimated tensor directions with 2-crossing fiber model; (C) T1-weighted structural MRI data; (D) Parcellated structural image based on Desikan-Killiany Atlas; (E) Seed masks in diffusion space, binarized and transformed from structural space; (F) Symmetric and weighted 78 × 78 connectivity matrix. The edges were calculated based on the number of fibers in tractography.

Finally, the DTI probabilistic fiber tracking was performed using a streamline tractography algorithm, FSL/PROBTRACKX2. To prevent the generated fibers from running into GM and cerebrospinal fluid, a WM mask was used for the probabilistic tractography. Five thousand streamlines per voxel were then initiated from each seed mask, with 0.5 step distance. A fiber was terminated when 1) it reached other seed masks; 2) it exceeded 2000 step limits; 3) it looped back to the same streamline; 4) its curvature exceeded 80 degree 5) it left the WM mask. Once all fibers terminated, fibers that reached one of the seed masks were retained and counted to determine the connectivity between ROIs.

3.2.3 Construction of structural brain network

To construct the structural brain network for each subject, the 78 cortical and subcortical ROIs were used as network nodes. A pair of nodes were considered to have no anatomical connectivity (i.e., no edge in the network), if fiber tracts from neither of the two nodes successfully reached to the other one, during the probabilistic tractography step. The weight of a non-zero edge was first evaluated by averaging the number of fibers on both directions. This raw value was then transformed using logarithm function and normalized by dividing the maximum edge weight in the same network (Rubinov and Sporns, 2011). In addition, a non-zero edge was further set as zero if at least 60% of the whole study sample had a zero weight on this edge (de Reus and van den Heuvel, 2013). This cutoff threshold was validated in previous studies for efficacy of controlling false positive and false negative rates of the generated connections (Misic et al., 2018; Verhelst et al., 2018; Bathelt et al., 2019). Then for each subject, the 78 × 78 symmetric connectivity matrix was generated for construction of the weighted structural brain (**Figure 3.1F**).

The global and regional topological properties of the structural brain network from each subject were then estimated, including the network global and local efficiencies, network overall strength, and nodal global efficiency, nodal local efficiency, and nodal clustering coefficient of each node. All network topological property were calculated using Brain Connectivity Toolbox (Rubinov and Sporns, 2010).

For each node in a WM structural brain network, its nodal global efficiency represents the integration of its associated WM structural subnetworks; whereas its nodal local efficiency and nodal clustering coefficient represent the modularity, and BC represents the connectivity of its associated WM subnetworks (Fagerholm et al., 2015; Jolly et al., 2020).

3.2.4 Group statistical analyses

Group statistics were carried out using SPSS 25 on macOS Mojave 10.14.1. Between-group comparisons in demographic, clinical, behavioral, and neurocognitive performance measures were conducted using chi-square test for categorical data (sex and ethics), and independent two sample t-test for numerical measures.

Group comparisons in the network topological measures were performed using a mixed-effects general linear model by setting TBI-A and controls as group variables, and adding IQ, age, SES as random-effect, and sex as fixed-effect covariates, respectively. In addition, the group-specific network hubs of each diagnostic group were examined using one-sample t test in the nodal strength and BC measures, respectively, with a threshold of 2 standard deviations higher than the group mean. Group comparisons in all of these network measures were controlled for potential multiple comparisons (in the total of 78 network nodes), using Bonferroni correction with a threshold of significance at corrected $\alpha \leq 0.05$ (Green and Diggle, 2007).

Brain-behavior relationships in the TBI-A group were assessed using Pearson correlation between the T scores of the inattentive and hyperactive/impulsive subscales from Conners 3-PS and the network measures that showed significant between-group differences. The correlation analyses were controlled for potential multiple comparisons (in the total number of comparisons), by using Bonferroni correction with a threshold of significance at corrected $\alpha \leq 0.05$.

3.3 Results

3.3.1 Clinical, behavioral, and demographic measures

As shown in **Table 3.1**, there were no significant between-group differences in the demographic and neurocognitive performance measures. Compared to the controls, the children with TBI-A showed significantly more inattentive ($p<0.001$) and hyperactive/impulsive ($p<0.001$) symptoms measured using the T scores in Conners 3-PS.

3.3.2 Topological properties of the structural brain network

The global network properties did not show significant between-group differences. Compared to controls, the TBI-A group showed significantly increased nodal local efficiency ($p=0.005$) and nodal clustering coefficient ($p<0.001$) in left inferior frontal gyrus; significantly increased BC ($p=0.037$) in left superior frontal gyrus; and significantly increased nodal local efficiency ($p=0.036$) and nodal clustering coefficient ($p=0.043$) in right transverse temporal gyrus. Meanwhile, relative to controls, the TBI-A group also demonstrated significantly decreased nodal local efficiency ($p=0.026$) in left parahippocampal gyrus; and greatly reduced nodal clustering coefficient ($p=0.017$) in left supramarginal gyrus (**Table 3.2**).

Table 3.2 Anatomical Regions That Showed Significant Between-group Differences in Nodal Topological Properties of the Structural Brain Network

Anatomical Region	**Measure**	**Controls** Mean (SD)	**TBI-A** Mean (SD)	**F value**	***p***
Left Inferior Frontal Gyrus	NLE	0.397 (0.041)	0.437 (0.042)	16.738	*0.005*
	NCC	0.326 (0.048)	0.376 (0.043)	20.879	*<0.001*
Right Transverse Temporal Gyrus	NLE	0.420 (0.064)	0.478 (0.062)	12.128	*0.036*
	NCC	0.412 (0.063)	0.471 (0.061)	11.736	*0.043*
Left Parahippocampal Gyrus	NLE	0.534 (0.058)	0.489 (0.042)	12.834	*0.026*
Left Supramarginal Gyrus	NCC	0.519 (0.050)	0.476 (0.045)	13.802	*0.017*
Left Superior Frontal Gyrus	BC	0.100 (0.032)	0.127 (0.030)	12.044	*0.037*

NLE: Nodal Local Efficiency; NCC: Nodal Clustering Coefficient; BC: Betweenness Centrality; TBI-A: TBI induced attention deficit; SD: Standard deviation.

In addition, distinct patterns of the within-group hub distribution were observed in the two diagnostic groups (**Figure 3.2**), with the precentral gyrus and putamen nucleus in the right hemisphere showing as hubs (measured by BC) in the TBI-A group but not in controls. Left precentral gyrus was identified as a hub in controls but not in the TBI-A group.

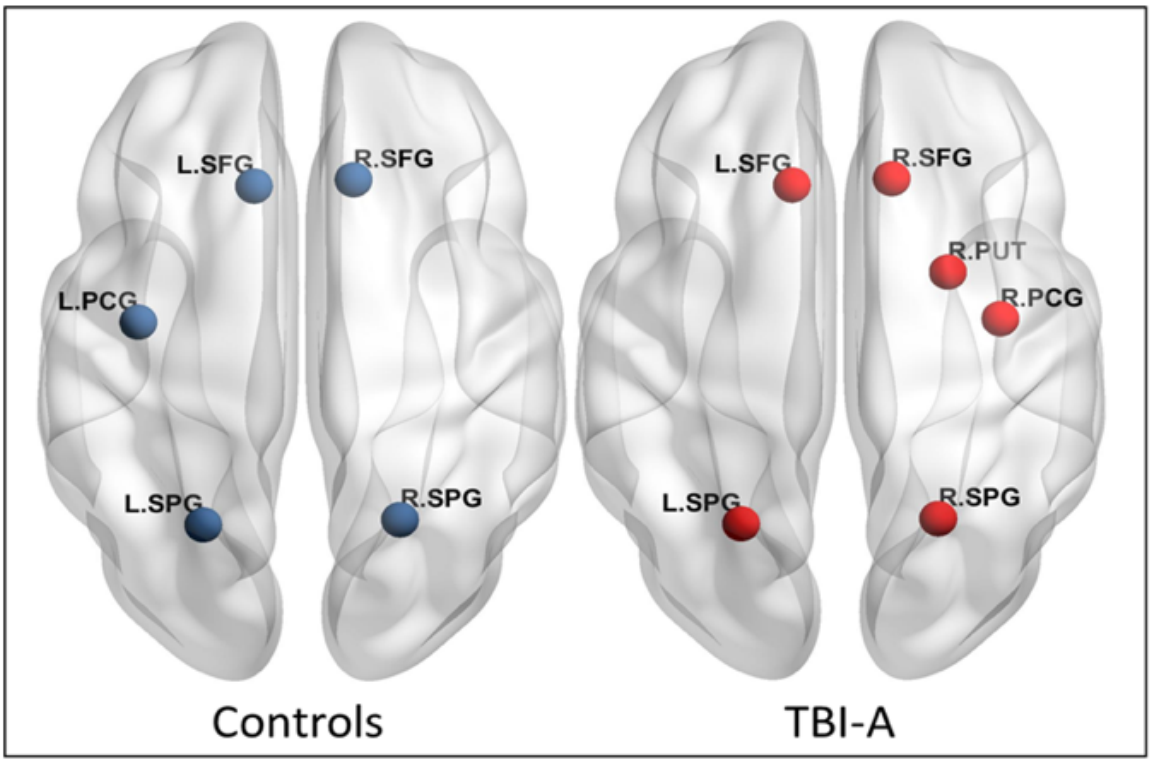

Figure 3.2 Network hubs identified using the betweenness-centrality measure in the groups of controls and TBI-A. TBI-A: TBI-induced attention deficits; SFG: Superior frontal gyrus; SPG: Superior parietal gyrus; PCG: Precentral gyrus; PUT: Putamen; L.: Left hemisphere; R.: Right hemisphere.

3.3.3 Brain-behavior correlations

In the TBI-A group, increased nodal local efficiency of left parahippocampal gyrus was significantly associated with increased inattentive (r=0.405, p=0.024) and hyperactive/impulsive (r=0.457, p=0.01) symptoms; while greater nodal clustering coefficient of right transverse temporal gyrus was strongly associated with decreased hyperactive/impulsive symptoms (r=-0.468, p=0.008) (**Figure 3.3**).

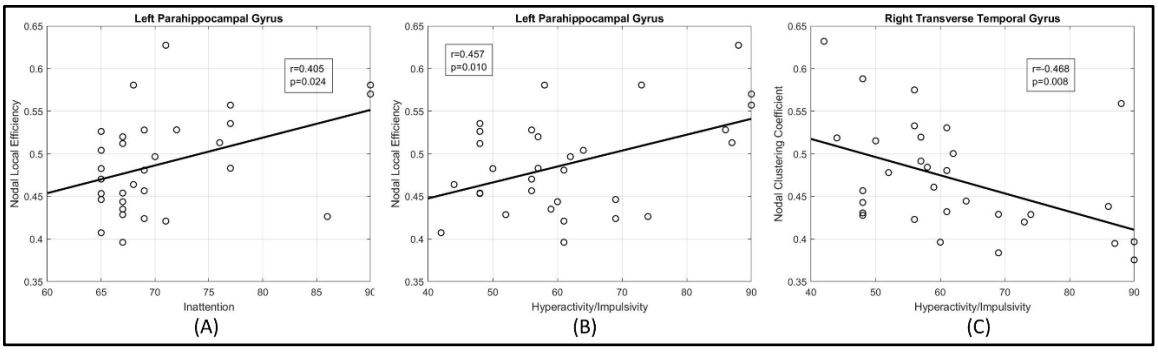

Figure 3.3 Regions that showed significant brain-behavior correlations in the TBI-A Group. The *p* values reported in the figure were after Bonferroni correction. (A) Correlation between hyperactive/impulsive symptoms severity score and nodal local efficiency of left parahippocampal gyrus. (B) Correlation between inattentive symptoms severity score and nodal local efficiency of left parahippocampal gyrus. (C) Correlation between hyperactive/impulsive symptoms severity score and nodal lustering coefficient of right transverse temporal gyrus.

3.4 Discussion

This aim depicted for the first time that aberrant regional topological properties of the WM structural brain network play critical role in severe post-TBI attention deficits in children. Specifically, we found that relative to the group-matched controls, children with TBI-A had significantly increased nodal local efficiency and nodal clustering coefficient in the left inferior frontal gyrus, as well as significantly higher BC in the left superior frontal gyrus. These results suggest significantly increased structural connectivity and modularity of the subnetworks associated with left inferior and superior frontal gyri in children with severe post-TBI attention deficits. Chronic tissue abnormalities in children with mild and moderate TBI have been found to be mainly resulted from diffuse axonal injury (DAI), due to the abrupt stretching, twisting, and shearing of axons in the event of a mechanical blow (Roberts et al., 2016). Frontal lobe, located class to the anterior fossa of the skull, is one of the most vulnerable brain regions to DAI (Bigler, 2007). Existing neuroimaging studies in children with chronic TBI have consistently demonstrated structural anomalies in frontal

cortex GM and the WM pathways connect it and other brain regions. For instance, multiple structural MRI and DTI studies have reported frontal GM volumetric reduction and cortical thinning (Wilde et al., 2012b; Bigler et al., 2013; Mayer et al., 2015b; Dennis et al., 2016), as well as disrupted frontal WM integrity, represented by reduced WM FA and increased apparent diffusion coefficient in children with chronic TBI relative to group-matched controls (Wozniak et al., 2007a; Wilde et al., 2011; Wilde et al., 2012a). Frontal tissue anomalies in children with TBI have also been found to link to long-term neurobehavioral impairments in domains such as executive control (Lipszyc et al., 2014) and learning and memory (Lindsey et al., 2019); whereas no evidence from previous quantitative clinical and neuroimaging studies have suggested strong correlations between frontal GM/WM tissue alterations and post-TBI attention deficits in children. Along with these existing studies, results from the current study suggest that abnormal structural connectivity and modularity of the subnetworks associated with frontal lobe may be caused by TBI-induced structural damages in frontal cortex and associated WM structures, while these regional topological alterations of the WM structural network might not necessarily play the key role in long-term and severe post-TBI attention deficits in the affected individuals.

Compared to controls, the TBI-A group demonstrated significantly reduced nodal clustering coefficient in left supramarginal gyrus. This result of reduced topological modularity of the structural subnetwork in parietal regions is consistent with findings from a previous structural network study using deterministic tractography (Caeyenberghs et al., 2012). In addition, several previous DTI studies in children with chronic TBI have consistently reported significantly decreased FA of the superior longitudinal fasciculus, which is a major association tract that connects parietal lobe with frontal lobe (Ewing-

Cobbs et al., 2016; Konigs et al., 2018; Molteni et al., 2019). An early structural MRI study reported significantly reduced cortical thickness of bilateral supramarginal gyri in children with chronic TBI children, relative to matched controls (Merkley et al., 2008); while a more recent longitudinal study reported significant correlation between greater volume of left supramarginal gyrus and worse overall cognitive performance (Dennis et al., 2016). Meanwhile, task-based functional MRI studies have demonstrated abnormal supramarginal gyrus activation in children with chronic TBI, when performing a motor task (Caeyenberghs et al., 2009) and a working memory task (Newsome et al., 2008). However, similar to the fact from investigations in frontal regions, no evidence has yet suggested strong linkage between parietal lobe GM/WM tissue alterations and post-TBI attention deficits in children.

Intriguingly, the current study found that relative to controls, the TBI-A group had significantly decreased nodal local efficiency in left parahippocampal gyrus and significantly increased nodal local efficiency and nodal clustering coefficient in right transverse temporal gyrus. Furthermore, nodal local efficiency in left parahippocampal gyrus showed significant positive correlations with the post-TBI inattentive and hyperactive symptoms, and nodal local efficiency in right transverse temporal gyrus showed significant negative correlations with the post-TBI hyperactive symptoms, in the group of TBI-A. These paradoxes may suggest compensatory or scaffolding mechanisms where reduced efficiency in left parahippocampal gyrus and increased efficiency in right transverse temporal gyrus both illustrate potential structural brain recovery from TBI-induced behavioral impairment in attention domain. Similar to the frontal lobe, temporal lobe is also among the most vulnerable brain regions for DAI, due to its anatomical location

as the close proximity to the bony structure of the middle fossa of the skull (Bigler, 2007). TBI-related cortical GM atrophy and disrupted WM integrity in temporal lobe have been reported in several studies in children with chronic TBI (Wilde et al., 2005; Caeyenberghs et al., 2012; Wilde et al., 2012a; Dennis et al., 2016; Diez et al., 2017). The transverse temporal gyrus, also call Heschl's gyrus, is the primary auditory cortex responsible for early processing related to speech understanding (Recanzone and Cohen, 2010; Arnott and Alain, 2011). It was also found to be part of the dorsal pathway in the bottom-up visual attention stream (Katsuki and Constantinidis, 2014), as well as subject to top-down influences of attention (Voisin et al., 2006). Parahippocampal gyrus belongs to the medial temporal system for visuospatial processing, which has intensive WM connections with frontal, parietal, occipital cortices, and midbrain structures. It was found to involve in selective attention during shifting and orienting processes through the ventral attention pathways (Corbetta and Shulman, 2002; Wager et al., 2004; Ochsner et al., 2012; Vossel et al., 2014). Both the transverse temporal and parahippocampal gyri are critical components in the multisensory integration system for attention processing (Cappe et al., 2009). These existing studies in cognitive neuroscience have provided strong scientific premise of our novel findings in the temporal lobe in children with TBI-A. Therefore, we suggest that TBI-related local re-modularity associated with the transverse temporal region, and structural segregation of the subnetworks connecting the parahippocampal gyrus with other brain regions, may have significant linkage with the onset of post-TBI inattentive and hyperactive/impulsive symptoms in children.

There are some limitations of the present study. First, the sample size is relatively modest. Compared to other existing studies with similar sample sizes, the effect size of our

study is larger, because of the inclusion criteria of the two diagnostic groups (the T-scores of inattentive and hyperactive subscales were ≥ 65 for TBI-A, while ≤60 for controls). The increased effect size can help improve statistical power of our study. Second, the study did not include a clinical control group of TBI children without clinically significant attention deficits. Therefore, the current study by itself could not testify whether the structural anomalies in the TBI-A group might also be seen in TBI patients more generally who do not have attention deficits. Nevertheless, the main findings of the current study reviewed in the above paragraphs, the structural alterations in left frontal, supramarginal, and parahippocampal gyri, have also been reported by other research groups to exist in TBI children without showing significant attention deficits (or studies without including post-TBI attention problems as inclusion/exclusion criteria). In addition, previous clinical studies have consistently reported that in children with TBI, 15% develop attention deficits 6 -12 months after the injury and 21% during the second year (Max et al., 2005), and more than 50% from one year up to ten years post-injury (Narad et al., 2018). However, we acknowledge that ADHD is a neurodevelopmental problem that can develop in this age range independently from any TBI episode. To minimize the number of potential primary ADHD subjects, we included detailed parent report to assess the pre-injury behavioral problems and have excluded subjects with uncertain responses and subjects with family history of ADHD. Considering the majority of ADHD onset is before age of 7 (Polanczyk et al., 2010), the number of potential primary ADHD in the TBI-A group is minimal. Third, sex-related topological differences of the structural brain network, and their interactions with the two diagnostic groups were not investigated, considering the sample size limitation of the study. Recently, several studies have reported effects of sex and SES on

the long-term cognitive and behavioral outcomes in children with TBI (Yeates et al., 2012; Anderson et al., 2013; Scholten et al., 2015; Wade et al., 2016). Additional analyses of our sample did not show any trends of significant correlations of the SES and time from injury with any clinical/behavioral measures in the TBI-A group. To partially remove the potential effects of these factors, we added sex as a fixed effect covariate, and SES as a random effect covariate, in the group-level analyses. Future work in a sample with a much larger size and a broader behavioral spectrum in terms of inattentiveness is expected to further elucidate how the results of the current study would provide new leads in structural brain network changes associated with TBI-A, and their interactions with the critical biological and social environmental factors. Finally, the DTI acquisition parameters were not optimal. The voxel size of our data was 2x2x2.5 mm^3. A previous study suggested that anisotropy in the z-plane may affect the estimation of FA values and fiber directions (Oouchi et al., 2007(Soares et al., 2013). In addition, the percentage of voxels that contain at least two crossing fibers was relatively low in this study when compared to a previous one (22% vs 63%) (Jeurissen et al., 2013). The reduced sensitivity in detecting the orientations of small fibers may be due to the relative low diffusion weighting (Jones et al., 2013). Since the major long-distance WM tracts are most vulnerable to TBI (Sharp et al., 2014) and both groups were applied with same settings, this limitation should not bias the group comparison.

3.5 Conclusion

In summary, aim 1 demonstrated significantly altered regional topological organizations of the WM brain network in frontal, parietal, and temporal regions, in a more homogeneous subgroup of children with chronic TBI who had severe post-TBI attention deficits. The

results further suggest that TBI-related WM structural re-modularity in the subnetworks associated with temporal lobe may significantly link to onset of severe post-TBI attention deficits in the affected children. These findings provide valuable implication for understanding the neurobiological substrates of TBI-A, and have the potential to serve as quantitatively measurable criteria guiding the development of more timely and tailored strategies for diagnoses and treatments to the affected individuals.

CHAPTER 4

ABNORMAL FUNCTIONAL NETWORK TOPOLOGY AND ITS DYNAMICS DURING SUSTAINED ATTENTION PROCESSING IN CHILDREN WITH POST-TRAUMATIC BRAIN INJURY ATTENTION DEFICITS

4.1 Introduction

Pediatric traumatic brain injury (TBI) is a significant public health issue, which occurs in more than 3 million children each year globally (Dewan et al., 2016; Hooper et al., 2004; Konigs et al., 2015; Polinder et al., 2015; Emery et al., 2016). Attention deficits are among the most common and persistent cognitive and behavioral consequences that can be observed in at least 35% of children within two years of their injuries (Max et al., 2005; Narad et al., 2018). Childhood post-TBI attention deficits (TBI-A) have been found to link with significantly heightened risk for development of severe psychopathology and impairments in overall functioning in late adolescence (Le Fur et al., 2019; Narad et al., 2019). The neural substrates associated with TBI-A in children have not yet been well investigated. Understanding the early brain mechanisms of TBI-A have considerable heuristic value for informing novel and timely strategies of prevention and intervention in affected individuals.

4.1.1 Task-based functional magnetic resonance imaging studies of traumatic brain injury in children

The blood-oxygen level dependent (BOLD) response-based functional MRI (fMRI) has been widely implemented to examine the neurophysiological alterations associated with TBI-related functional brain damages (Mayer et al., 2015a). The majority of task-based fMRI studies in TBI have used working memory paradigms and have reported abnormal functional activation in cortical and subcortical areas, such as the prefrontal cortex,

superior temporal gyrus, and hippocampus, which were associated with working memory impairments in subjects with TBI (Newsome et al., 2008; Kramer et al., 2009; Sinopoli et al., 2014; Westfall et al., 2015), while a recent study reported no significant working memory-related brain differences between children with TBI and controls (Brooks et al., 2020). Other fMRI studies have also reported functional alterations in frontal, parietal, temporal, and occipital regions in children with TBI during motor task (Caeyenberghs et al., 2009), language task (Karunanayaka et al., 2007), and social cognition task (Newsome et al., 2010). Only a few pediatric TBI studies have investigated brain activations during attention-related tasks (Kramer et al., 2008; Tlustos et al., 2011; Strazzer et al., 2015; Tlustos et al., 2015). Studies have reported that, during sustained attention processing, children with TBI demonstrated reduced activations in frontal, parietal, and occipital regions when compared to healthy controls (Strazzer et al., 2015) and children with orthopedic injuries (Kramer et al., 2008). Tlustos and colleagues reported that children with TBI, relative to controls, showed decreased activation in anterior cingulate and motor cortex during inhibitory control processing (Tlustos et al., 2015). Children with TBI also showed hyperactivations in middle frontal gyrus, precentral gyrus, and parietal lobule during interference control processing (Tlustos et al., 2011). The discrepancies of findings from the existing studies might be partially explained by the differences of task design, techniques implemented for data analyses, sample size, environmental factors, and subject-related biases without controlling the heterogeneity of neurocognitive/behavioral outcomes induced by TBI (Babikian et al., 2015).

4.1.2 Functional connectivity and functional brain network analysis studies of traumatic brain injury

Resting-state fMRI (rs-fMRI) studies in TBI have also reported inconsistent results. Relative to matched controls, children with chronic TBI have been found to have reduced functional connectivity (FC) between caudate and motor network (Stephens et al., 2017), increased FC between frontal and fusiform gyrus (Tuerk et al., 2020), or reduced FC between rostral anterior cingulate cortex and amygdala (Newsome et al., 2013). In addition, graph theoretical technique (GTT)-based rs-fMRI studies have reported systems-level topological alterations in adults with TBI, relative to controls (Caeyenberghs et al., 2017). For instance, studies have shown decreased functional network integration, including decreased network global efficiency and increased characteristic path length, in adult with TBI when compared to healthy controls (Nomura et al., 2010; Pandit et al., 2013; Han et al., 2016). A more recent longitudinal study reported that increased functional integrations were associated with better cognitive recovery in adults with TBI (Kuceyeski et al., 2019).

4.1.3 Dynamics analyses of the functional brain network

With the help of the advances in recent techniques and methodologies, dynamic FC patterns during both resting-state and cognitive processes have been increasingly observed and linked to neurobehavioral variations in normal controls and subjects with mental disorders (Braun et al., 2015; Hutchison and Morton, 2015; Kucyi et al., 2017; Gilbert et al., 2018). Relative to the procedure of constructing the functional network using overall time duration (referred to as static functional network), dynamic analysis evaluates the functional network topology at a temporal basis. Gilbert et al. reported that during a working memory and information processing task, adults with TBI demonstrated more brain states than controls but with less between-state transitions (Gilbert et al., 2018). A rs-

fMRI study found both static and dynamic alterations in adult with TBI at the acute stage, which were associated with persistent symptoms at chronic stage (Hou et al., 2019).

Indeed, the GTT- and dynamic FC-based investigations in functional brain networks during resting-state and cognitive tasks have allowed a new dimension in understanding the neural mechanisms associated with post-TBI neurocognitive and behavioral impairments in adults. However, the systems-level functional brain organizations, their temporal dynamics, and their associations with TBI-related cognitive/behavioral deficits have not yet been sufficiently revealed in children. The current study proposed to utilize the GTT- and dynamic FC-based techniques to study the topological properties and their dynamics of the functional network for attention processing, and their relations with TBI-related attention deficits in a homogeneous group of children with TBI-A and matched controls. Our previous research has showed disrupted structural network topological properties in frontal, parietal, and temporal regions in children with TBI-A (Cao et al., 2021b). Based on the existing findings from our and other groups, we hypothesize that relative to matched controls, children with TBI-A may exhibit significantly altered topological properties and their dynamic features in frontal, parietal, and temporal areas; and these systems-level anomalies in the functional network for attention processing strongly link to the severe attention problems in children with TBI-A.

4.2 Materials and Methods

4.2.1 Participants

A total of 89 children, including 42 children with TBI-A and 47 controls were involved in the study. The TBI-A subjects were recruited from the New Jersey Pediatric Neuroscience Institute, Saint Peter's University Hospital, and local communities in New Jersey. Controls

were solicited from the local communities by advertisement in public places. The study received institutional review board approval at the New Jersey Institute of Technology and Saint Peter's University Hospital. Prior the study, all the participants and their parents or guardians provided written informed assents and consents, respectively.

The inclusion criteria for the TBI-A group were: 1) history of clinically diagnosed mild-to-moderate non-penetrating TBI with the severity scores ranging from 9 to 15 using the Glasgow Coma Scale (GCS) (Teasdale and Jennett, 1974) and no overt focal brain damages or hemorrhages; 2) the first TBI incidence happened at least 6 month prior to the study; 3) T score ≥ 65 in inattention subscale, hyperactivity subscale, or both in the Conners 3rd Edition-Parent Short form (Conners 3-PS) (Conners, 2008) assessed during the study visit. In addition, subjects with a history of diagnosed attention-deficit/hyperactivity disorder (ADHD) (any sub-presentations) prior the diagnosis of TBI, or severe pre-TBI inattentive and/or hyperactive behaviors that were reported by a parent, were not included, to minimize confounding factors. The control group included children with 1) no history of TBI; 2) no history of diagnosed ADHD (any sub-presentation); 3) T-scores ≤ 60 in all the subscales in the Conners 3-PS assessed during the study visit. The two groups were matched on age, sex (male/female) distribution, and socioeconomic status (SES) (estimated using the average education year of both parents).

To further improve the homogeneity of the study sample, the general inclusion criteria for both groups included 1) only right-handed, to remove handedness-related potential effects on brain structures; 2) full scale IQ ≥ 80, to minimize neurobiological heterogeneities in the study sample; 3) ages of 11 – 15 years, to reduce neurodevelopment-introduced variations in brain structures. In the current study, handedness was evaluated

using the Edinburgh Handedness Inventory (Oldfield, 1971). Full scale IQ was estimated by the Wechsler Abbreviated Scale of Intelligence II (WASI-II) (Wechsler, 2011). None of the subjects involved in this study had 1) current or previous diagnosis of Autism Spectrum Disorders, Pervasive Development Disorder, psychotic, Major Mood Disorders (except dysthymia not under treatment), Post-Traumatic Stress Disorder, Obsessive-Compulsive Disorder, Conduct Disorder, Anxiety (except simple phobias), or substance use disorders, based on Diagnostic and Statistical Manual of Mental Disorders 5 (DSM-5) and supplemented by the Kiddie Schedule for Affective Disorders and Schizophrenia for School-Age Children-Present and Lifetime Version (K-SADS-PL) (Kaufman et al., 2000); 2) any types of diagnosed chronic medical illnesses, neurological disorders, or learning disabilities, from the medical history; 3) treatment with long-acting stimulants or non-stimulant psychotropic medications within the past month; 4) any contraindications for MRI scanning, such as claustrophobia, tooth braces or other metal implants. In addition, pre-puberty subjects were also excluded to reduce confounders associated with different pubertal stages (Blakemore and Choudhury, 2006). Puberty status was evaluated using the parent version of Carskadon and Acebo's self-administered rating scale (Carskadon and Acebo, 1993). After initial processing of the neuroimaging data from each subject, 3 subjects were excluded from further analyses, due to heavy head motion. Therefore, a total of 40 patients with TBI-A and 46 controls were included in group-level analyses. All the demographic and clinical measures were summarized in **Table 4.1**.

Table 4.1 Demographic and Clinical Characteristics of the Study Sample

	Controls Mean (SD)	**TBI-A** Mean (SD)	**t or χ^2 value**	***p* value**
N	46	40		
Male/Female	26/20	24/16	0.106 (χ^2)	*0.744*
Socioeconomic Status	16.19 (1.80)	15.57 (4.19)	1.450	*0.151*
Full Scale IQ	115.00 (10.60)	110.48 (12.68)	1.802	*0.075*
Age	13.24 (1.47)	13.27 (1.72)	-0.075	*0.940*
Ethnicity/Race			2.411 (χ^2)	*0.300*
Caucasian	27	29		
Hispanic	8	3		
Others	11	8		
Inattention	46.67 (6.22)	71.75 (8.09)	-16.366	*< 0.001*
Hyperactivity/Impulsivity	47.91 (5.68)	63.50 (14.23)	-6.835	*< 0.001*

Socioeconomic status was estimated using the average education year of both parents. The Inattention and Hyperactivity/impulsivity were T-scores of Conner 3-PS. TBI-A: children with traumatic brain injury related attention deficits; SD: standard deviation; N: number of subjects; Conners 3-PS: Conners 3rd Edition-Parent Short Form T-score.

4.2.2 Visual sustained attention task for functional magnetic resonance imaging

Clinical studies have suggested that sustained attention in children is vulnerable to the TBI-induced damages (Wassenberg et al., 2004; Ornstein et al., 2014). Continuous performance task (CPT) is one of the most widely used task to measure sustained attention and was shown to be a robust instrument to challenge the sustained attention in children with TBI (Ginstfeldt and Emanuelson, 2010). In the current study, all subjects were asked to perform an enhanced CPT, the Visual Sustained Attention Task (VAST), during fMRI data

acquisition. The VAST is a block-designed task that was established and validated in our previous functional imaging studies for achieving optimal power in maintaining sustained attention and assessing related functional brain pathways in children (Li et al., 2012; Xia et al., 2014; Wu et al., 2018b). The task contains 5 task stimulation blocks that interleaved with 5 resting blocks, as shown in **Figure 4.1A**. Each block lasts 30 seconds, with a total scan time of 5 minutes. Within each task stimulation block, a sequence of 3 single digit numbers was first shown in red to serve as the target, followed by 9 stimulus sequences in black, when subjects were asked to response if each sequence matches the target. Subjects were instructed to stay focused and respond only after the third number of each sequence was shown. To ensure full understanding of the instructions, practical trials of the task were provided to each subject before the scan session.

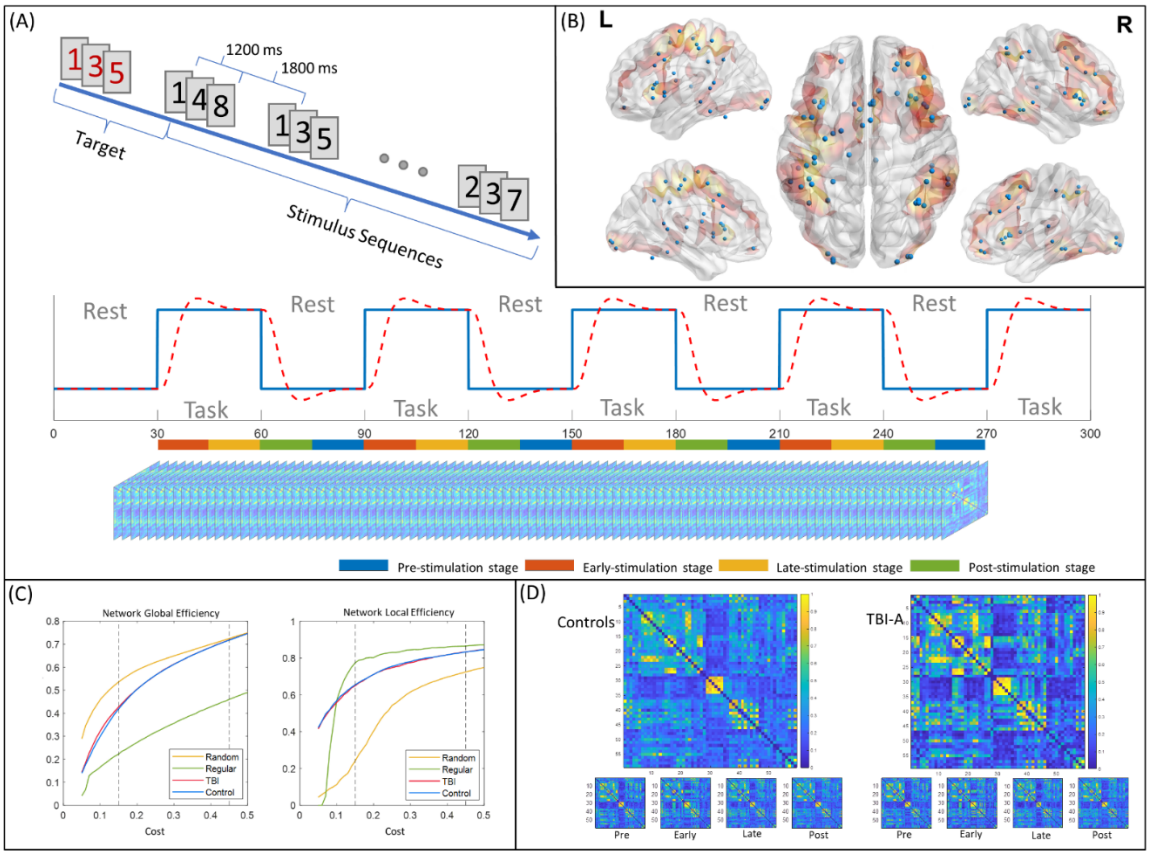

Figure 4.1 Functional network construction steps. (A) Block design and sub-stage definitions. (B) Selected nodes for functional network construction; (C) The network global and local efficiency curves of TBI-A and controls over the cost range of 0.05 to 0.5; (D) The group connectivity matrices of controls and TBI-A. L: left hemisphere; R: right hemisphere; TBI-A: children with severe post-traumatic brain injury attention deficits; Pre: pre-stimulation stage; Early: early-stimulation stage; Late: late-stimulation stage; Post: post-stimulation stage.

4.2.3 Preprocessing and individual-level analysis of functional magnetic resonance imaging data

Pre-processing of each fMRI data was carried out using the FEAT Toolbox from FMRIB Software Library v6.0 (FSL) (Woolrich et al., 2001). The data was first manually checked for any missing volumes and heavy head motions. Then the motion artifacts were corrected using rigid-body transformation by registering all volumes to the first volume. The motions for each subject were measured by extracting the six translational and rotational

displacement parameters. Due to the critical impacts of the head motions on the construction of both static and dynamic functional networks (Power et al., 2012; Satterthwaite et al., 2012), we applied strict cutoff threshold of 1.5 mm. Three subjects (2 TBI-A subjects and 1 control) were excluded due to heavy head motion. After corrected for slice timing, fMRI data of each subject was then smoothed with a 5-mm full-width at half maximum gaussian kernel to improve the signal-to-noise ratio. A high-pass filter was applied to the time series to remove the low frequency noise and signal drifting. Finally, the fMRI data was co-registered to a MNI152 template, with a voxel size of 2 mm × 2 mm × 2 mm, using each subject's T1-weighted structural image. Hemodynamic response to task-related condition was modeled using the general linear model, with 24 motion parameters, including the 6 basic displacement parameters (Rt), and the derivatives (Rt') and squares (Rt2 and Rt-12, where t and t-1 refer to current and preceding timepoints) of these parameters, and nuisance signals (white matter, cortical spinal fluid, and global signal), as additional regressors. The Z statistic images were thresholded using clusters determined by $Z>2.3$ and a cluster-based method for multiple comparison correction at $p<0.05$ (Woolrich et al., 2001).

4.2.4 Construction of functional brain network

To construct the overall functional brain network responding to the sustained attention processing task, pairwise Pearson's correlation coefficients of the BOLD signals in the 59 network nodes were first calculated to form the 59 x 59 FC matrix. The matrix was then binarized by thresholding using the network cost, which was defined as the fraction of existing edges relative to all possible edges within a network. To determine the proper threshold range for functional network construction, the network global efficiency and

network local efficiency were calculated over the cost range from 0.1 to 0.5. The network global efficiency is a metric of the network integration that reflects the ability of information transferring across distributed brain areas (Latora and Marchiori, 2001). It was defined as the average of the inversed shortest distance between each node pair in the network. The network local efficiency estimates the network segregation and represents the fault tolerance level of the network (Latora and Marchiori, 2001). The network local efficiency is the average nodal local efficiency of all nodes in the network, where the nodal local efficiency was defined as the network global efficiency of the subnetwork that consisted of all neighbor nodes of that specific node. Then both global metrics of the constructed network were compared with the node- and degree-matched regular and random networks. A network is considered to be small-world if both measures fall in between the measure of regular and random networks. (Achard and Bullmore, 2007). The proper cost range for functional network construction in both TBI-A and control groups was from 0.15 to 0.45, as shown in **Figure 4.1C**.

The global and regional topological properties of the overall functional brain network from each subject were then calculated and averaged over the cost range, including the network/nodal global efficiency, network/nodal local efficiency, network/nodal clustering coefficient, nodal degree, and betweenness centrality. clustering coefficient describing the likelihood of whether the neighboring nodes of node are interconnected with each other (Onnela et al., 2005), indirectly connected nodes by counting the number of shortest paths that pass through a certain node's nodal local efficiency and nodal clustering coefficient represent the modularity (Fagerholm et al., 2015; Jolly et al., 2020). All network topological property calculation were performed using Brain Connectivity Toolbox

(Rubinov and Sporns, 2010). Since the methods for calculations of these properties have been well established, we won't repeat the details here.

4.2.5 Analysis of functional network dynamics

A sliding-window approach was used to investigate the functional network dynamics during the task procedure. A temporal window was defined to include 17 consecutive volumes in the fMRI data. Therefore, a total of 284 temporal windows were generated, with a sliding-step of 1 TR applied along the 300 TRs during the entire task period. For each of the 284 temporal windows, a 59 x 59 FC matrix was formed by the pairwise Pearson's correlation coefficients of the 59 network nodes each contained only 17 time points within that temporal window.

Based on the task design, the task duration consisted of pre-, early-, late-, and post-stimulation stages (**Figure 4.1A**). The pre-stimulation stage was defined as the 15 seconds (15 TRs) right before each task-stimulation block. The early-stimulation stage was defined as the first 15 TRs of each task-stimulation block, and the late-stimulation stage was defined as the last 15 TRs of each task-stimulation block. The post-stimulation stage was defined as the 15 TRs after each task-stimulation block. Based on the estimated hemodynamic response function, the early-stimulation stage corresponds to the recruiting response stage while the late-stimulation stage corresponds to the stable response stage, also shown in **Figure 4.1A**. During the network dynamics analyses introduced in the following paragraphs, the temporal window-based FC matrices of the early- and late-stimulation stages were extracted from only the first four task-stimulation blocks, to match the involved duration of the pre- and post-stimulation stages.

A temporal window-based functional network for each sliding step was constructed

using the same strategy for static network construction introduced in Section 2.6. The thresholding for network topological property estimations in this step utilized the Pearson's correlation coefficients ranging from 0.55 to 0.85, which corresponded to the top 45% to top 15% strongest FCs among the 284 FC matrices. The network topological properties, including global efficiency, local efficiency, and clustering coefficient at both network and nodal levels, plus degree and betweenness centrality at nodal level, were then calculated for the functional network in each temporal window. The mean and the standard deviation values of each network property were calculated among the temporal networks involved in each of the four task-stimulation stages. The standard deviation characterizes the stability of the network property, which was defined as:

$$S = \sqrt{\frac{1}{N-1}\sum_{i=1}^{N}|A_i - \mu|^2}, \tag{4.1}$$

where N is the number of steps in a stage, A_i is the specific topological property at step i, and μ is the mean of the topological property over all steps in a stage.

4.2.6 Group statistical analyses

Group statistics were carried out using R 4.0.3 on macOS Mojave 10.14.1. Between-group comparisons in demographic, clinical, behavioral, and neurocognitive performance measures were conducted using chi-square test for categorical data (sex and ethics), and independent two sample t-test for numerical measures.

Group comparisons in the static network topological properties were performed using a mixed-effects general linear model by setting TBI-A and controls as group variables, and adding IQ, age, SES as random-effect, and sex as fixed-effect covariates,

respectively. Group comparisons in the static network topological properties were controlled for potential multiple comparisons, using Bonferroni correction with a threshold of significance at corrected $\alpha \leq 0.05$ (Green and Diggle, 2007).

To test the group difference in sub-stages and the transition between each adjacent stage-pair, a mixed-model analysis of covariance (ANCOVA) with topological properties at adjacent stages as repeated measure, sex as fixed-effect covariate, and IQ, age, SES as random-effect covariates. Topological properties that showed significant group effects or significant group-stage interaction (corrected using false discovery rate) were selected for post-hoc analysis. Group comparison of the selected measures were performed using independent-sample t-tests as the post-hoc analysis. Post-hoc analysis were controlled for potential multiple comparisons (in the total of 4 stages), using Bonferroni correction with a threshold of significance at corrected $\alpha \leq 0.05$ (Green and Diggle, 2007).

Brain-behavior associations in the TBI-A group were assessed using Pearson correlation between the T-scores of the inattentive and hyperactive/impulsive subscales from Conners 3-PS and the network measures that showed significant between-group differences. The correlation analyses were controlled for potential multiple comparisons (in the total number of comparisons), by using Bonferroni correction with a threshold of significance at corrected $\alpha \leq 0.05$.

4.3 Results

4.3.1 Clinical, behavioral, and demographic measures

No demographic information was found to have significant group difference. In addition, children with TBI-A did not demonstrate any significant differences in the performance measures of VSAT when compared with controls. Relative to the controls, the children

with TBI-A showed significantly more inattentive (t=-16.366, p<0.001) and hyperactive/impulsive (t=-6.835, p<0.001) symptoms measured using the T scores in Conners 3-PS. The demographic information was shown in **Table 4.1**.

4.3.2 Topological properties of the overall functional brain network

Compared to controls, children with TBI-A showed significantly decreased nodal clustering coefficient in left precentral gyrus (F=7.649, p-$_{Bonferroni}$=0.035), and significantly decreased nodal local efficiency (F=20.626, p-$_{Bonferroni}$<0.001) and nodal clustering coefficient (F=18.804, p-$_{Bonferroni}$<0.001) in left postcentral gyrus. No significant between-group differences were observed in topological measures at global level.

4.3.3 Dynamics of the functional topological properties

The network topological properties at each stage were calculated using the average network properties of all steps within each stage. Relative to controls, the TBI-A group showed significantly decreased nodal local efficiency (t=2.560, p-$_{Bonferroni}$=0.049) in left postcentral gyrus at early-stimulation stage (**Figure 4.2A**); significantly decreased nodal local efficiency (t=2.798, p-$_{Bonferroni}$=0.026) and nodal degree (t=2.603, p-$_{Bonferroni}$=0.044) in left inferior parietal lobule at early-stimulation stage (**Figure 4.2B**); significantly decreased nodal local efficiency (t=2.870, p-$_{Bonferroni}$=0.021) and nodal clustering coefficient (t=2.750, p-$_{Bonferroni}$=0.029) in left inferior temporal gyrus at late-stimulation stage (**Figure 4.2C**); and significantly increased nodal global efficiency (t=-2.702, p-$_{Bonferroni}$=0.033) in right putamen at late-stimulation stage (**Figure 4.2D**).

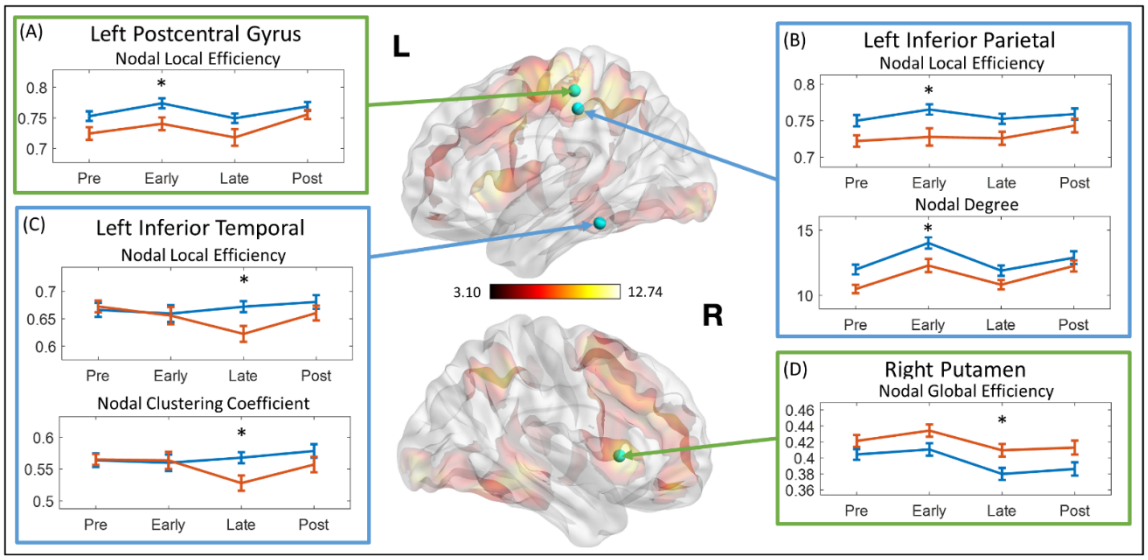

Figure 4.2 Mean network topological properties at different stages. The topological properties that showed significant group difference were marked with asterisk. L: left hemisphere; R: right hemisphere; Pre: pre-stimulation stage; Early: early-stimulation stage; Late: late-stimulation stage; Post: post-stimulation stage.

The stability of each network topological property at each stage was represented by the standard deviation within each stage. Relative to controls, children with TBI-A demonstrated significantly increased standard deviation of network global efficiency at the late-stimulation stage (t=2.519, p-$_{\text{Bonferroni}}$=0.048) (**Figure 4.3A**). At the late-stimulation stage, the TBI-A group also showed significantly decreased standard deviations of the right insula nodal local efficiency (t=3.206, p-$_{\text{Bonferroni}}$=0.007) and nodal clustering coefficient (t=3.052, p-$_{\text{Bonferroni}}$=0.012) (**Figure 4.3B**); significantly increased standard deviations of the left fusiform gyrus nodal local efficiency (t=-2.707, p-$_{\text{Bonferroni}}$=0.033) and nodal clustering coefficient (t=-2.732, p-$_{\text{Bonferroni}}$=0.031) (**Figure 4.3C**); and significantly increased standard deviation of left inferior temporal gyrus nodal local efficiency (t=-3.174, p-$_{\text{Bonferroni}}$=0.008) (**Figure 4.3D**).

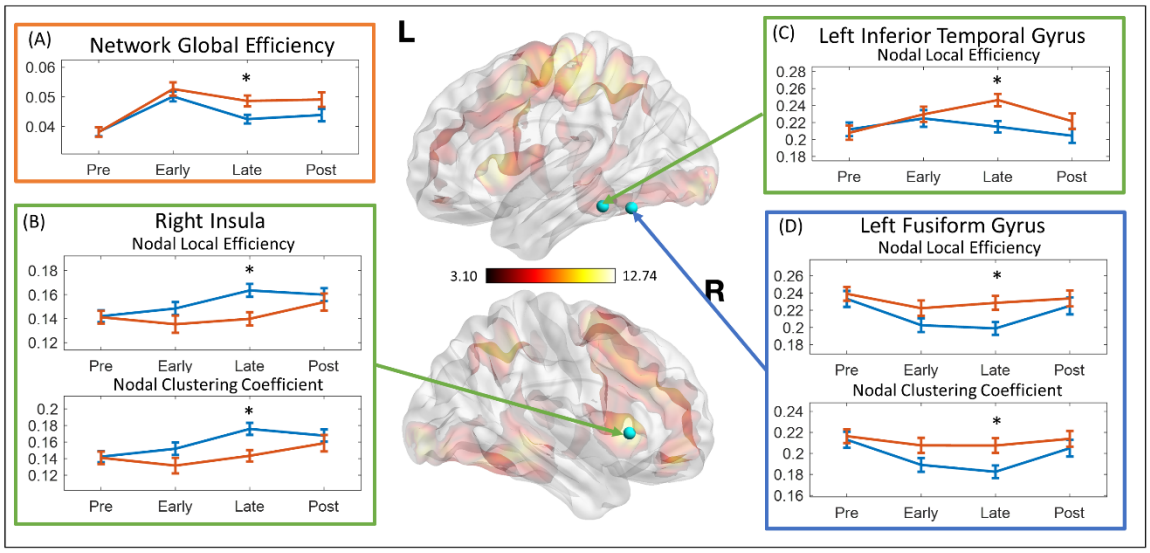

Figure 4.3 Standard deviation of network topological properties at different stages. The topological properties that showed significant group difference were marked with asterisk (*). (A) Standard deviation of the network global efficiency. (B) Standard deviation of the nodal local efficiency and the nodal clustering coefficient at right insula. (C) Standard deviation of the nodal local efficiency at left inferior temporal gyrus. (D) Standard deviation of the nodal local efficiency and the nodal clustering coefficient at left fusiform gyrus. L: left hemisphere; R: right hemisphere; Pre: pre-stimulation stage; Early: early stimulation stage; Late: late-stimulation stage; Post: post-stimulation stage

4.3.4 Brain-behavior correlations

As shown in **Figure 4.4,** higher T-score of the inattention subscale in the Conners 3-PS were significantly correlated with lower nodal global efficiency in left postcentral gyrus ($r=-0.460$, $p\text{-}_{Bonferroni}=0.015$) and lower nodal degree in left inferior parietal lobule ($r=-0.443$, $p\text{-}_{Bonferroni}=0.020$) in children with TBI-A at the early-stimulation stage. No significant brain-behavior correlations were found in the group of controls.

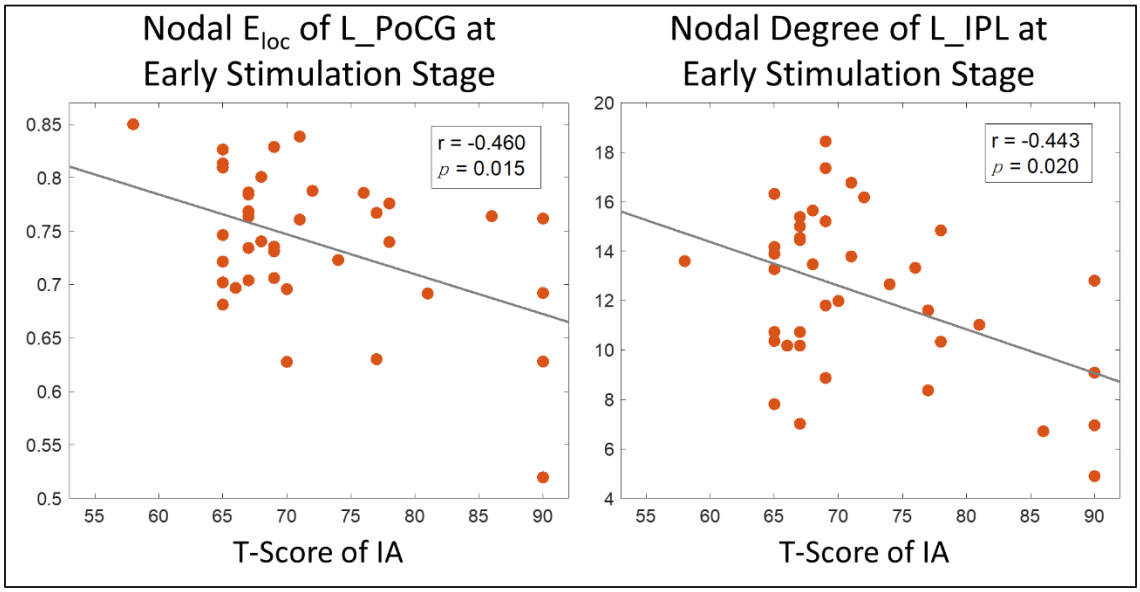

Figure 4.4 Brain-behavior correlation analysis results. Eloc: local efficiency; L_PoCG: left postcentral gyrus; IA: inattention; L_IPL: left inferior parietal lobule.

4.4 Discussion

In this aim, we found that relative to matched controls, the left precentral gyrus in children with TBI-A showed significantly lower capacity for functional information transferring (represented by significantly lower nodal clustering coefficient) during sustained attention processing. Precentral gyrus, as the location of the primary motor cortex, has been proven to significantly involve in response inhibition function (Li et al., 2006). Previous fMRI studies in pediatric TBI have found significantly decreased precentral activation in children with TBI during performance of sustained attention (Kramer et al., 2008), inhibitory control (Tlustos et al., 2015), and language processing (Karunanayaka et al., 2007). Clinical studies have also suggested that children with TBI is vulnerable to deficits in inhibitory control (Levin et al., 2004; Levin et al., 2008), and children with post-TBI attention deficits have even more severe impairments than children with normal outcomes

after TBI (Konrad et al., 2000).

Meanwhile, the left parietal cortex, particularly the left postcentral and inferior parietal gyri, showed significantly suboptimal regional efficiency for functional communications with other brain regions during sustained attention processing, especially at the early-stimulation stage; and these systems-level functional anomalies associated with the left parietal cortex were found to greatly link to the severe inattentive symptoms in children with TBI-A. The parietal cortex is a key component of the attention network, involving in both the bottom-up selection and top-down control processes (Buschman and Miller, 2007; Katsuki and Constantinidis, 2014). Within the attention network, the postcentral gyrus is responsible for transferring tactile information during the spatial attention (Macaluso et al., 2000), while the inferior parietal gyrus for information integration in the frontoparietal pathways during cognitive control (Vincent et al., 2008). Functional brain alterations associated with parietal cortex have been frequently reported in previous studies in children with TBI when performing task of attention (Kramer et al., 2008; Tlustos et al., 2015), interference control (Tlustos et al., 2011), working memory (Kramer et al., 2009; Westfall et al., 2015), and motor control (Caeyenberghs et al., 2009).

Indeed, both frontal and parietal lobes are core components subserving attention processing and cognitive control in human brain. There has been growing consensus that dynamic disruptions of the frontal and parietal systems play the central role in chronical post-TBI neurocognitive and behavioral impairment, especially in the attention and cognitive control domains (Venkatesan and Hillary, 2019). Together with the existing findings, results of the present study further suggest that the suboptimal efficiency of left parietal regions for functional interactions with other brain areas, especially during the

initiation stage of attention processing, significantly implicate the TBI-A-specific impairment of the attention network, which can together contribute to severe behavioral inattentiveness and hyperactivity/impulsivity in children with TBI.

Compared to the control group, our study also found that at the late-stimulation stage, the left fusiform gyrus in children with TBI-A had significantly decreased stability for maintaining the efficiency of functional interactions with other brain regions. Fusiform gyrus is part of the temporal and occipital lobes, which has been found to be a key structure for high-order visual (such as face, body and high special frequency objects) and imagery processing (Haxby et al., 2001; Grill-Spector and Weiner, 2014). Functional brain activation and connectivity studies in children with TBI have also reported fusiform gyrus-related abnormalities, such as reduced activations during sustained attention processing (Strazzer et al., 2015), significantly increased activation during working memory processing (Kramer et al., 2009), and altered functional connectivity between fusiform gyrus and frontal lobe during resting state (Tuerk et al., 2020). On the other hand, studies have demonstrated significant involvement of the fusiform gyrus in severe psychopathology, especially psychosocial and emotional dysregulation and thought problems in patients with Major Depression Disorder (Ho et al., 2016; Wang et al., 2017), Schizophrenia (Lee et al., 2002; Silverstein et al., 2010), and other mental disorders (Strakowski et al., 2004; Perlman et al., 2013). psychosis (Molloy et al., 2011; Fujii and Ahmed, 2014; Rabner et al., 2016), On the basis of these prior studies from our and other groups, we hypothesize that post-TBI functional alterations associated with the left fusiform gyrus may significantly link to the development of severe late adolescence psychopathology, such as anxious/depressed, social and thought problems, in those with

childhood TBI-A. Longitudinal follow-up of children with TBI-A will help to test this hypothesis.

There are several limitations associated with the current study. First, the sample size is relatively modest, which can limit the statistic power of the proposed analyses. Compared with other existing studies with similar sample sizes, the effect size of our study is relatively larger, because of the inclusion criteria of the two diagnostic groups (the T-scores of inattentive and hyperactive subscales were ≥65 for TBI-A, whereas ≤60 for controls). The increased effect size can help improve statistical power of our study. Future research with a larger sample size is expected to further validate the results. Second, due to the nature of the sliding window approach, functional dynamics analysis is highly sensitive to head motions. Therefore, we had taken extra precaution during the setup before each scan and applied restrictive cut-off threshold of 1.5 mm to minimize potential errors caused by head motions. In addition, factors such as injury severity, number of injuries, and time interval between injury and study visit may introduce confounders of the results. Nevertheless, our supplementary analyses showed that the detected functional alterations did not show significant correlations with injury severity, number of injuries and time intervals.

4.5 Conclusion

In summary, aim 2 reported significant alterations of the topological properties of the sustained attention processing network and their temporal dynamics in children with severe post-TBI attention deficits, especially in the temporal and parietal regions. And these systems-level functional alterations were significantly linked with the elevated inattentive behaviors in the group of TBI-A. These findings provide valuable insight into the

neurobiological and neurophysiological substrates associated with the onset of post-TBI attention deficits in children. This study also provided positive evidence that analysis of functional network dynamics can demonstrate the temporal instability of the functional brain pathways characteristics of TBI-related attention deficits in children.

CHAPTER 5

MULTIMODAL NEUROIMAGING-BASED PREDICTION OF ATTENTION DEFICITS IN CHILDREN WITH TRAUMATIC BRAIN INJURY

5.1 Introduction

5.1.1 Neuroimaging evidence of attention deficits in children with traumatic brain Injury

In the past two decades, a number of clinical and neuroimaging studies have tried to investigate the neuroanatomical and functional substrates associated with TBI-related attention problems in children. Several diffusion tensor imaging (DTI) studies reported that the white matter integrity in corpus collosum, superior longitudinal fasciculus, and inferior fronto-occipital fasciculus were linked with impaired attention function in children with chronic TBI (Wozniak et al., 2007a; Kurowski et al., 2009; Dennis et al., 2015; Konigs et al., 2018). Task-based functional magnetic resonance imaging (fMRI) studies have also reported functional alterations in frontal, parietal, and occipital regions during inhibition and sustained attention process (Kramer et al., 2008; Tlustos et al., 2011; Strazzer et al., 2015; Tlustos et al., 2015).

Known as a foundation of neuroscience, human brain regions do not work in an isolated manner. The existing voxel- and region-of-interest (ROI)-based studies have limitations in addressing how, in the systems-level, certain brain regions are vulnerable to TBI and contribute to related cognitive and behavioral consequences. The graph theoretical technique (GTT)-based approaches have been increasingly implemented in human brain imaging data to construct structural and/or functional brain networks in a systems-level, and to characterize the network integration, segregation, centrality, and small-worldness in both the global and regional (sub-network) scales (Bullmore and Sporns, 2009). Studies

have reported that children with TBI demonstrated a less integrated structural or functional brain network compared to healthy controls (Caeyenberghs et al., 2012; Konigs et al., 2017; Yuan et al., 2017a; Botchway et al., 2022; Ware et al., 2022). Our recent GTT-based studies in both DTI and task-based fMRI data reported that, compared to group-matched typically developing children (TDC), children with diagnosed TBI-related attention deficits (TBI-A) had significant regional topological alterations associated with frontal, parietal, and temporal lobes in both structural and functional networks, with the altered regional topological properties associated with parietal and temporal regions significantly linking to elevated inattentive symptoms in children with TBI-A (Cao et al., 2021a; Cao et al., 2021b). These existing studies suggest that TBI-related attention deficits in children have close relationships with systems-level functional and structural abnormalities associated with multiple brain regions. However, all these studies have adopted conventional parametric models (such as t-test, analysis of variance, etc.) for group comparisons, which have very limited capacities to deal with the large-scale and nonlinearly related neuroimaging measures.

5.1.2 Machine learning studies of traumatic brain injury

Compared to conventional parametrical models, machine learning techniques have the capacity in learning the joint effects of measures in high dimensional space and have the sensitivity in detecting subtle information that have high discriminative/predictive power (Nielsen et al., 2020). When aided with feature selection methods and cross-validation methods, machine learning techniques can deliver efficient and robust classifications between different groups. A few existing studies in children with TBI have applied machine learning techniques. By constructing classification model using support vector

machine (SVM) and edge density image, one study was able to differentiate 14 children with TBI and 10 controls with an area under the receiver-operating-characteristic-curve (AUC) of 0.94 (Raji et al., 2020). Another study built an SVM-based classification model using structural MRI data and DTI data from 29 student athletes (aged from 15 to 20 years) and 27 controls and achieved an AUC of 0.84 (Tamez-Pena et al., 2021). A longitudinal study reported that when combining resting-state MRI data and structural MRI data in 99 children with TBI at 4 weeks after the injury, SVM algorithm was able to predict the recovery of post-concussion symptoms at 8 weeks with an AUC of 0.86 (Iyer et al., 2019). However, the majority of these machine learning studies in children with TBI applied supervised models that only focused on discriminating labels of the two diagnostic groups, and none of these studies have intended to detect the neurobiological features associated with the most common TBI-related cognitive deficits.

In this aim, we propose to utilize a deep learning technique, semi-supervised autoencoder, to identify the robust functional and structural brain signatures of TBI-related attention deficits in children. Deep learning techniques were highly effective in generating feature representations by learning the deep linear or nonlinear relationships within a high dimensional space of the study measures (LeCun et al., 2015). Based on results of previous study from our and other teams (Wozniak et al., 2007a; Kramer et al., 2008; Kurowski et al., 2009; Tlustos et al., 2011; Dennis et al., 2015; Strazzer et al., 2015; Tlustos et al., 2015; Konigs et al., 2018; Cao et al., 2021a; Cao et al., 2021b), we hypothesize that topological anomalies associated with frontal, parietal, and temporal regions in the functional and structural brain networks not only play the most important role in characterizing children with TBI when compared to controls, but also most significantly contribute to TBI-related

attention deficits in the affected children.

5.2 Materials and Methods

5.2.1 Participants

A total of 110 children, including 55 children with TBI and 55 group-matched controls, were initially involved in this study. The TBI subjects were recruited from the New Jersey Pediatric Neuroscience Institute, Saint Peter's University Hospital, and local communities in New Jersey. Controls were solicited from the local communities by advertisement in public places. The study received institutional review board approval at the New Jersey Institute of Technology and Saint Peter's University Hospital. Prior the study, all the participants and their parents or guardians provided written informed assent and consent, respectively.

The inclusion criteria for the TBI group were: (1) has history of at least one clinical diagnosed mild or moderate non-penetrating TBI (Teasdale and Jennett, 1974); (2) has no overt focal brain damages or hemorrhages during all the TBI incidences; (3) the first TBI incidence was at least 6 months prior to the study date; (4) has no significant inattention or hyperactive problems before the injury. The control group included children with no history of diagnosed TBI or no history of diagnosed attention deficit/hyperactivity disorder (ADHD). Conners 3rd Edition-Parent Short form (Conners 3-PS) were assessed during the study visit to characterize the inattention problems and hyperactivity/impulsivity problems in both groups (Conners, 2008).

To further improve the homogeneity of the study sample, the general inclusion criteria for both groups included (1) only right-handed, to remove handedness-related potential effects on brain structures, which the handedness were evaluated using the

Edinburgh Handedness Inventory (Oldfield, 1971); (2) full scale IQ ≥ 80, which were estimated by the Wechsler Abbreviated Scale of Intelligence II (WASI-II) (Wechsler, 2011); (3) has no current or previous diagnosis of Autism spectrum disorders, pervasive development disorder, psychosis, major mood disorders (except dysthymia not under treatment), post-traumatic stress disorder, obsessive compulsive disorder, conduct disorder, anxiety (except simple phobias), or substance use disorders, based on Diagnostic and Statistical Manual of Mental Disorders 5 (DSM-5) and supplemented by the Kiddie Schedule for Affective Disorders and Schizophrenia for School-Age Children-Present and Lifetime Version (K-SADS-PL) (Kaufman et al., 2000); (4) has no learning disabilities, neurological disorders, or any types of diagnosed chronic medical illnesses, from the medical history. None of the subjects involved in this study had any treatments with long-acting stimulants or non-stimulant psycho-tropic medications within the past month nor any contraindications for MRI scanning, such as claustrophobia, tooth braces, or other metal implants.

After initial processing of the neuroimaging data from each subject, 3 subjects from the TBI group and 2 subjects from the control group were excluded due to low imaging quality or excessive motions in either DTI data or functional MRI data. Therefore, a total of 52 children with TBI and 53 controls were included in the group-level analyses. All the demographic information was shown in **Table 5.1**.

Table 5.1. Demographic and Clinical Characteristics in the Study Sample.

	Controls Mean (SD)	**TBI Mean (SD)**	**t or χ^2 value**	***p* value**
N	55	55		
Male/female	30/25	33/22	0.334 (χ^2)	*0.563*
Socio-economic status	16.47 (2.13)	15.70 (2.09)	1.450	*0.151*
Full scale IQ	113.00 (11.23)	110.97 (13.72)	1.402	*0.165*
Age	13.06 (2.03)	13.63 (2.28)	-1.370	*0.174*
Ethnicity/race				*0.119*
Caucasian	30	36		
Hispanic	8	11		
Others	17	8	4.259 (χ^2)	
Conners 3rd edition-parent short form (T-score)				
Inattention	46.15 (6.02)	64.73 (13.49)	-9.145	*< 0.001*
Hyperactivity/impulsivity	48.38 (5.42)	58.44 (14.43)	-4.747	*< 0.001*

TBI: Children with traumatic brain injury; SD: Standard deviation; N: Number of subjects; M: Males; F: Females.

5.2.2 Individual level structural magnetic resonance imaging and diffusion tensor imaging data processing and structural brain feature generation

Each individual's structural MRI data was visually checked for artifacts and excessive motions. Then the preprocessing steps, including registration into Talairach space, skull-stripping, and intensity normalization, were performed using Freesurfer v6.0.0 (Fischl, 2012). The preprocessed structural MRI data were parcellated using Desikan atlas and were used for node generation in constructing the structural brain network.

To construct the structural network, the DTI data were preprocessed using the

Diffusion Toolbox from FMRIB Software Library v6.0 (FSL) (Woolrich et al., 2001). The preprocessing steps included head-motions correction, non-brain voxels removal, and intensities normalization. The head motions and eddy-current distortion were then corrected with affine transformation and predictions estimated by a Gaussian Process (Andersson and Sotiropoulos, 2016). Heavy head movement is a critical issue that can significantly affect the quality of imaging data and cause inaccurate results of tractography. In this study, the cutoffs of heavy head movements were defined as data with > 2mm translational displacement, > 5° rotational displacement, or > 0.2 mm mean volume-by-volume displacement. Three subjects from TBI group and 1 subject from control group were excluded due to heavy head motion. Then, the probabilistic tractography parameters of each voxel were estimated with a two-fiber model in each individual's native space. For each subject, a total of 78 ROIs were selected as the nodes for structural brain network, including 34 cortical regions and 5 subcortical regions per hemisphere. The mask for each ROI was generated based on the parcellation in the preprocessed structural MRI data and transformed into the native diffusion space. Probabilistic tractography were used to estimate the connecting fibers between each pair of the seed masks. Five thousand streamlines per voxel were then initiated from each seed mask, with 0.5 step distance. A fiber was terminated when (1) it reached other seed masks; (2) it exceeded 2000 step limits; (3) it looped back to the same streamline; or (4) its curvature exceeded 80. The streamlines between seed masks were averaged in both directions to determine the structural connectivity between network nodes. Due to the connection density bias, the white matter bundle with higher anisotropy usually generate significantly higher streamline counts in the probabilistic tractography process (Jones, 2010; Zhang et al., 2022). Therefore, in this

study, the weight of a non-zero edge was evaluated by log-transformed streamline count and normalized by dividing the maximum edge weight in the same network to increase the discriminability of low edge weights (Ashourvan et al., 2019; Hansen et al., 2022). Then for each subject, a 78 × 78 symmetric connectivity matrix was generated for construction of the weighted structural brain network.

After the weighted structural brain network was constructed for each subject, the network topological properties were calculated (technical details for computations were provided in our previous publications (Cao et al., 2021b)). The nodal-level topological properties for weighted network, including the nodal strength, nodal global efficiency, nodal local efficiency, clustering coefficient, and betweenness centrality, were calculated for each node in the structural brain networks to serve as structural brain features. All structural network topological properties were calculated using the Brain Connectivity Toolbox (Rubinov and Sporns, 2010). A total of 390 structural brain features were generated for building the semi-supervised autoencoder.

5.2.3 Individual level functional magnetic resonance imaging data processing and functional brain feature generation

The preprocessing of the fMRI data was carried out using FEAT Toolbox from FSL v6.0 (Woolrich et al., 2001). For fMRI data, the same cutoffs of heavy head motions that used in DTI preprocessing were applied, with which 2 subjects from TBI group (overlapped with excluded subjects in DTI preprocessing) and 1 subject from control group were excluded. After motion correction and slice timing correction, the fMRI data of each subject was co-registered to standard Montreal Neurological Institute (MNI) space using high-resolution structural MRI. The hemodynamic response to the task-related condition was modeled using the general linear model with 24 motion parameters. The activated

voxels were identified by cluster-based thresholding on the Z statistic map with $Z > 2.3$ and $p < 0.05$. To construct the functional brain network for each subject, the network nodes were generated by defining a spherical region with a radius of 5 mm at the local maximum of any clusters that have more than 100 activated voxels. A total of 59 ROIs were generated based on the automatic anatomical labeling atlas (Tzourio-Mazoyer et al., 2002). The connectivity of a ROI-pair was represented by the Pearson's correlation coefficient of the blood-oxygen-level-dependent (BOLD) signal in each of the two ROIs. The connectivity matrix was then binarized using the network cost range that satisfied small-network property to construct the binarized functional brain network (Achard and Bullmore, 2007). The nodal-level topological properties for binarized network, including the nodal degree, nodal global efficiency, nodal local efficiency, clustering coefficient, and betweenness centrality, were calculated for each node in the functional brain networks (technical details for computations were provided in our previous publications (Cao et al., 2021a)). The individual-level analysis was performed using pipeline tool GAT-FD (Cao et al., 2022), where all network topological properties were calculated by calling functions from the Brain Connectivity Toolbox (Rubinov and Sporns, 2010). A total of 295 nodal topological properties were calculated from the functional brain networks to serve as the functional brain features of each subject for building the semi-supervised autoencoder.

5.2.4 Modeling of semi-supervised autoencoder

To increase training robustness and reduce overfitting risk, combination of 3 approaches, including two-sample t-test, mutual information-based method (Ross, 2014), and Lasso-based method (Muthukrishnan and Rohini, 2016), were utilized for feature reduction. At the end, a total of 60 top features from the 685 source brain features derived from structural

and functional brain networks were selected for training in the model. Before passing to the autoencoder model, all these features were normalized to a range of 0 to 1 using min-max normalization.

The semi-supervised autoencoder consisted of 3 major components, the encoder, the decoder, and the classifier, as shown in **Figure 5.1**. The encoder and decoder were part of a regular autoencoder model, which learns a compressed representation of the original brain features by optimizing the reconstructed brain features in an unsupervised manner (Hinton and Salakhutdinov, 2006). The encoder transformed inputs from original feature space into a latent space by compressing the information in the inputs. The encoder in the proposed model contained one input layer with a size of 60, one hidden layer of 40 neurons, and one output layer of 20 neurons. Then the autoencoder-generated features, i.e., AE-features, in the latent space were passed into the decoder to reconstruct the original input. The decoder included an input layer with a size of 20, a hidden layer of 40 neurons, and one output layer of 60 neurons. An additional classifier was included in the proposed autoencoder to work as a constrain in the learning of the compressed AE-features in the latent space. The classifier took 20 AE-features in the latent space to predict the group label for each sample. The classifier included a hidden layer with 20 neurons and an output layer of 1 neuron. Sigmoid function was used as the activation function for all the artificial neurons in the semi-supervised autoencoder neural network.

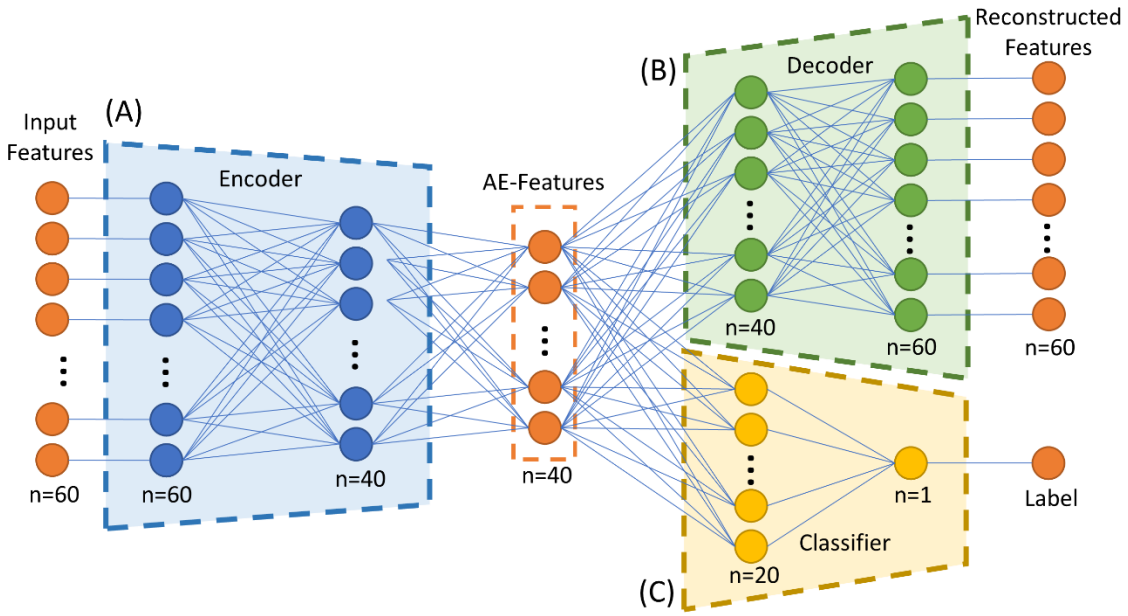

Figure 5.1 Overall structure of the semi-supervised autoencoder. (A) The encoder model, which transform the inputs from original brain feature space into a latent space. (B) The decoder model, which reconstruct the input by transforming the encoded features. (C) The classifier model, which predict if a subject is in the TBI group or in the control group based on the encoded features. AE-Features: autoencoder-generated features.

Two different loss functions were used compensate the different training speeds of the regression task (the decoder) and the classification task (the classifier). Mean squared error (MSE) was selected as the loss function of the reconstruction process, which was calculated using the following formula,

$$MSE = \frac{1}{n}\sum_{i=1}^{n}\left[\frac{1}{f}\sum_{j=1}^{f}\left(x'_{ij} - x_{ij}\right)^2\right] \tag{5.1}$$

where n is the number of subjects in the training data, f is the number of brain features, x'_{ij} is the reconstructed value for feature j of subject i, and $x_{ij}$is original value for feature

j of subject i. Binary cross-entropy were selected as the loss function of the classification process, which was calculated using the following formula,

$$H_{binary} = -\frac{1}{n}\sum_{i=1}^{n}[y \log p + (1-y)\log(1-p)] \quad (5.2)$$

where H_{binary} is binary cross-entropy, n is the number of subjects in the training data, y is the binary indicator of the class label, and p is probability of y is 1.

In order to force the model to learn the latent AE-features for reconstruction earlier than for classification, loss of the decoder model was assigned with a higher weight than the loss of the classifier model. The loss function of the full model was calculated using the following formula,

$$L_{full-model} = 0.7 \times MSE + 0.3 \times H_{binary} \quad (5.3)$$

where the weight of the decoder loss is 0.7 and the weight of the classifier loss is 0.3.

5.2.5 Model training and evaluation

Training of the model was performed using python v3.8.0 and Tensorflow v2.10 (Abadi et al., 2016). Adam optimizer was used for the back-propagation process (Kingma and Ba, 2014). To increase the robustness of the model, a 5-fold cross validation were employed in the training process. For details, the data were split into five stratified folds such that each fold consisted of balanced 20% of the entire data. For each iteration, four folds were dedicated for training data and the remaining one for validation. To avoid potential leakage

effect in the training process, the feature selection algorithms only used training data in each cross validation (Pereira et al., 2009). To further minimize the risk of overfitting in the training process, a gaussian noise with a mean of zero and standard deviation of 0.02 was randomly induced to 20% of the input features, before feeding into the encoder model. The training process stops when the accuracy of the training data exceeds 95% or reach a total of 1000 epochs.

The performance of the reconstruction process of the semi-supervised autoencoder model were measured using the MSE of the validation data and averaged for all the five cross validations. The classification performance was measured in terms of classification accuracy and AUC in the validation data, which also averaged for all five cross validations. In comparison, a conventional machine learning model was also constructed using the same training and validation procedure. The model used principal component analysis (PCA) for feature reduction and SVM for classification.

5.2.6 Feature importance

To identify the most important brain features for successful classification process, a permutation-based method was used to calculate the importance score of each input feature (Breiman, 2001). A feature's importance was determined by the amount of error caused by shuffling the feature's value over all the samples (Fisher et al., 2019). For the classification process, the feature importance for a feature was characterized by the binary cross-entropy, which was calculated using the following formula,

$$FI_{class} = \frac{1}{m}\sum_{k=1}^{m}\left(H_{binary} - H'_{binary}\right)^2 \tag{5.4}$$

where m is the number of random shuffling, H_{binary} is the cross-entropy of the original input, and H'_{binary} is the cross-entropy of the shuffled input. The importance score for features in the current study was calculated by shuffling for 1000 times. Features with importance score that 2 standard deviation higher than the mean importance score of all features were identified as important features (Sun et al., 2020).

5.2.7 Modeling of brain-behavior relationships

Regression-based machine learning, a support vector regression (SVR) model, was first constructed to study the relations between the most important brain features for successful group discriminations and the severity measures of inattentive and hyperactive/impulsive symptoms (T-scores derived from Conners 3-PS) in the whole study sample. To minimize overfitting, 5-fold cross validation were used for training and validation. The R^2 and MSE were used to evaluate the performance of the SVR model. Permutation importance score were used to evaluate the importance of the brain features.

To further validate the robustness of the relationships between the identified important brain features and clinical measures, a partial least squares structural equation modeling (PLS-SEM) was conducted (Hair et al., 2011). The rationale of the PLS-SEM was to test whether the important brain features for classification were associated with any AE-features, and whether those AE-features were associated with the clinical measures, while accounting for the effects of age, sex, handedness, SES, and IQ. The PLS-SEM analysis was carried out using R 4.1.3 and SEMinR 2.3.2 (Hair Jr et al., 2021). First, Pearson's correlation between the AE-features in the latent space and T-scores of the inattentive and hyperactive/impulsive subscales from Conners 3-PS were performed within

the whole study sample. The correlation analyses were controlled for potential multiple comparisons (for 20 features in the latent space), by using the Bonferroni correction with a threshold of significance at corrected $\alpha \leq 0.05$. The AE-features in the latent space that showed significant correlation with the clinical scores were selected as the intermediate variables in the PLS-SEM. Bootstrap with 5000 random samples were performed to determine the significant levels of the path coefficients in the PLS-SEM analysis (Henseler and Chin, 2010).

5.3 Results

5.3.1 Clinical, behavioral, and demographic measures

There were no significant between-group differences in any demographic measures in our sample. Among the subjects in TBI group, 14 subjects had no significant inattentive or hyperactive problems, 27 had significant inattentive problems, 2 had significant hyperactive/impulsive problems, and 12 had significant problems in both inattention and hyperactivity/impulsivity. In the TBI group, the range between first TBI incidence and MRI scan was from 6 months to 90 months (7 years 6 months), with average of 33.8 months ± 24.2 months. The results showed that children with TBI had significantly more inattentive ($t = -9.145$, $p < 0.001$) and hyperactive/impulsive ($t = -4.747$, $p < 0.001$) symptoms measured using the T-scores in Conners 3-PS, when compared to controls. No significant correlations were observed between the time after injury and inattention or hyperactivity/impulsivity T-scores. The demographic and clinical information was shown in **Table 5.1**.

5.3.2 Performance of semi-supervised autoencoder

The semi-supervised autoencoder model was able to differentiate children with TBI and controls with a classification accuracy of 82.86% ± 07.97% and an AUC of 0.860 ± 0.061. At the same time, the model was able to reconstruct the original brain features with an MSE of 0.035 ± 0.005, as shown in **Figure 5.2**. In comparison, the PCA+SVM model was able to achieve a classification accuracy of 78.09% ± 11.47% with an AUC of 0.825 ± 0.114.

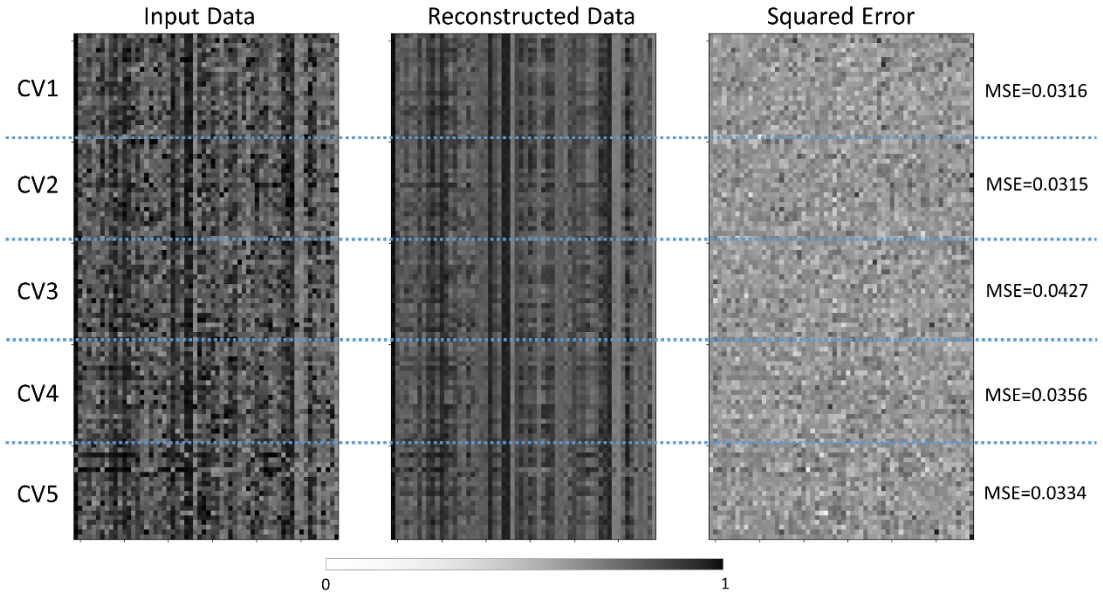

Figure 5.2 Comparisons between the normalized features and reconstructed features by the semi-supervised autoencoder model. The normalized input data was shown on the left, the reconstructed data was shown in the middle, and the squared error was shown on the right. The vertical axis represented the subjects in each cross-validation set, and the horizontal axis represented the features. CV: cross-validation. MSE: mean squared error.

5.3.3 Important brain features for classification

Network topological properties associated with left inferior and superior frontal, postcentral, inferior temporal and medial occipitotemporal regions were identified as the most important brain features for successful discrimination between children with TBI and

controls. Specifically, the functional nodal clustering coefficient of left inferior temporal gyrus and left medial occipitotemporal gyrus, the functional nodal local efficiency of left postcentral gyrus, the structural nodal local efficiency of left inferior frontal gyrus, the structural nodal clustering coefficient of left frontal pole, and the structural betweenness centrality of left superior frontal gyrus had significantly higher importance scores than other selected brain features (**Table 5.2**).

Table 5.2 Importance Score of the Most Important Brain Features in Accurately Differentiating Children With TBI and Controls.

Region	Topological property	Network	Importance score
Left inferior temporal gyrus	Nodal clustering coefficient	Functional	0.0430
Left superior frontal gyrus	Betweenness centrality	Structural	0.0421
Left inferior frontal gyrus	Nodal local efficiency	Structural	0.0339
Left medial occipitotemporal gyrus	Nodal clustering coefficient	Functional	0.0338
Left postcentral gyrus	Nodal local efficiency	Functional	0.0308
Left frontal pole	Nodal clustering coefficient	Structural	0.0277

5.3.4 Performance of regression model for brain-behavior relationships

The SVR model using the top 6 most important brain features was able to explain 9.44% of the variance (R^2 of 9.44% ± 4.02%) in the inattentive symptom T-score in the study sample (**Figure 5.3A**). And the predicted inattentive symptom T-score yielded an MSE of 0.057 ± 0.015. The functional nodal clustering coefficient of left medial occipitotemporal gyrus and the functional nodal local efficiency of left postcentral gyrus showed the highest predictive values, with feature importance scores of 0.132 and 0.104, respectively. For the

SVR model in predicting hyperactive/impulsive symptom T-score, the R^2 was 7.25% ± 2.69% and the MSE was 0.039 ± 0.009 (**Figure 5.3B**). The most important brain features for predicting hyperactive/impulsive symptoms were the structural betweenness centrality of left superior frontal gyrus, with an importance score of 0.114, and the functional nodal clustering coefficient of left medial occipitotemporal gyrus, with an importance score of 0.050 (**Table 5.3**).

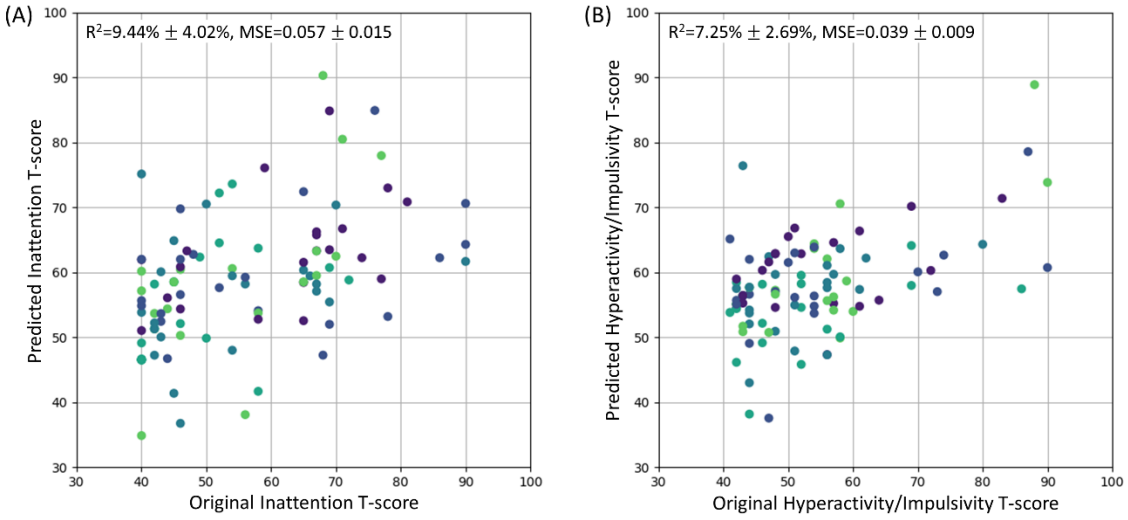

Figure 5.3 The original T-scores of the inattentive and hyperactive/impulsive subscales vs the predicted T-scores using regression model. The predicted values were scaled back to the normal T-score range. The R2 and MSE were reported as mean ± standard deviation. Different cross-validation sets were represented with different colors. (A) Original inattention T-score vs Predicted inattention T-score. (B) Original hyperactivity/impulsivity T-score vs Predicted hyperactivity/impulsivity T-score. MSE: Mean squared error.

Table 5.3 Importance Score of the Most Important Brain Features in the Regression-based Machine Learning Model.

Region	Topological property	Network	Importance score
Importance scores for predicting inattentive T-score			
Left medial occipitotemporal gyrus	Nodal clustering coefficient	Functional	0.132
Left postcentral gyrus	Nodal local efficiency	Functional	0.104
Left inferior temporal gyrus	Nodal clustering coefficient	Functional	0.061
Left superior frontal gyrus	Betweenness centrality	Structural	0.014
Left frontal pole	Nodal clustering coefficient	Structural	0.013
Left inferior frontal gyrus	Nodal local efficiency	Structural	0.011
Importance scores for predicting hyperactive/impulsive T-score			
Left superior frontal gyrus	Betweenness centrality	Structural	0.114
Left medial occipitotemporal gyrus	Nodal clustering coefficient	Functional	0.050
Left inferior frontal gyrus	Nodal local efficiency	Structural	0.021
Left inferior temporal gyrus	Nodal clustering coefficient	Functional	0.017
Left postcentral gyrus	Nodal local efficiency	Functional	0.016
Left frontal pole	Nodal clustering coefficient	Structural	-0.007

In the PLM-SEM analysis, AE-feature 17 showed significant direct effect on the inattentive symptoms T-score, and both AE-features 4 and 17 showed significant direct effects on the hyperactive/impulsive symptoms T-score in the whole study sample. Important brain features in left inferior temporal, medial occipitotemporal, postcentral, and superior frontal regions showed significant direct effects on AE-features 4 and 17. The detailed results of the PLM-SEM analysis were shown in **Figure 5.4**.

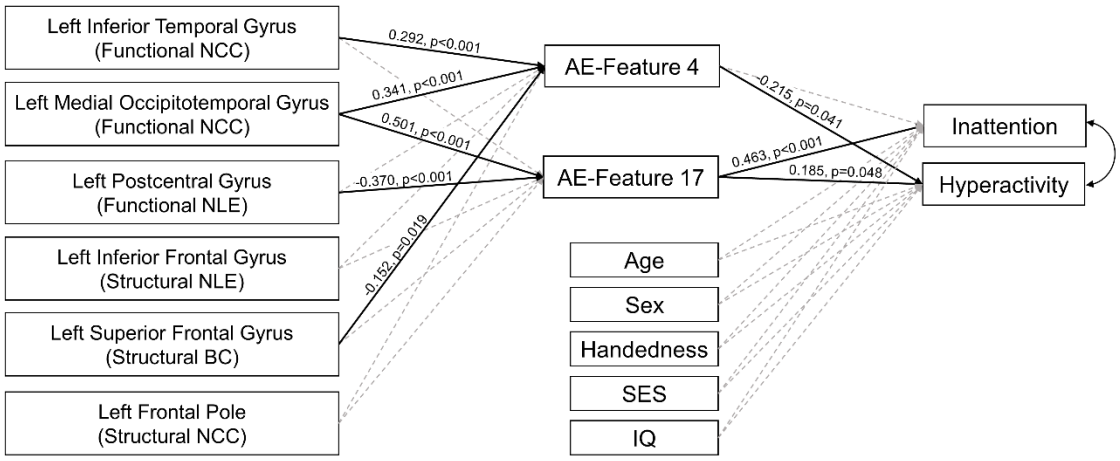

Figure 5.4 Results of partial least square structural equation modeling analysis. The paths with significant direct effects were shown in black solid line. The paths without significant effects were shown in grey dashed line. The numbers next to the significant paths were standardized path coefficient. The *p* values were calculated by applying bootstrapping with 5000 random samples. AE-Features: autoencoder-generated features; NCC: Nodal clustering coefficient; NLE: nodal local efficiency; BC: Betweenness centrality; SES: socioeconomic status, was calculated using the average education years of the parents.

5.4 Discussion

To our best knowledge, this is the first study in the field applying deep learning approach in multimodal neuroimaging data to identify the neural signatures associated with post-TBI attention deficits in children. By constructing a semi-supervised autoencoder in task-based fMRI and DTI data from 110 children, this study has identified 6 most predictive brain features, involving functional and structural network topological properties associated with left frontal, parietal, temporal and occipital lobes. Regression-based machine learning analysis in our study sample further showed that, among these most important brain features, those associated with left postcentral area showed significant predictive value for inattentive symptoms; those associated with left superior frontal gyrus showed significant predictive value for hyperactive/impulsive symptoms; while those associated with left

medial occipitotemporal gyrus showed significant predictive value for both inattentive and hyperactive/impulsive symptoms.

In this aim, our semi-supervised autoencoder model has well-behaved in terms of effectiveness and robustness in successful discrimination between children with TBI and controls, with satisfactory accuracy and AUC. The reconstructed features also showed minimal error, measured using MSE, when compared to the input features. Compared to the conventional PCA+SVM model, our semi-supervised autoencoder model achieved higher classification accuracy and AUC. The reconstruction process preserved the distinctive information while reducing the feature dimensionality for the classification process (Hinton and Salakhutdinov, 2006; Kamal and Bae, 2022). In addition, the added gaussian noise to input features during the training process of the semi-supervised autoencoder model further improve the generalization performance of the constructed deep neural network model (Audhkhasi et al., 2016; Noh et al., 2017). Therefore, relative to those reported in the majority of existing conventional model-based studies, our identified brain substrates for childhood TBI and its related attention deficits are more reliable and have more significant value in guiding tailored diagnoses and interventions in affected children.

Our study observed the important roles of the structural topological alterations of left inferior frontal gyrus, left superior frontal gyrus, and left frontal pole in differentiating children with TBI and controls. In addition, the betweenness centrality (which represent the capacity of serving as a bridging node) of left superior frontal gyrus showed significant value for successfully predicting severity of the hyperactive/impulsive symptoms in the whole study sample. Those regions were part of the prefrontal cortex, which is an essential

component in the top-down control pathway that facilitate the selective attention, inhibition, and sensory modulation (Buschman and Miller, 2007; Rossi et al., 2009; Katsuki and Constantinidis, 2014). Structural MRI and DTI studies have consistently reported decreased gray matter volume, reduced cortical thickness, and disrupted white matter integrity in left prefrontal area in children with TBI (Wilde et al., 2012a; Mayer et al., 2015b; Dennis et al., 2016). Our previous investigation also reported significant structural topological alterations in left inferior frontal gyrus in children with TBI-A (Cao et al., 2021b). Linking with these existing findings, our findings of altered structural connectivity within left prefrontal cortex and between left prefrontal and other brain regions may be related to the axonal damages caused TBI; and the persisted structural alterations in the left prefrontal area in children with chronic TBI might disrupt the attention processing pathways and contribute to the emergence of hyperactive/impulsive symptoms.

Meanwhile, the functional nodal local efficiency (which represent regional integration in the whole network) in the left postcentral gyrus were identified as one of the most important brain features for accurate group classification as well as one of the most valuable brain features in predicting severity of inattentive symptoms in the whole study sample. The postcentral gyrus is responsible for transferring tactile information during the spatial attention, which is a key region in the attention top-down and bottom-up pathways (Macaluso et al., 2000; Buschman and Miller, 2007; Katsuki and Constantinidis, 2014). Existing task-based fMRI studies have reported functional alterations of postcentral gyrus in children with TBI during inhibitory control (Tlustos et al., 2015) and sustained attention (Cao et al., 2021b). Our functional network study also reported that the increased nodal

local efficiency in left postcentral gyrus was significantly correlated with reduced inattentive symptoms in children with TBI-A (Cao et al., 2021b). Together with existing evidence, this study further validated that functional alterations associated with left postcentral gyrus are highly vulnerable that may disrupt normal attention processing and contribute to the onset of attention deficits in children with TBI.

Intriguingly, our study also found that the functional nodal clustering coefficient (which represent the regional connectivity) in left medial occipitotemporal gyrus was an important brain feature in differentiating TBI and control, as well as a significant predictor for both inattentive and hyperactive/impulsive symptoms. The occipitotemporal gyrus has been associated with visual information processing, especially letter process (Mechelli et al., 2003; Vinckier et al., 2007), and was also found to play important role in visual imagery and internally directed cognition (Benedek et al., 2016; Ceh et al., 2021). Structural MRI studies have reported reductions in gray matter volume of the medial occipitotemporal gyrus in children with TBI, and the reduction can persist years after the injury (Wilde et al., 2012b; Dennis et al., 2016). However, no existing studies have reported functional alterations in medial occipitotemporal gyrus in children with TBI. One of the reasons might be that the conventional parametric models lack the sensitivity in detecting the subtle functional alterations in medial occipitotemporal gyrus.

There are some limitations associates with the current study. First, although we have a total of 110 subjects involved in the study, this sample size is still relatively modest in the deep learning field. Such sample size still has potential risk for having overfitted model and limited generalizability. To minimize such risk, we utilized multiple feature selection methods, applied cross-validation, and implemented an additional gaussian noise

layer during the training process. Future research with an even larger sample size is expected to further validate the findings of this study. Second, streamline count-based structural brain network can be biased using probabilistic tractography (Zhang et al., 2022). To reduce potential effects, estimation of streamline count was performed in the native diffusion space using individualized brain parcellations and edge weights were normalized in the individual-level analysis. Other graph theory techniques on structural brain network, like fiber density-based (Smith et al., 2015), connectivity probability-based (Cao et al., 2013), and microstructural measure-based (Girard et al., 2017), can be explored to validate the significance of the current findings. Third, the sex factor associated with post-TBI attention deficits was not investigated in this study. Recent clinical studies with large sample size (>500) reported that girls with TBI had significantly higher risk in developing attention problems than boys (Keenan et al., 2018; Wade et al., 2020). We did not investigate sex-specific neural markers, considering the sample size limitation mentioned above. To partially remove the potential confounding effects, sex was added in our post hoc analysis and showed no significant associations with inattentive or hyperactive symptoms. Future studies with much larger samples are required to thoroughly investigate the sex-specific neural markers of post-TBI attention deficits in children.

5.5 Conclusion

In summary, aim 3 has constructed a semi-supervised autoencoder to effectively and robustly discriminate children with TBI and controls while preserve the intrinsic neuroimaging characteristics in the reconstruction of brain features. All the predominant brain features in differentiating children with TBI and controls were in the left hemisphere, including the functional and structural topological alterations involving left frontal regions,

postcentral regions, and temporal regions. More importantly, the highly discriminative brain features in left frontal regions, parietal regions, and medial occipitotemporal regions demonstrated significant value for predicting elevated inattentive and/or hyperactive/impulsive symptoms in children post-TBI. The findings of this study suggest that deep learning techniques may have the potential to help identifying robust neurobiological markers for post-TBI attention deficits; and the left superior frontal, postcentral, and medial occipitotemporal regions may serve as reliable targets for the diagnosis and interventions of TBI-related attention problems in children.

CHAPTER 6

CONCLUSION

This dissertation is the first study to investigate neurobiological substrates associated with post-TBI attention deficits in children using both anatomical and functional neuroimaging data. In the first aim, the results demonstrated significantly altered regional topological organizations of the WM brain network in frontal, parietal, and temporal regions, in a more homogeneous subgroup of children with chronic TBI who had severe post-TBI attention deficits. The results further suggest that TBI-related WM structural re-modularity in the subnetworks associated with temporal lobe may significantly link to onset of severe post-TBI attention deficits in the affected children. In the second aim, the results showed significant alterations of the topological properties of the sustained attention processing network and their temporal dynamics in children with severe post-TBI attention deficits, especially in the temporal and parietal regions. And these systems-level functional alterations were significantly linked with the elevated inattentive behaviors in the group of TBI-A. Semi-supervised deep learning model applied in the third aim further confirms the significant contributions of these brain features in the prediction of elevated attention deficits in children post-TBI.

These findings provide valuable insight into the neurobiological and neurophysiological substrates associated with the onset of post-TBI attention deficits in children. This project provides valuable foundations for future research on developing neural markers for TBI-induced attention deficits in children, which may significantly assist more effective and individualized diagnostic and treatment strategies. Future research with an even larger sample size and a longitudinal design is expected to further

validate the findings of this study.

The implementation of deep learning models in the third aim in identifying potential biomarkers for post-TBI attention deficits suggests that deep learning has great potential in study the neurocognitive and behavioral consequence post-TBI. Relative to conventional machine learning algorithms, deep learning techniques, such as semi-supervised learning, provide better generalizability and classification performance. Other than based on traditional classification, future studies can take different approaches, such as generative approaches and dimensional approaches. Generative models characterize samples by identifying subgroups that cluster together, which may be beneficial in detecting homogeneous subgroups that have similar consequences in children after TBI. Dimensional approaches associate biological features multiple clinical dimensions simultaneously to link heterogeneities in both clinical presentations and biological properties to increase the interpretability. Deep learning opens the opportunities for future research in exploring the phenotypes or endophenotypes of post-TBI attention deficits and explain the heterogeneities in TBI consequences.

REFERENCES

Abadi, M., Agarwal, A., Barham, P., Brevdo, E., Chen, Z., Citro, C., Corrado, G.S., Davis, A., Dean, J., and Devin, M. (2016). Tensorflow: large-scale machine learning on heterogeneous distributed systems. *arXiv preprint arXiv:1603.04467*.

Achard, S., and Bullmore, E. (2007). Efficiency and cost of economical brain functional networks. *PLoS Computational Biology* 3**,** e17.

Adamson, C., Yuan, W., Babcock, L., Leach, J.L., Seal, M.L., Holland, S.K., and Wade, S.L. (2013). Diffusion tensor imaging detects white matter abnormalities and associated cognitive deficits in chronic adolescent TBI. *Brain Injury* 27**,** 454-463.

Aitken, M.E., Mccarthy, M.L., Slomine, B.S., Ding, R., Durbin, D.R., Jaffe, K.M., Paidas, C.N., Dorsch, A.M., Christensen, J.R., Mackenzie, E.J., and Group, C.S. (2009). Family burden after traumatic brain injury in children. *Pediatrics* 123**,** 199-206.

Anderson, V., Beauchamp, M.H., Yeates, K.O., Crossley, L., Hearps, S.J., and Catroppa, C. (2013). Social competence at 6 months following childhood traumatic brain injury. *Journal of the International Neuropsychological Society* 19**,** 539-550.

Andersson, J.L.R., and Sotiropoulos, S.N. (2016). An integrated approach to correction for off-resonance effects and subject movement in diffusion MR imaging. *Neuroimage* 125**,** 1063-1078.

Arbabshirani, M.R., Plis, S., Sui, J., and Calhoun, V.D. (2017). Single subject prediction of brain disorders in neuroimaging: Promises and pitfalls. *Neuroimage* 145**,** 137-165.

Arbogast, K.B., Curry, A.E., Pfeiffer, M.R., Zonfrillo, M.R., Haarbauer-Krupa, J., Breiding, M.J., Coronado, V.G., and Master, C.L. (2016). Point of health care entry for youth with concussion within a large pediatric care network. *The Journal of the American Medical Association Pediatrics* 170**,** e160294-e160294.

Arnott, S.R., and Alain, C. (2011). The auditory dorsal pathway: orienting vision. *Neuroscience and Biobehavioral Reviews* 35**,** 2162-2173.

Ashourvan, A., Telesford, Q.K., Verstynen, T., Vettel, J.M., and Bassett, D.S. (2019). Multi-scale detection of hierarchical community architecture in structural and functional brain networks. *PLoS One* 14**,** e0215520.

Audhkhasi, K., Osoba, O., and Kosko, B. (2016). Noise-enhanced convolutional neural networks. *Neural Network* 78**,** 15-23.

Babikian, T., Merkley, T., Savage, R.C., Giza, C.C., and Levin, H. (2015). Chronic aspects of pediatric traumatic brain injury: review of the literature. *Journal of Neurotrauma* 32**,** 1849-1860.

Backeljauw, B., and Kurowski, B.G. (2014). Interventions for attention problems after pediatric traumatic brain injury: what is the evidence? *Physical Medicine and Rehabilitation: The Journal of Injury, Function and Rehabilitation* 6**,** 814-824.

Barnett, M., and Reid, L. (2020). The effectiveness of methylphenidate in improving cognition after brain injury in adults: a systematic review. *Brain Injury* 34**,** 1-10.

Bassett, D.S., Wymbs, N.F., Porter, M.A., Mucha, P.J., Carlson, J.M., and Grafton, S.T. (2011). Dynamic reconfiguration of human brain networks during learning. *Proceedings of the National Academy of Sciences of the United States of America* 108**,** 7641-7646.

Bathelt, J., Johnson, A., Zhang, M., and Astle, D.E. (2019). The cingulum as a marker of individual differences in neurocognitive development. *Scientific Reports* 9**,** 2281.

Baum, G.L., Ciric, R., Roalf, D.R., Betzel, R.F., Moore, T.M., Shinohara, R.T., Kahn, A.E., Vandekar, S.N., Rupert, P.E., Quarmley, M., Cook, P.A., Elliott, M.A., Ruparel, K., Gur, R.E., Gur, R.C., Bassett, D.S., and Satterthwaite, T.D. (2017). Modular segregation of structural brain networks supports the development of executive function in youth. *Current Biology* 27**,** 1561-1572 e1568.

Behrens, T.E., Berg, H.J., Jbabdi, S., Rushworth, M.F., and Woolrich, M.W. (2007). Probabilistic diffusion tractography with multiple fibre orientations: What can we gain? *Neuroimage* 34**,** 144-155.

Benedek, M., Jauk, E., Beaty, R.E., Fink, A., Koschutnig, K., and Neubauer, A.C. (2016). Brain mechanisms associated with internally directed attention and self-generated thought. *Scientific Reports* 6**,** 22959.

Bigler, E.D. (2007). Anterior and middle cranial fossa in traumatic brain injury: relevant neuroanatomy and neuropathology in the study of neuropsychological outcome. *Neuropsychology* 21**,** 515-531.

Bigler, E.D., Abildskov, T.J., Petrie, J., Farrer, T.J., Dennis, M., Simic, N., Taylor, H.G., Rubin, K.H., Vannatta, K., Gerhardt, C.A., Stancin, T., and Owen Yeates, K. (2013). Heterogeneity of brain lesions in pediatric traumatic brain injury. *Neuropsychology* 27**,** 438-451.

Blakemore, S.J., and Choudhury, S. (2006). Development of the adolescent brain: implications for executive function and social cognition. *Journal of Child Psychology and Psychiatry* 47**,** 296-312.

Botchway, E., Kooper, C.C., Pouwels, P.J.W., Bruining, H., Engelen, M., Oosterlaan, J., and Konigs, M. (2022). Resting-state network organisation in children with traumatic brain injury. *Cortex* 154**,** 89-104.

Braun, U., Schafer, A., Walter, H., Erk, S., Romanczuk-Seiferth, N., Haddad, L., Schweiger, J.I., Grimm, O., Heinz, A., Tost, H., Meyer-Lindenberg, A., and Bassett, D.S. (2015). Dynamic reconfiguration of frontal brain networks during executive cognition in humans. *Proceedings of the National Academy of Sciences of the United States of America* 112**,** 11678-11683.

Breiman, L. (2001). Random forests. *Machine Learning* 45**,** 5-32.

Brooks, B.L., Virani, S., Khetani, A., Carlson, H., Jadavji, Z., Mauthner, M., Low, T.A., Plourde, V., Macmaster, F.P., Bray, S., Harris, A.D., Lebel, C., Lebel, R.M., Esser, M.J., Yeates, K.O., and Barlow, K.M. (2020). Functional magnetic resonance imaging study of working memory several years after pediatric concussion. *Brain Injury* 34**,** 895-904.

Bullmore, E., and Sporns, O. (2009). Complex brain networks: graph theoretical analysis of structural and functional systems. *Nature Review Neuroscience* 10**,** 186-198.

Buschman, T.J., and Miller, E.K. (2007). Top-down versus bottom-up control of attention in the prefrontal and posterior parietal cortices. *Science* 315**,** 1860-1862.

Caeyenberghs, K., Leemans, A., De Decker, C., Heitger, M., Drijkoningen, D., Linden, C.V., Sunaert, S., and Swinnen, S.P. (2012). Brain connectivity and postural control in young traumatic brain injury patients: A diffusion MRI based network analysis. *Neuroimage Clinical* 1**,** 106-115.

Caeyenberghs, K., Leemans, A., Leunissen, I., Gooijers, J., Michiels, K., Sunaert, S., and Swinnen, S.P. (2014). Altered structural networks and executive deficits in traumatic brain injury patients. *Brain Structure and Function* 219**,** 193-209.

Caeyenberghs, K., Leemans, A., Leunissen, I., Michiels, K., and Swinnen, S.P. (2013). Topological correlations of structural and functional networks in patients with traumatic brain injury. *Frontiers in Human Neuroscience* 7**,** 726.

Caeyenberghs, K., Verhelst, H., Clemente, A., and Wilson, P.H. (2017). Mapping the functional connectome in traumatic brain injury: What can graph metrics tell us? *Neuroimage* 160**,** 113-123.

Caeyenberghs, K., Wenderoth, N., Smits-Engelsman, B.C., Sunaert, S., and Swinnen, S.P. (2009). Neural correlates of motor dysfunction in children with traumatic brain injury: exploration of compensatory recruitment patterns. *Brain* 132**,** 684-694.

Cao, M., Halperin, J.M., and Li, X. (2021a). Abnormal functional network topology and its dynamics during sustained attentionp significantly implicate post-TBI attention deficits in children. *Brain Sciences* 11.

Cao, M., Luo, Y., Wu, Z., Mazzola, C.A., Catania, L., Alvarez, T.L., Halperin, J.M., Biswal, B., and Li, X. (2021b). Topological aberrance of structural brain network provides quantitative substrates of post-traumatic brain injury attention deficits in children. *Brain Connectivity* 11**,** 651-662.

Cao, M., Wu, Z., and Li, X. (2022). GAT-FD: An integrated MATLAB toolbox for graph theoretical analysis of task-related functional dynamics. *PLoS One* 17**,** e0267456.

Cao, Q., Shu, N., An, L., Wang, P., Sun, L., Xia, M.R., Wang, J.H., Gong, G.L., Zang, Y.F., Wang, Y.F., and He, Y. (2013). Probabilistic diffusion tractography and graph theory analysis reveal abnormal white matter structural connectivity networks in drug-naive boys with attention deficit/hyperactivity disorder. *Journal of Neuroscience* 33**,** 10676-10687.

Cappe, C., Rouiller, E.M., and Barone, P. (2009). Multisensory anatomical pathways. *Hearing Research* 258**,** 28-36.

Carskadon, M.A., and Acebo, C. (1993). A self-administered rating scale for pubertal development. *Journal of Adolescent Health* 14**,** 190-195.

Ceh, S.M., Annerer-Walcher, S., Koschutnig, K., Korner, C., Fink, A., and Benedek, M. (2021). Neurophysiological indicators of internal attention: An fMRI-eye-tracking coregistration study. *Cortex* 143**,** 29-46.

Chu, S.H., Parhi, K.K., and Lenglet, C. (2018). Function-specific and enhanced brain structural connectivity mapping via Joint modeling of diffusion and functional MRI. *Scientific Reports* 8**,** 4741.

Corbetta, M., and Shulman, G.L. (2002). Control of goal-directed and stimulus-driven attention in the brain. *Nature Review Neuroscience* 3**,** 201-215.

Dall'acqua, P., Johannes, S., Mica, L., Simmen, H.P., Glaab, R., Fandino, J., Schwendinger, M., Meier, C., Ulbrich, E.J., Muller, A., Baetschmann, H., Jancke, L., and Hanggi, J. (2017). Functional and structural network recovery after mild traumatic brain injury: a 1-year longitudinal study. *Frontiers in Human Neuroscience* 11**,** 280.

De Reus, M.A., and Van Den Heuvel, M.P. (2013). Estimating false positives and negatives in brain networks. *Neuroimage* 70**,** 402-409.

Dennis, E.L., Babikian, T., Alger, J., Rashid, F., Villalon-Reina, J.E., Jin, Y., Olsen, A., Mink, R., Babbitt, C., Johnson, J., Giza, C.C., Thompson, P.M., and Asarnow, R.F. (2018). Magnetic resonance spectroscopy of fiber tracts in children with traumatic brain injury: a combined MRS - diffusion MRI study. *Human Brain Mapping* 39**,** 3759-3768.

Dennis, E.L., Faskowitz, J., Rashid, F., Babikian, T., Mink, R., Babbitt, C., Johnson, J., Giza, C.C., Jahanshad, N., Thompson, P.M., and Asarnow, R.F. (2017). Diverging volumetric trajectories following pediatric traumatic brain injury. *Neuroimage Clinical* 15**,** 125-135.

Dennis, E.L., Hua, X., Villalon-Reina, J., Moran, L.M., Kernan, C., Babikian, T., Mink, R., Babbitt, C., Johnson, J., Giza, C.C., Thompson, P.M., and Asarnow, R.F. (2016). Tensor-based morphometry reveals volumetric deficits in moderate-severe pediatric traumatic brain injury. *Journal of Neurotrauma* 33**,** 840-852.

Dennis, E.L., Jin, Y., Villalon-Reina, J.E., Zhan, L., Kernan, C.L., Babikian, T., Mink, R.B., Babbitt, C.J., Johnson, J.L., Giza, C.C., Thompson, P.M., and Asarnow, R.F. (2015). White matter disruption in moderate/severe pediatric traumatic brain injury: advanced tract-based analyses. *Neuroimage Clinical* 7**,** 493-505.

Dennis, M., Simic, N., Bigler, E.D., Abildskov, T., Agostino, A., Taylor, H.G., Rubin, K., Vannatta, K., Gerhardt, C.A., Stancin, T., and Yeates, K.O. (2013). Cognitive, affective, and conative theory of mind (ToM) in children with traumatic brain injury. *Developmental Cognitive Neuroscience* 5**,** 25-39.

Dewan, M.C., Mummareddy, N., Wellons, J.C., 3rd, and Bonfield, C.M. (2016). Epidemiology of Global Pediatric Traumatic Brain Injury: Qualitative Review. *World Neurosurgery* 91**,** 497-509 e491.

Diez, I., Drijkoningen, D., Stramaglia, S., Bonifazi, P., Marinazzo, D., Gooijers, J., Swinnen, S.P., and Cortes, J.M. (2017). Enhanced prefrontal functional-structural networks to support postural control deficits after traumatic brain injury in a pediatric population. *Network Neuroscience* 1**,** 116-142.

Eckner, J.T., Kutcher, J.S., and Richardson, J.K. (2011). Effect of concussion on clinically measured reaction time in 9 NCAA division I collegiate athletes: a preliminary study. *Physical Medicine and Rehabilitation: The Journal of Injury, Function and Rehabilitation* 3**,** 212-218.

Emery, C.A., Barlow, K.M., Brooks, B.L., Max, J.E., Villavicencio-Requis, A., Gnanakumar, V., Robertson, H.L., Schneider, K., and Yeates, K.O. (2016). A systematic review of psychiatric, psychological, and behavioural outcomes following mild traumatic brain injury in children and adolescents. *Canada Journal of Psychiatry* 61**,** 259-269.

Ewing-Cobbs, L., Johnson, C.P., Juranek, J., Demaster, D., Prasad, M., Duque, G., Kramer, L., Cox, C.S., and Swank, P.R. (2016). Longitudinal diffusion tensor imaging after pediatric traumatic brain injury: impact of age at injury and time since injury on pathway integrity. *Human Brain Mapping* 37**,** 3929-3945.

Ewing-Cobbs, L., Prasad, M.R., Swank, P., Kramer, L., Cox, C.S., Jr., Fletcher, J.M., Barnes, M., Zhang, X., and Hasan, K.M. (2008). Arrested development and disrupted callosal microstructure following pediatric traumatic brain injury: relation to neurobehavioral outcomes. *Neuroimage* 42**,** 1305-1315.

Faber, J., Wilde, E.A., Hanten, G., Ewing-Cobbs, L., Aitken, M.E., Yallampalli, R., Macleod, M.C., Mullins, S.H., Chu, Z.D., Li, X., Hunter, J.V., Noble-Haeusslein, L., and Levin, H.S. (2016). Ten-year outcome of early childhood traumatic brain injury: Diffusion tensor imaging of the ventral striatum in relation to executive functioning. *Brain Injury* 30**,** 1635-1641.

Fagerholm, E.D., Hellyer, P.J., Scott, G., Leech, R., and Sharp, D.J. (2015). Disconnection of network hubs and cognitive impairment after traumatic brain injury. *Brain* 138**,** 1696-1709.

Fischl, B. (2012). FreeSurfer. *Neuroimage* 62**,** 774-781.

Fisher, A., Rudin, C., and Dominici, F. (2019). All models are wrong, but many are useful: learning a variable's importance by studying an Entire class of prediction Models Simultaneously. *Journal of Machine Learning Research* 20**,** 1-81.

Freeman, L.C.J.S.N. (1978). Centrality in social networks conceptual clarification. *Social Networks* 1**,** 215-239.

Fujii, D.E., and Ahmed, I. (2014). Psychotic disorder caused by traumatic brain injury. *Psychiatric Clinics of North America* 37**,** 113-124.

Gerring, J.P., Brady, K.D., Chen, A., Vasa, R., Grados, M., Bandeen-Roche, K.J., Bryan, R.N., Denckla, M.B.J.J.O.T.a.a.O.C., and Psychiatry, A. (1998). Premorbid prevalence of ADHD and development of secondary ADHD after closed head injury. *Journal of the American Academy of Child and Adolescent Psychiatry* 37**,** 647-654.

Gilbert, N., Bernier, R.A., Calhoun, V.D., Brenner, E., Grossner, E., Rajtmajer, S.M., and Hillary, F.G. (2018). Diminished neural network dynamics after moderate and severe traumatic brain injury. *PLoS One* 13**,** e0197419.

Ginstfeldt, T., and Emanuelson, I. (2010). An overview of attention deficits after paediatric traumatic brain injury. *Brain Injury* 24**,** 1123-1134.

Girard, G., Daducci, A., Petit, L., Thiran, J.P., Whittingstall, K., Deriche, R., Wassermann, D., and Descoteaux, M. (2017). AxTract: Toward microstructure informed tractography. *Human Brain Mapping* 38**,** 5485-5500.

Green, G.H., and Diggle, P.J. (2007). On the operational characteristics of the Benjamini and Hochberg false discovery rate procedure. *Statistical Applications in Genetics and Molecular Biology* 6.

Grill-Spector, K., and Weiner, K.S. (2014). The functional architecture of the ventral temporal cortex and its role in categorization. *Nature Review Neuroscience* 15**,** 536-548.

Hair, J.F., Ringle, C.M., and Sarstedt, M. (2011). PLS-SEM: Indeed a silver bullet. *Journal of Marketing Theory and Practice* 19**,** 139-152.

Hair Jr, J.F., Hult, G.T.M., Ringle, C.M., Sarstedt, M., Danks, N.P., and Ray, S. (2021). "Partial least squares structural equation modeling (PLS-SEM) using R: A workbook". New York, NY: Springer Nature.

Han, K., Chapman, S.B., and Krawczyk, D.C. (2016). Disrupted intrinsic connectivity among default, dorsal attention, and frontoparietal control networks in Individuals with chronic traumatic brain injury. *Journal of the International Neuropsychological Society* 22**,** 263-279.

Hansen, J.Y., Shafiei, G., Vogel, J.W., Smart, K., Bearden, C.E., Hoogman, M., Franke, B., Van Rooij, D., Buitelaar, J., Mcdonald, C.R., Sisodiya, S.M., Schmaal, L., Veltman, D.J., Van Den Heuvel, O.A., Stein, D.J., Van Erp, T.G.M., Ching, C.R.K., Andreassen, O.A., Hajek, T., Opel, N., Modinos, G., Aleman, A., Van Der Werf, Y., Jahanshad, N., Thomopoulos, S.I., Thompson, P.M., Carson, R.E., Dagher, A., and Misic, B. (2022). Local molecular and global connectomic contributions to cross-disorder cortical abnormalities. *Nature Communications* 13**,** 4682.

Haxby, J.V., Gobbini, M.I., Furey, M.L., Ishai, A., Schouten, J.L., and Pietrini, P. (2001). Distributed and overlapping representations of faces and objects in ventral temporal cortex. *Science* 293**,** 2425-2430.

Hellyer, P.J., Scott, G., Shanahan, M., Sharp, D.J., and Leech, R. (2015). Cognitive flexibility through metastable neural dynamics is disrupted by damage to the structural connectome. *Journal of Neuroscience* 35**,** 9050-9063.

Henseler, J., and Chin, W.W. (2010). A comparison of approaches for the analysis of interaction effects between latent variables using partial least squares path modeling. *Structural Equation Modeling* 17**,** 82-109.

Hinton, G.E., and Salakhutdinov, R.R. (2006). Reducing the dimensionality of data with neural networks. *Science* 313**,** 504-507.

Ho, T.C., Zhang, S., Sacchet, M.D., Weng, H., Connolly, C.G., Henje Blom, E., Han, L.K., Mobayed, N.O., and Yang, T.T. (2016). Fusiform gyrus dysfunction is associated with perceptual processing efficiency to emotional faces in adolescent Depression: a model-based approach. *Frontiers in Psychology* 7**,** 40.

Hooper, S.R., Alexander, J., Moore, D., Sasser, H.C., Laurent, S., King, J., Bartel, S., and Callahan, B.J.N. (2004). Caregiver reports of common symptoms in children following a traumatic brain injury. *Journal of Pediatric Rehabilitation Medicine* 19**,** 175-189.

Hou, W., Sours Rhodes, C., Jiang, L., Roys, S., Zhuo, J., Jaja, J., and Gullapalli, R.P. (2019). Dynamic functional network analysis in mild traumatic brain injury. *Brain Connectivity* 9**,** 475-487.

Hutchison, R.M., and Morton, J.B. (2015). Tracking the brain's functional coupling dynamics over development. *Journal of Neuroscience* 35**,** 6849-6859.

Imms, P., Clemente, A., Cook, M., D'souza, W., Wilson, P.H., Jones, D.K., and Caeyenberghs, K. (2019). The structural connectome in traumatic brain injury: A meta-analysis of graph metrics. *Neuroscience and Biobehavioral Reviews* 99**,** 128-137.

Iyer, K.K., Zalesky, A., Barlow, K.M., and Cocchi, L. (2019). Default mode network anatomy and function is linked to pediatric concussion recovery. *Annals of Clinical and Translational Neurology* 6**,** 2544-2554.

Janssen, R.J., Mourao-Miranda, J., and Schnack, H.G. (2018). Making individual prognoses in psychiatry using neuroimaging and machine learning. *Biological Psychiatry Cognitive Neuroscience and Neuroimaging* 3**,** 798-808.

Jenkinson, M., Beckmann, C.F., Behrens, T.E., Woolrich, M.W., and Smith, S.M. (2012). FSL. *Neuroimage* 62**,** 782-790.

Jeurissen, B., Leemans, A., Tournier, J.D., Jones, D.K., and Sijbers, J. (2013). Investigating the prevalence of complex fiber configurations in white matter tissue with diffusion magnetic resonance imaging. *Human Brain Mapping* 34**,** 2747-2766.

Jolly, A.E., Scott, G.T., Sharp, D.J., and Hampshire, A.H. (2020). Distinct patterns of structural damage underlie working memory and reasoning deficits after traumatic brain injury. *Brain* 143**,** 1158-1176.

Jones, D.K. (2010). Challenges and limitations of quantifying brain connectivity in vivo with diffusion MRI. *Imaging in Medicine* 2**,** 341.

Jones, D.K., Knosche, T.R., and Turner, R. (2013). White matter integrity, fiber count, and other fallacies: the do's and don'ts of diffusion MRI. *Neuroimage* 73**,** 239-254.

Kalin, N.H. (2021). Understanding the value and limitations of MRI neuroimaging in psychiatry. *American Journal of Psychiatry* 178**,** 673-676.

Kalmady, S.V., Greiner, R., Agrawal, R., Shivakumar, V., Narayanaswamy, J.C., Brown, M.R.G., Greenshaw, A.J., Dursun, S.M., and Venkatasubramanian, G. (2019). Towards artificial intelligence in mental health by improving schizophrenia prediction with multiple brain parcellation ensemble-learning. *Schizophrenia* 5**,** 2.

Kamal, I.M., and Bae, H. (2022). Super-encoder with cooperative autoencoder networks. *Pattern Recognition* 126**,** 108562.

Karunanayaka, P.R., Holland, S.K., Yuan, W., Altaye, M., Jones, B.V., Michaud, L.J., Walz, N.C., and Wade, S.L. (2007). Neural substrate differences in language networks and associated language-related behavioral impairments in children with TBI: a preliminary fMRI investigation. *NeuroRehabilitation* 22**,** 355-369.

Katsuki, F., and Constantinidis, C. (2014). Bottom-up and top-down attention: different processes and overlapping neural systems. *Neuroscientist* 20**,** 509-521.

Kaufman, J., Birmaher, B., Brent, D.A., Ryan, N.D., and Rao, U. (2000). K-Sads-Pl. *Journal of the American Academy of Child and Adolescent Psychiatry* 39(10), 1208

Keenan, H.T., Clark, A.E., Holubkov, R., Cox, C.S., and Ewing-Cobbs, L. (2018). Psychosocial and executive function recovery trajectories one year after pediatric traumatic brain injury: the influence of age and injury severity. *Journal of Neurotrauma* 35**,** 286-296.

Kim, J., Parker, D., Whyte, J., Hart, T., Pluta, J., Ingalhalikar, M., Coslett, H.B., and Verma, R. (2014). Disrupted structural connectome is associated with both psychometric and real-world neuropsychological impairment in diffuse traumatic brain injury. *Journal of the International Neuropsychological Society* 20**,** 887-896.

Kim, S.G., and Ogawa, S. (2012). Biophysical and physiological origins of blood oxygenation level-dependent fMRI signals. *Journal of Cerebral Blood Flow and Metabolism* 32**,** 1188-1206.

King, D.J., Ellis, K.R., Seri, S., and Wood, A.G. (2019). A systematic review of cross-sectional differences and longitudinal changes to the morphometry of the brain following paediatric traumatic brain injury. *Neuroimage Clinical* 23**,** 101844.

Kingma, D.P., and Ba, J. (2014). Adam: A method for stochastic optimization. *arXiv preprint arXiv:1412.6980*.

Konigs, M., Heij, H.A., Van Der Sluijs, J.A., Vermeulen, R.J., Goslings, J.C., Luitse, J.S., Poll-The, B.T., Beelen, A., Van Der Wees, M., Kemps, R.J., Catsman-Berrevoets, C.E., and Oosterlaan, J. (2015). Pediatric traumatic brain injury and attention deficit. *Pediatrics* 136**,** 534-541.

Konigs, M., Pouwels, P.J., Ernest Van Heurn, L.W., Bakx, R., Jeroen Vermeulen, R., Goslings, J.C., Carel Goslings, J., Poll-The, B.T., Van Der Wees, M., Catsman-Berrevoets, C.E., and Oosterlaan, J. (2018). Relevance of neuroimaging for neurocognitive and behavioral outcome after pediatric traumatic brain injury. *Brain Imaging and Behavior* 12**,** 29-43.

Konigs, M., Van Heurn, L.W.E., Bakx, R., Vermeulen, R.J., Goslings, J.C., Poll-The, B.T., Van Der Wees, M., Catsman-Berrevoets, C.E., Oosterlaan, J., and Pouwels, P.J.W. (2017). The structural connectome of children with traumatic brain injury. *Human Brain Mapping* 38**,** 3603-3614.

Konrad, K., Gauggel, S., Manz, A., and Scholl, M. (2000). Inhibitory control in children with traumatic brain injury (TBI) and children with attention deficit/hyperactivity disorder (ADHD). *Brain Injury* 14**,** 859-875.

Kramer, M.E., Chiu, C.Y., Shear, P.K., and Wade, S.L. (2009). Neural correlates of verbal associative memory and mnemonic strategy use following childhood traumatic brain injury. *The Journal of Pediatric Rehabilitation Medicine* 2**,** 255-271.

Kramer, M.E., Chiu, C.Y., Walz, N.C., Holland, S.K., Yuan, W., Karunanayaka, P., and Wade, S.L. (2008). Long-term neural processing of attention following early childhood traumatic brain injury: fMRI and neurobehavioral outcomes. *Journal of the International Neuropsychological Society* 14**,** 424-435.

Kuceyeski, A.F., Jamison, K.W., Owen, J.P., Raj, A., and Mukherjee, P. (2019). Longitudinal increases in structural connectome segregation and functional connectome integration are associated with better recovery after mild TBI. *Human Brain Mapping* 40**,** 4441-4456.

Kucyi, A., Hove, M.J., Esterman, M., Hutchison, R.M., and Valera, E.M. (2017). Dynamic brain network correlates of spontaneous fluctuations in attention. *Cerebral Cortex* 27**,** 1831-1840.

Kurowski, B., Wade, S.L., Cecil, K.M., Walz, N.C., Yuan, W., Rajagopal, A., and Holland, S.K. (2009). Correlation of diffusion tensor imaging with executive function measures after early childhood traumatic brain injury. *The Journal of Pediatric Rehabilitation Medicine* 2**,** 273-283.

Kurowski, B.G., Epstein, J.N., Pruitt, D.W., Horn, P.S., Altaye, M., and Wade, S.L. (2019). Benefits of methylphenidate for long-term attention problems after traumatic brain injury in childhood: A randomized, double-masked, placebo-controlled, dose-titration, crossover trial. *Journal of Head Trauma Rehabilitation* 34**,** E1-E12.

Latora, V., and Marchiori, M. (2001). Efficient behavior of small-world networks. *Physical Review Letters* 87**,** 198701.

Le Fur, C., Camara-Costa, H., Francillette, L., Opatowski, M., Toure, H., Brugel, D., Laurent-Vannier, A., Meyer, P., Watier, L., Dellatolas, G., and Chevignard, M. (2019). Executive functions and attention 7 years after severe childhood traumatic brain injury: Results of the Traumatisme Grave de l'Enfant (TGE) cohort. *Annals of Physical and Rehabilitation Medicine*.

Leblond, E., Smith-Paine, J., Riemersma, J.J., Horn, P.S., Wade, S.L., and Kurowski, B.G. (2019). Influence of methylphenidate on long-term neuropsychological and everyday executive functioning After traumatic brain injury in children with secondary attention problems. *Journal of the International Neuropsychological Society* 25**,** 740-749.

Lecun, Y., Bengio, Y., and Hinton, G. (2015). Deep learning. *Nature* 521**,** 436-444.

Lee, C.U., Shenton, M.E., Salisbury, D.F., Kasai, K., Onitsuka, T., Dickey, C.C., Yurgelun-Todd, D., Kikinis, R., Jolesz, F.A., and Mccarley, R.W. (2002). Fusiform gyrus volume reduction in first-episode schizophrenia: a magnetic resonance imaging study. *Archives of General Psychiatry* 59**,** 775-781.

Levin, H.S., Hanten, G., Zhang, L., Swank, P.R., and Hunter, J. (2004). Selective impairment of inhibition after TBI in children. *Journal of Clinical and Experimental Neuropsychology* 26**,** 589-597.

Levin, H.S., Wilde, E.A., Chu, Z., Yallampalli, R., Hanten, G.R., Li, X., Chia, J., Vasquez, A.C., and Hunter, J.V. (2008). Diffusion tensor imaging in relation to cognitive and functional outcome of traumatic brain injury in children. *Journal of Head Trauma Rehabilitation* 23**,** 197-208.

Li, C.S., Huang, C., Constable, R.T., and Sinha, R. (2006). Imaging response inhibition in a stop-signal task: neural correlates independent of signal monitoring and post-response processing. *Journal of Neuroscience* 26**,** 186-192.

Li, X., Sroubek, A., Kelly, M.S., Lesser, I., Sussman, E., He, Y., Branch, C., and Foxe, J.J. (2012). Atypical pulvinar-cortical pathways during sustained attention performance in children with attention-deficit/hyperactivity disorder. *Journal of the American Academy of Child and Adolescent Psychiatry* 51**,** 1197-1207 e1194.

Liegeois, F.J., Mahony, K., Connelly, A., Pigdon, L., Tournier, J.D., and Morgan, A.T. (2013). Pediatric traumatic brain injury: language outcomes and their relationship to the arcuate fasciculus. *Brain and Language* 127**,** 388-398.

Lindsey, H.M., Lalani, S.J., Mietchen, J., Gale, S.D., Wilde, E.A., Faber, J., Macleod, M.C., Hunter, J.V., Chu, Z.D., Aitken, M.E., Ewing-Cobbs, L., and Levin, H.S. (2019). Acute pediatric traumatic brain injury severity predicts long-term verbal memory performance through suppression by white matter integrity on diffusion tensor imaging. *Brain Imaging and Behavior*.

Lipszyc, J., Levin, H., Hanten, G., Hunter, J., Dennis, M., and Schachar, R. (2014). Frontal white matter damage impairs response inhibition in children following traumatic brain injury. *Archives of Clinical Neuropsychology* 29**,** 289-299.

Liu, M., Zhang, D., Shen, D., and Alzheimer's Disease Neuroimaging, I. (2012). Ensemble sparse classification of Alzheimer's disease. *Neuroimage* 60**,** 1106-1116.

Lui, Y.W., Xue, Y., Kenul, D., Ge, Y., Grossman, R.I., and Wang, Y. (2014). Classification algorithms using multiple MRI features in mild traumatic brain injury. *Neurology* 83**,** 1235-1240.

Lumba-Brown, A., Yeates, K.O., Sarmiento, K., Breiding, M.J., Haegerich, T.M., Gioia, G.A., Turner, M., Benzel, E.C., Suskauer, S.J., Giza, C.C., Joseph, M., Broomand, C., Weissman, B., Gordon, W., Wright, D.W., Moser, R.S., Mcavoy, K., Ewing-Cobbs, L., Duhaime, A.C., Putukian, M., Holshouser, B., Paulk, D., Wade, S.L., Herring, S.A., Halstead, M., Keenan, H.T., Choe, M., Christian, C.W., Guskiewicz, K., Raksin, P.B., Gregory, A., Mucha, A., Taylor, H.G., Callahan, J.M., Dewitt, J., Collins, M.W., Kirkwood, M.W., Ragheb, J., Ellenbogen, R.G., Spinks, T.J., Ganiats, T.G., Sabelhaus, L.J., Altenhofen, K., Hoffman, R., Getchius, T., Gronseth, G., Donnell, Z., O'connor, R.E., and Timmons, S.D. (2018). Diagnosis and management of mild traumatic brain injury in children: A systematic review. *Journal of the American Medical Association Pediatrics* 172**,** e182847.

Luo, Y., Alvarez, T.L., Halperin, J.M., and Li, X. (2020). Multimodal neuroimaging-based prediction of adult outcomes in childhood-onset ADHD using ensemble learning techniques. *Neuroimage Clinical* 26**,** 102238.

Macaluso, E., Frith, C.D., and Driver, J. (2000). Modulation of human visual cortex by crossmodal spatial attention. *Science* 289**,** 1206-1208.

Max, J.E., Schachar, R.J., Levin, H.S., Ewing-Cobbs, L., Chapman, S.B., Dennis, M., Saunders, A., and Landis, J. (2005). Predictors of secondary attention-deficit/hyperactivity disorder in children and adolescents 6 to 24 months after traumatic brain injury. *Journal of the American Academy of Child and Adolescent Psychiatry* 44**,** 1041-1049.

Mayer, A.R., Bellgowan, P.S., and Hanlon, F.M. (2015a). Functional magnetic resonance imaging of mild traumatic brain injury. *Neuroscience and Biobehavioral Reviews* 49**,** 8-18.

Mayer, A.R., Hanlon, F.M., and Ling, J.M. (2015b). Gray matter abnormalities in pediatric mild traumatic brain injury. *Journal of Neurotrauma* 32**,** 723-730.

Mechelli, A., Gorno-Tempini, M.L., and Price, C.J. (2003). Neuroimaging studies of word and pseudoword reading: consistencies, inconsistencies, and limitations. *Journal of Cognitive Neuroscience* 15**,** 260-271.

Merkley, T.L., Bigler, E.D., Wilde, E.A., Mccauley, S.R., Hunter, J.V., and Levin, H.S. (2008). Diffuse changes in cortical thickness in pediatric moderate-to-severe traumatic brain injury. *Journal of Neurotrauma* 25**,** 1343-1345.

Miller, G.F., Depadilla, L., and Xu, L. (2021). Costs of nonfatal traumatic brain injury in the United States, 2016. *Medical Care* 59**,** 451-455.

Mishra, V.R., Sreenivasan, K.R., Zhuang, X., Yang, Z., Cordes, D., Banks, S.J., and Bernick, C. (2019). Understanding white matter structural connectivity differences between cognitively impaired and nonimpaired active professional fighters. *Human Brain Mapping* 40**,** 5108-5122.

Misic, B., Betzel, R.F., Griffa, A., De Reus, M.A., He, Y., Zuo, X.N., Van Den Heuvel, M.P., Hagmann, P., Sporns, O., and Zatorre, R.J. (2018). Network-based asymmetry of the human auditory system. *Cerebral Cortex* 28**,** 2655-2664.

Mitra, J., Shen, K.K., Ghose, S., Bourgeat, P., Fripp, J., Salvado, O., Pannek, K., Taylor, D.J., Mathias, J.L., and Rose, S. (2016). Statistical machine learning to identify traumatic brain injury (TBI) from structural disconnections of white matter networks. *Neuroimage* 129**,** 247-259.

Molloy, C., Conroy, R.M., Cotter, D.R., and Cannon, M. (2011). Is traumatic brain injury a risk factor for schizophrenia? A meta-analysis of case-controlled population-based studies. *Schizophrenia Bulletin* 37**,** 1104-1110.

Molteni, E., Pagani, E., Strazzer, S., Arrigoni, F., Beretta, E., Boffa, G., Galbiati, S., Filippi, M., and Rocca, M.A. (2019). Fronto-temporal vulnerability to disconnection in paediatric moderate and severe traumatic brain injury. *The European Journal of Neurology* 26**,** 1183-1190.

Mukherjee, P., Berman, J.I., Chung, S.W., Hess, C.P., and Henry, R.G. (2008). Diffusion tensor MR imaging and fiber tractography: theoretic underpinnings. *American Journal of Neuroradiology* 29**,** 632-641.

Muthukrishnan, R., and Rohini, R. (2016). "LASSO: A feature selection technique in predictive modeling for machine learning", in: *IEEE International Conference on Advances in Computer Applications (ICACA)*), 18-20.

Napolitano, E., Elovic, E.P., and Qureshi, A.I. (2005). Pharmacological stimulant treatment of neurocognitive and functional deficits after traumatic and non-traumatic brain injury. *Medical Science Monitor* 11**,** RA212-220.

Narad, M.E., Kennelly, M., Zhang, N., Wade, S.L., Yeates, K.O., Taylor, H.G., Epstein, J.N., and Kurowski, B.G. (2018). Secondary attention-deficit/hyperactivity disorder in children and adolescents 5 to 10 Years after traumatic brain injury. *Journal of the American Medical Association Pediatrics* 172**,** 437-443.

Narad, M.E., Riemersma, J., Wade, S.L., Smith-Paine, J., Morrison, P., Taylor, H.G., Yeates, K.O., and Kurowski, B.G. (2019). Impact of secondary ADHD on long-term outcomes after early childhood traumatic brain injury. *Journal of Head Trauma Rehabilitation*.

Newsome, M.R., Scheibel, R.S., Hanten, G., Chu, Z., Steinberg, J.L., Hunter, J.V., Lu, H., Vasquez, A.C., Li, X., Lin, X., Cook, L., and Levin, H.S. (2010). Brain activation while thinking about the self from another person's perspective after traumatic brain injury in adolescents. *Neuropsychology* 24**,** 139-147.

Newsome, M.R., Scheibel, R.S., Mayer, A.R., Chu, Z.D., Wilde, E.A., Hanten, G., Steinberg, J.L., Lin, X., Li, X., Merkley, T.L., Hunter, J.V., Vasquez, A.C., Cook, L., Lu, H., Vinton, K., and Levin, H.S. (2013). How functional connectivity between emotion regulation structures can be disrupted: preliminary evidence from adolescents with moderate to severe traumatic brain injury. *Journal of the International Neuropsychological Society* 19**,** 911-924.

Newsome, M.R., Steinberg, J.L., Scheibel, R.S., Troyanskaya, M., Chu, Z., Hanten, G., Lu, H., Lane, S., Lin, X., Hunter, J.V., Vasquez, C., Zientz, J., Li, X., Wilde, E.A., and Levin, H.S. (2008). Effects of traumatic brain injury on working memory-related brain activation in adolescents. *Neuropsychology* 22**,** 419-425.

Nielsen, A.N., Barch, D.M., Petersen, S.E., Schlaggar, B.L., and Greene, D.J. (2020). Machine learning with neuroimaging: evaluating its applications in psychiatry. *Biological Psychiatry Cognitive Neuroscience and Neuroimaging* 5**,** 791-798.

Noh, H., You, T., Mun, J., and Han, B. (2017). Regularizing deep neural networks by noise: Its interpretation and optimization. *Advances in Neural Information Processing Systems* 30.

Nomura, E.M., Gratton, C., Visser, R.M., Kayser, A., Perez, F., and D'esposito, M. (2010). Double dissociation of two cognitive control networks in patients with focal brain lesions. *Proceedings of the National Academy of Sciences of the United States of America* 107**,** 12017-12022.

Ochsner, K.N., Silvers, J.A., and Buhle, J.T. (2012). Functional imaging studies of emotion regulation: a synthetic review and evolving model of the cognitive control of emotion. *Annals of the New York Academy of Sciences* 1251**,** E1-24.

Oldfield, R.C. (1971). The assessment and analysis of handedness: the Edinburgh inventory. *Neuropsychologia* 9**,** 97-113.

Olsen, A., Babikian, T., Dennis, E.L., Ellis-Blied, M.U., Giza, C., Marion, S.D., Mink, R., Johnson, J., Babbitt, C.J., Thompson, P.M., and Asarnow, R.F. (2020). Functional brain hyperactivations are linked to an electrophysiological measure of slow interhemispheric transfer time after pediatric moderate/severe traumatic brain injury. *Journal of Neurotrauma* 37**,** 397-409.

Onnela, J.P., Saramaki, J., Kertesz, J., and Kaski, K. (2005). Intensity and coherence of motifs in weighted complex networks. *Physical Review E: Statistical, Nonlinear, and Soft Matter Physics* 71**,** 065103.

Ornstein, T.J., Sagar, S., Schachar, R.J., Ewing-Cobbs, L., Chapman, S.B., Dennis, M., Saunders, A.E., Yang, T.T., Levin, H.S., and Max, J.E. (2014). Neuropsychological performance of youth with secondary attention-deficit/hyperactivity disorder 6- and 12-months after traumatic brain injury. *Journal of the International Neuropsychological Society* 20**,** 971-981.

Pandit, A.S., Expert, P., Lambiotte, R., Bonnelle, V., Leech, R., Turkheimer, F.E., and Sharp, D.J. (2013). Traumatic brain injury impairs small-world topology. *Neurology* 80**,** 1826-1833.

Pangilinan, P.H., Giacoletti-Argento, A., Shellhaas, R., Hurvitz, E.A., and Hornyak, J.E. (2010). Neuropharmacology in pediatric brain injury: a review. *Physical medicine and rehabilitation: The Journal of Injury, Function and Rehabilitation* 2**,** 1127-1140.

Pereira, F., Mitchell, T., and Botvinick, M. (2009). Machine learning classifiers and fMRI: a tutorial overview. *Neuroimage* 45**,** S199-209.

Perlman, S.B., Fournier, J.C., Bebko, G., Bertocci, M.A., Hinze, A.K., Bonar, L., Almeida, J.R., Versace, A., Schirda, C., Travis, M., Gill, M.K., Demeter, C., Diwadkar, V.A., Sunshine, J.L., Holland, S.K., Kowatch, R.A., Birmaher, B., Axelson, D., Horwitz, S.M., Arnold, L.E., Fristad, M.A., Youngstrom, E.A., Findling, R.L., and Phillips, M.L. (2013). Emotional face processing in pediatric bipolar disorder: evidence for functional impairments in the fusiform gyrus. *Journal of the American Academy of Child and Adolescent Psychiatry* 52**,** 1314-1325 e1313.

Polanczyk, G., Caspi, A., Houts, R., Kollins, S.H., Rohde, L.A., and Moffitt, T.E. (2010). Implications of extending the ADHD age-of-onset criterion to age 12: results from a prospectively studied birth cohort. *Journal of the American Academy of Child and Adolescent Psychiatry* 49**,** 210-216.

Polinder, S., Haagsma, J.A., Van Klaveren, D., Steyerberg, E.W., and Van Beeck, E.F. (2015). Health-related quality of life after TBI: a systematic review of study design, instruments, measurement properties, and outcome. *Population Health Metrics* 13**,** 4.

Power, J.D., Barnes, K.A., Snyder, A.Z., Schlaggar, B.L., and Petersen, S.E. (2012). Spurious but systematic correlations in functional connectivity MRI networks arise from subject motion. *Neuroimage* 59**,** 2142-2154.

Quaak, M., Van De Mortel, L., Thomas, R.M., and Van Wingen, G. (2021). Deep learning applications for the classification of psychiatric disorders using neuroimaging data: Systematic review and meta-analysis. *Neuroimage Clinical* 30**,** 102584.

Rabner, J., Gottlieb, S., Lazdowsky, L., and Lebel, A. (2016). Psychosis following traumatic brain injury and cannabis use in late adolescence. *American Journal of Addiction* 25**,** 91-93.

Raizman, R., Tavor, I., Biegon, A., Harnof, S., Hoffmann, C., Tsarfaty, G., Fruchter, E., Tatsa-Laur, L., Weiser, M., and Livny, A. (2020). Traumatic brain injury severity in a network perspective: A diffusion MRI based connectome study. *Scientific Reports* 10**,** 9121.

Raji, C.A., Wang, M.B., Nguyen, N., Owen, J.P., Palacios, E.M., Yuh, E.L., and Mukherjee, P. (2020). Connectome mapping with edge density imaging differentiates pediatric mild traumatic brain injury from typically developing controls: proof of concept. *Pediatric Radiology* 50**,** 1594-1601.

Rangaprakash, D., Deshpande, G., Daniel, T.A., Goodman, A.M., Robinson, J.L., Salibi, N., Katz, J.S., Denney, T.S., Jr., and Dretsch, M.N. (2017). Compromised hippocampus-striatum pathway as a potential imaging biomarker of mild-traumatic brain injury and posttraumatic stress disorder. *Human Brain Mapping* 38**,** 2843-2864.

Recanzone, G.H., and Cohen, Y.E. (2010). Serial and parallel processing in the primate auditory cortex revisited. *Behavioural Brain Research* 206**,** 1-7.

Resch, C., Rosema, S., Hurks, P., De Kloet, A., and Van Heugten, C. (2018). Searching for effective components of cognitive rehabilitation for children and adolescents with acquired brain injury: A systematic review. *Brain Injury* 32**,** 679-692.

Roberts, R.M., Mathias, J.L., and Rose, S.E. (2016). Relationship between diffusion tensor imaging (DTI) findings and cognition following pediatric TBI: A meta-analytic review. *Developmental Neuropsychology* 41**,** 176-200.

Ross, B.C. (2014). Mutual information between discrete and continuous data sets. *PLoS One* 9**,** e87357.

Rossi, A.F., Pessoa, L., Desimone, R., and Ungerleider, L.G. (2009). The prefrontal cortex and the executive control of attention. *Experimental Brain Research* 192**,** 489-497.

Rubinov, M., and Sporns, O. (2010). Complex network measures of brain connectivity: uses and interpretations. *Neuroimage* 52**,** 1059-1069.

Rubinov, M., and Sporns, O. (2011). Weight-conserving characterization of complex functional brain networks. *Neuroimage* 56**,** 2068-2079.

Satterthwaite, T.D., Wolf, D.H., Loughead, J., Ruparel, K., Elliott, M.A., Hakonarson, H., Gur, R.C., and Gur, R.E. (2012). Impact of in-scanner head motion on multiple measures of functional connectivity: relevance for studies of neurodevelopment in youth. *Neuroimage* 60**,** 623-632.

Scheinost, D., Noble, S., Horien, C., Greene, A.S., Lake, E.M., Salehi, M., Gao, S., Shen, X., O'connor, D., Barron, D.S., Yip, S.W., Rosenberg, M.D., and Constable, R.T. (2019). Ten simple rules for predictive modeling of individual differences in neuroimaging. *Neuroimage* 193**,** 35-45.

Scholten, A.C., Haagsma, J.A., Andriessen, T.M., Vos, P.E., Steyerberg, E.W., Van Beeck, E.F., and Polinder, S. (2015). Health-related quality of life after mild, moderate and severe traumatic brain injury: patterns and predictors of suboptimal functioning during the first year after injury. *Injury* 46**,** 616-624.

Senior, H.E., Mckinlay, L., Nikles, J., Schluter, P.J., Carmont, S.A., Waugh, M.C., Epps, A., Lloyd, O., and Mitchell, G.K. (2013). Central nervous system stimulants for secondary attention deficit-hyperactivity disorder after paediatric traumatic brain injury: a rationale and protocol for single patient (n-of-1) multiple cross-over trials. *BioMed Central Pediatrics* 13**,** 89.

Sharp, D.J., Scott, G., and Leech, R. (2014). Network dysfunction after traumatic brain injury. *Nature Review Neurology* 10**,** 156-166.

Silverstein, S.M., All, S.D., Kasi, R., Berten, S., Essex, B., Lathrop, K.L., and Little, D.M. (2010). Increased fusiform area activation in schizophrenia during processing of spatial frequency-degraded faces, as revealed by fMRI. *Psychological Medicine* 40**,** 1159-1169.

Simundic, A.M. (2009). Measures of diagnostic accuracy: basic definitions. *The Electronic Journal of the International Federation of Clinical Chemistry and Laboratory Medicine* 19**,** 203-211.

Sinopoli, K.J., Chen, J.K., Wells, G., Fait, P., Ptito, A., Taha, T., and Keightley, M. (2014). Imaging "brain strain" in youth athletes with mild traumatic brain injury during dual-task performance. *Journal of Neurotrauma* 31**,** 1843-1859.

Sinopoli, K.J., Schachar, R., and Dennis, M. (2011). Traumatic brain injury and secondary attention-deficit/hyperactivity disorder in children and adolescents: the effect of reward on inhibitory control. *Journal of Clinical and Experimental Neuropsychology* 33**,** 805-819.

Smith, R.E., Tournier, J.D., Calamante, F., and Connelly, A. (2015). SIFT2: Enabling dense quantitative assessment of brain white matter connectivity using streamlines tractography. *Neuroimage* 119**,** 338-351.

Soares, J.M., Marques, P., Alves, V., and Sousa, N. (2013). A hitchhiker's guide to diffusion tensor imaging. *Frontiers in Neuroscience* 7**,** 31.

Spreng, R.N., Sepulcre, J., Turner, G.R., Stevens, W.D., and Schacter, D.L. (2013). Intrinsic architecture underlying the relations among the default, dorsal attention, and frontoparietal control networks of the human brain. *Journal of Cognitive Neuroscience* 25**,** 74-86.

Stancin, T., Wade, S.L., Walz, N.C., Yeates, K.O., and Taylor, H.G. (2010). Family adaptation 18 months after traumatic brain injury in early childhood. *Journal of Developmental and Behavioral Pediatrics* 31**,** 317-325.

Stephens, J.A., Salorio, C.F., Barber, A.D., Risen, S.R., Mostofsky, S.H., and Suskauer, S.J. (2018). Preliminary findings of altered functional connectivity of the default mode network linked to functional outcomes one year after pediatric traumatic brain injury. *Developmental Neurorehabilitiation* 21**,** 423-430.

Stephens, J.A., Salorio, C.F., Gomes, J.P., Nebel, M.B., Mostofsky, S.H., and Suskauer, S.J. (2017). Response Inhibition Deficits and Altered Motor Network Connectivity in the Chronic Phase of Pediatric Traumatic Brain Injury. *Journal of Neurotrauma* 34**,** 3117-3123.

Strakowski, S.M., Adler, C.M., Holland, S.K., Mills, N., and Delbello, M.P. (2004). A preliminary FMRI study of sustained attention in euthymic, unmedicated bipolar disorder. *Neuropsychopharmacology* 29**,** 1734-1740.

Strazzer, S., Rocca, M.A., Molteni, E., De Meo, E., Recla, M., Valsasina, P., Arrigoni, F., Galbiati, S., Bardoni, A., and Filippi, M. (2015). Altered recruitment of the attention network is associated with disability and cognitive impairment in pediatric patients with acquired brain injury. *Neural Plasticity* 15**,** 104282.

Suk, H.I., Lee, S.W., Shen, D., and Alzheimer's Disease Neuroimaging, I. (2017). Deep ensemble learning of sparse regression models for brain disease diagnosis. *Medical Image Analysis* 37**,** 101-113.

Sun, Y., Zhao, L., Lan, Z., Jia, X.Z., and Xue, S.W. (2020). Differentiating boys with ADHD from those with typical development based on whole-brain functional connections using a machine learning approach. *Neuropsychiatric Disease and Treatment* 16**,** 691-702.

Tamez-Pena, J., Rosella, P., Totterman, S., Schreyer, E., Gonzalez, P., Venkataraman, A., and Meyers, S.P. (2021). Post-concussive mTBI in student athletes: MRI features and machine learning. *Frontiers in Neurology* 12**,** 734329.

Taylor, C.A., Bell, J.M., Breiding, M.J., and Xu, L. (2017). Traumatic brain injury–related emergency department visits, hospitalizations, and deaths—United States, 2007 and 2013. *Morbidity and Mortality Weekly Report Surveillance Summaries* 66**,** 1.

Teasdale, G., and Jennett, B. (1974). Assessment of coma and impaired consciousness. A practical scale. *Lancet* 2**,** 81-84.

Tlustos, S.J., Chiu, C.Y., Walz, N.C., Holland, S.K., Bernard, L., and Wade, S.L. (2011). Neural correlates of interference control in adolescents with traumatic brain injury: functional magnetic resonance imaging study of the counting stroop task. *Journal of the International Neuropsychological Society* 17**,** 181-189.

Tlustos, S.J., Peter Chiu, C.Y., Walz, N.C., and Wade, S.L. (2015). Neural substrates of inhibitory and emotional processing in adolescents with traumatic brain injury. *The Journal of Pediatric Rehabilitation Medicine* 8**,** 321-333.

Treble, A., Hasan, K.M., Iftikhar, A., Stuebing, K.K., Kramer, L.A., Cox, C.S., Jr., Swank, P.R., and Ewing-Cobbs, L. (2013a). Working memory and corpus callosum microstructural integrity after pediatric traumatic brain injury: a diffusion tensor tractography study. *Journal of Neurotrauma* 30**,** 1609-1619.

Treble, A., Hasan, K.M., Iftikhar, A., Stuebing, K.K., Kramer, L.A., Cox, C.S., Jr., Swank, P.R., and Ewing-Cobbs, L. (2013b). Working memory and corpus callosum microstructural integrity after pediatric traumatic brain injury: a diffusion tensor tractography study. *Journal of Neurotrauma* 30**,** 1609-1619.

Tuerk, C., Degeilh, F., Catroppa, C., Dooley, J.J., Kean, M., Anderson, V., and Beauchamp, M.H. (2020). Altered resting-state functional connectivity within the developing social brain after pediatric traumatic brain injury. *Human Brain Mapping* 41**,** 561-576.

Tzourio-Mazoyer, N., Landeau, B., Papathanassiou, D., Crivello, F., Etard, O., Delcroix, N., Mazoyer, B., and Joliot, M. (2002). Automated anatomical labeling of activations in SPM using a macroscopic anatomical parcellation of the MNI MRI single-subject brain. *Neuroimage* 15**,** 273-289.

Venkatesan, U.M., and Hillary, F.G. (2019). Functional connectivity within lateral posterior parietal cortex in moderate to severe traumatic brain injury. *Neuropsychology* 33**,** 893-910.

Vergara, V.M., Mayer, A.R., Damaraju, E., Kiehl, K.A., and Calhoun, V. (2017). Detection of mild traumatic brain injury by machine learning classification using resting state functional network connectivity and fractional anisotropy. *Journal of Neurotrauma* 34**,** 1045-1053.

Verhelst, H., Vander Linden, C., De Pauw, T., Vingerhoets, G., and Caeyenberghs, K. (2018). Impaired rich club and increased local connectivity in children with traumatic brain injury: Local support for the rich? *Human Brain Mapping* 39**,** 2800-2811.

Vincent, J.L., Kahn, I., Snyder, A.Z., Raichle, M.E., and Buckner, R.L. (2008). Evidence for a frontoparietal control system revealed by intrinsic functional connectivity. *Journal of Neurophysiology* 100**,** 3328-3342.

Vinckier, F., Dehaene, S., Jobert, A., Dubus, J.P., Sigman, M., and Cohen, L. (2007). Hierarchical coding of letter strings in the ventral stream: dissecting the inner organization of the visual word-form system. *Neuron* 55**,** 143-156.

Voisin, J., Bidet-Caulet, A., Bertrand, O., and Fonlupt, P. (2006). Listening in silence activates auditory areas: a functional magnetic resonance imaging study. *Journal of Neuroscience* 26**,** 273-278.

Vossel, S., Geng, J.J., and Fink, G.R. (2014). Dorsal and ventral attention systems: distinct neural circuits but collaborative roles. *Neuroscientist* 20**,** 150-159.

Wade, S.L., Kaizar, E.E., Narad, M.E., Zang, H., Kurowski, B.G., Miley, A.E., Moscato, E.L., Aguilar, J.M., Yeates, K.O., Taylor, H.G., and Zhang, N. (2020). Behavior Problems Following Childhood TBI: The Role of Sex, Age, and Time Since Injury. *Journal of Head Trauma Rehabilitation* 35**,** E393-E404.

Wade, S.L., Zhang, N., Yeates, K.O., Stancin, T., and Taylor, H.G. (2016). Social environmental moderators of long-term functional outcomes of early childhood brain injury. *Journal of the American Medical Association Pediatrics* 170**,** 343-349.

Wager, T.D., Jonides, J., and Reading, S. (2004). Neuroimaging studies of shifting attention: a meta-analysis. *Neuroimage* 22**,** 1679-1693.

Wang, J., Wei, Q., Bai, T., Zhou, X., Sun, H., Becker, B., Tian, Y., Wang, K., and Kendrick, K. (2017). Electroconvulsive therapy selectively enhanced feedforward connectivity from fusiform face area to amygdala in major depressive disorder. *Social Cognitive and Affective Neuroscience* 12**,** 1983-1992.

Ware, A.L., Yeates, K.O., Geeraert, B., Long, X., Beauchamp, M.H., Craig, W., Doan, Q., Freedman, S.B., Goodyear, B.G., Zemek, R., Lebel, C., and Pediatric Emergency Research Canada, A.C.a.P.S.T. (2022). Structural connectome differences in pediatric mild traumatic brain and orthopedic injury. *Human Brain Mapping* 43**,** 1032-1046.

Wassenberg, R., Max, J.E., Lindgren, S.D., and Schatz, A. (2004). Sustained attention in children and adolescents after traumatic brain injury: relation to severity of injury, adaptive functioning, ADHD and social background. *Brain Injury* 18**,** 751-764.

Watson, C.G., Demaster, D., and Ewing-Cobbs, L. (2019). Graph theory analysis of DTI tractography in children with traumatic injury. *Neuroimage Clinical* 21**,** 101673.

Wechsler, D. (2011). Wechsler abbreviated scale of intelligence–second edition (WASI-II). *American Psychological Association PsycTests*.

Wehmeier, P.M., Schacht, A., and Barkley, R.a.J.J.O.a.H. (2010). Social and emotional impairment in children and adolescents with ADHD and the impact on quality of life. *Journal of Adolescent Health* 46**,** 209-217.

Westfall, D.R., West, J.D., Bailey, J.N., Arnold, T.W., Kersey, P.A., Saykin, A.J., and Mcdonald, B.C. (2015). Increased brain activation during working memory processing after pediatric mild traumatic brain injury (mTBI). *The Journal of Pediatric Rehabilitation Medicine* 8**,** 297-308.

Wilde, E.A., Ayoub, K.W., Bigler, E.D., Chu, Z.D., Hunter, J.V., Wu, T.C., Mccauley, S.R., and Levin, H.S. (2012a). Diffusion tensor imaging in moderate-to-severe pediatric traumatic brain injury: changes within an 18 month post-injury interval. *Brain Imaging and Behavior* 6**,** 404-416.

Wilde, E.A., Hunter, J.V., Newsome, M.R., Scheibel, R.S., Bigler, E.D., Johnson, J.L., Fearing, M.A., Cleavinger, H.B., Li, X., Swank, P.R., Pedroza, C., Roberson, G.S., Bachevalier, J., and Levin, H.S. (2005). Frontal and temporal morphometric findings on MRI in children after moderate to severe traumatic brain injury. *Journal of Neurotrauma* 22**,** 333-344.

Wilde, E.A., Merkley, T.L., Bigler, E.D., Max, J.E., Schmidt, A.T., Ayoub, K.W., Mccauley, S.R., Hunter, J.V., Hanten, G., Li, X., Chu, Z.D., and Levin, H.S. (2012b). Longitudinal changes in cortical thickness in children after traumatic brain injury and their relation to behavioral regulation and emotional control. *International Journal of Developmental Neuroscience* 30**,** 267-276.

Wilde, E.A., Newsome, M.R., Bigler, E.D., Pertab, J., Merkley, T.L., Hanten, G., Scheibel, R.S., Li, X., Chu, Z., Yallampalli, R., Hunter, J.V., and Levin, H.S. (2011). Brain imaging correlates of verbal working memory in children following traumatic brain injury. *International Journal of Psychophysiology* 82**,** 86-96.

Woolrich, M.W., Ripley, B.D., Brady, M., and Smith, S.M. (2001). Temporal autocorrelation in univariate linear modeling of FMRI data. *Neuroimage* 14**,** 1370-1386.

Wozniak, J.R., Krach, L., Ward, E., Mueller, B.A., Muetzel, R., Schnoebelen, S., Kiragu, A., and Lim, K.O. (2007a). Neurocognitive and neuroimaging correlates of pediatric traumatic brain injury: a diffusion tensor imaging (DTI) study. *Archives of Clinical Neuropsychology* 22**,** 555-568.

Wozniak, J.R., Krach, L., Ward, E., Mueller, B.A., Muetzel, R., Schnoebelen, S., Kiragu, A., and Lim, K.O. (2007b). Neurocognitive and neuroimaging correlates of pediatric traumatic brain injury: a diffusion tensor imaging (DTI) study. *Arch Clin Neuropsychol* 22**,** 555-568.

Wu, T., Merkley, T.L., Wilde, E.A., Barnes, A., Li, X., Chu, Z.D., Mccauley, S.R., Hunter, J.V., and Levin, H.S. (2018a). A preliminary report of cerebral white matter microstructural changes associated with adolescent sports concussion acutely and subacutely using diffusion tensor imaging. *Brain Imaging and Behavior* 12**,** 962-973.

Wu, Z., Mazzola, C.A., Catania, L., Owoeye, O., Yaramothu, C., Alvarez, T., Gao, Y., and Li, X. (2018b). Altered cortical activation and connectivity patterns for visual attention processing in young adults post-traumatic brain injury: A functional near infrared spectroscopy study. *Central Nervous System Neuroscience and Therapeutics* 24**,** 539-548.

Xia, S., Foxe, J.J., Sroubek, A.E., Branch, C., and Li, X. (2014). Topological organization of the "small-world" visual attention network in children with attention deficit/hyperactivity disorder (ADHD). *Frontiers in Human Neuroscience* 8**,** 162.

Yang, L.Y., Huang, C.C., Chiu, W.T., Huang, L.T., Lo, W.C., and Wang, J.Y. (2016). Association of traumatic brain injury in childhood and attention-deficit/hyperactivity disorder: a population-based study. *Pediatric Research* 80**,** 356-362.

Yeates, K.O., Bigler, E.D., Abildskov, T., Dennis, M., Gerhardt, C.A., Vannatta, K., Rubin, K.H., Stancin, T., and Taylor, H.G. (2014). Social competence in pediatric traumatic brain injury: from brain to behavior. *Clinical Psychological Science* 2**,** 97-107.

Yeates, K.O., Taylor, H.G., Rusin, J., Bangert, B., Dietrich, A., Nuss, K., and Wright, M. (2012). Premorbid child and family functioning as predictors of post-concussive symptoms in children with mild traumatic brain injuries. *International Journal of Developmental Neuroscience* 30**,** 231-237.

Yuan, W., Treble-Barna, A., Sohlberg, M.M., Harn, B., and Wade, S.L. (2017a). Changes in structural connectivity following a cognitive intervention in children with traumatic brain injury. *Neurorehabilitation Neural Repair* 31**,** 190-201.

Yuan, W., Wade, S.L., and Babcock, L. (2015). Structural connectivity abnormality in children with acute mild traumatic brain injury using graph theoretical analysis. *Human Brain Mapping* 36**,** 779-792.

Yuan, W., Wade, S.L., Quatman-Yates, C., Hugentobler, J.A., Gubanich, P.J., and Kurowski, B.G. (2017b). Structural connectivity related to persistent symptoms after mild TBI in adolescents and response to aerobic training: preliminary investigation. *Journal of Head Trauma Rehabilitation* 32**,** 378-384.

Zhang, F., Daducci, A., He, Y., Schiavi, S., Seguin, C., Smith, R.E., Yeh, C.H., Zhao, T., and O'donnell, L.J. (2022). Quantitative mapping of the brain's structural connectivity using diffusion MRI tractography: A review. *Neuroimage* 249**,** 118870.

Zhang, H., Schneider, T., Wheeler-Kingshott, C.A., and Alexander, D.C. (2012). NODDI: practical in vivo neurite orientation dispersion and density imaging of the human brain. *Neuroimage* 61**,** 1000-1016.